THE UNIVERSITY OF QUEENSLAND

AUSTRALIA

Regulation and Cell Biology of Secondary Metabolite Production in *Fusarium graminearum* and *Fusarium pseudograminearum*

Ailisa Blum

MSc, BSc

A thesis submitted for the degree of Doctor of Philosophy at

The University of Queensland in 2017

School of Agriculture and Food Sciences

CSIRO Agriculture and Food

Abstract

Ascomycete fungi have the potential to produce a vast array of secondary metabolites, which are metabolites not required for normal growth and development. In any one species there is typically the potential for production of upward of fifty of these compounds. Many fungal secondary metabolites are used as medicines (e.g. penicillin or cyclosporine), or are of importance due to their toxicity in humans or animals (e.g. aflatoxins), or because they are virulence factors during crop plant infection (e.g. deoxynivalenol). Despite the vast potential encoded in ascomycete genomes, the vast majority of fungal secondary metabolites are yet to be discovered. This is in part due to our lack of understanding of how the production of these compounds is regulated. Moreover, even for the compounds we do know, we are just beginning to understand the complex interaction of external stimuli, signalling pathways, cellular and developmental biology that leads to their production. In this thesis, biological insights into these aspects of two fungal secondary metabolites, deoxynivalenol (DON) and fusatin are provided.

In chapter II a high-throughput fluorescence activated cell sorting (FACS) based mutant screen was developed and the regulation of DON production in *Fusarium graminearum* was analysed. DON is an economically very important mycotoxin, as it is the most common contaminant of wheat, barley and corn worldwide. It is produced by plant pathogenic filamentous fungi of the *Fusarium* family, which can cause *Fusarium* head blight as well as *Fusarium* crown rot. During plant infection, DON is an important virulence factor and it can be toxic for humans and animals. The regulation of DON production is not yet fully understood. To identify regulators, a mutant screen was developed using FACS to allow high throughput screening, coupled with whole genome sequencing to identify mutations. Segregation analyses were performed to determine the mutation causing the phenotype. The mutant screen identified an adenylyl cyclase allele, which resulted in production of DON under normally repressive conditions. In addition, the mutant developed cellular structures associated with toxin production under repressive conditions. The levels of the fundamental second messenger cAMP, which adenylyl cyclases produce, were increased in the identified mutant, suggesting it might be a gain-of-function adenylyl cyclase mutant. This mutant screening methodology can be adapted to identify regulators of different secondary metabolites as well as to identify mutants overproducing yet unknown secondary metabolites.

In chapter III the cell biology of DON production in *Fusarium graminearum* was elucidated with quantitative super resolution microscopy. During the last five years the first insights into the cell biology of DON production were gained, indicating complex cell biological mechanisms. During toxin production, *F. graminearum* develops endoplasmic reticulum proliferations, called toxisomes, at which two DON biosynthesis enzymes, TRI1 and TRI4, are localized. However, TRI5 which catalyses the first DON biosynthesis step is localized in the cytosol. Thus, the question arose, how DON biosynthesis is coordinated between the cytosol and toxisomes. The subcellular localization of TRI5-GFP was analysed with structured illumination super resolution microscopy. This indicated a potential accumulation of the cytosolic TRI5 around the toxisomes. Accordingly, a quantification system was developed which confirmed a significant enrichment of TRI5-GFP around the toxisomes in comparison to the general cytosol. It is not understood yet, how the cytosolic TRI5 could be recruited to the toxisomes, but it could be part of a potential DON biosynthesis multi-enzyme complex at the toxisomes.

In chapter IV the regulation of fusatin production was analysed in *Fusarium pseudograminearum*. *F. pseudograminearum* is another member of the *Fusarium* family and causes *Fusarium* crown rot of wheat and barley. Recently it was shown that *F. pseudograminearum* is able to produce cytokinins. Here, the regulation of cytokinin production was analysed *in vitro* and *in planta*. This revealed that cytokinin production in *F. pseudograminearum* can be induced by specific nitrogen sources similar to DON production in *F. graminearum*. DON and cytokinin quantifications showed that their production seems to be partially co-regulated. Fluorescence microscopy revealed that cytokinin production is induced during wheat seedling infection in hyphae in close association with the plant, indicating a potential role of cytokinin production during plant infection.

In summary, this thesis presents a novel tool for high throughput mutant screens, as well as novel insights into the regulation and cell biology of DON and fusatin production in *F. graminearum* and *F. pseudograminearum*. Using these two secondary metabolites as examples, the results presented here show how complex the regulation of the production of these compounds can be and that it often also involves complex developmental and cell biological programs.

Declaration by author

This thesis is composed of my original work, and contains no material previously published or written by another person except where due reference has been made in the text. I have clearly stated the contribution by others to jointly-authored works that I have included in my thesis.

I have clearly stated the contribution of others to my thesis as a whole, including statistical assistance, survey design, data analysis, significant technical procedures, professional editorial advice, and any other original research work used or reported in my thesis. The content of my thesis is the result of work I have carried out since the commencement of my research higher degree candidature and does not include a substantial part of work that has been submitted to qualify for the award of any other degree or diploma in any university or other tertiary institution. I have clearly stated which parts of my thesis, if any, have been submitted to qualify for another award.

I acknowledge that an electronic copy of my thesis must be lodged with the University Library and, subject to the policy and procedures of The University of Queensland, the thesis be made available for research and study in accordance with the Copyright Act 1968 unless a period of embargo has been approved by the Dean of the Graduate School.

I acknowledge that copyright of all material contained in my thesis resides with the copyright holder(s) of that material. Where appropriate I have obtained copyright permission from the copyright holder to reproduce material in this thesis.

Publication during candidature

Peer-reviewed paper

Blum, A., Benfield, A. H., Stiller, J., Kazan, K., Batley, J., Gardiner, D. M., 2016. High-throughput FACS-based mutant screen identifies a gain-of-function allele of the Fusarium graminearum adenylyl cyclase causing deoxynivalenol over-production. Fungal Genet. Biol. 90, 1–11.

Publication included in this thesis

Blum, A., Benfield, A. H., Stiller, J., Kazan, K., Batley, J., Gardiner, D. M., 2016. High-throughput FACS-based mutant screen identifies a gain-of-function allele of the Fusarium graminearum adenylyl cyclase causing deoxynivalenol over-production. Fungal Genet. Biol. 90, 1–11.Incorporated as Chapter II.

Contributor	Statement of contribution
Ailisa Blum	Designed experiments (70%) Wrote the paper (90%)
Aurélie H. Benfield	Created the *TRI5-GFP* reporter strain (100%)
Jiri Stiller	Wrote the customised perl script used to filter SNPs for high confidence SNPs (100%)
Kemal Kazan	Edited the paper (20%)
Jacqueline Batley	Edited the paper (20%)
Donald M. Gardiner	Designed experiments (30%) Wrote the paper (10%) Edited the paper (60%) Created the DNA construct for the *TRI5-GFP* reporter strain (100%)

Contributions by others to the thesis

The initial project idea, whose results are presented in chapter III was developed by Prof H. Corby Kistler and Marike J. Boenisch. The *F. graminearum TRI5-GFP/TRI4-RFP*, *HMS1-GFP/TRI4-RFP* and *TRI5-GFP/HMS1-RFP* strains used in chapter III were created by John Menke, Karen L. Broz and Marike J. Boenisch.

Statement of parts of the thesis submitted to qualify for the award of another degree

None.

Acknowledgements

I want to thank the University of Queensland for enabling me to do my PhD thanks to their research scholarship.

Further, I want to thank the Grains & Research Development Corporation for supporting my PhD with a GRDC top up scholarship and for funding the project, which I have been working on (GRS10658, CSP00154).

I also want to thank A/Prof Jacqueline Batley and Dr Donald Gardiner for their excellent supervision during my PhD.

I want to thank CSIRO Agriculture and Food and Dr Donald Gardiner for the opportunity to do my PhD with them and for funding my lab expenses.

I want to thank the University of Queensland Graduate School International Travel Award and the School of Agriculture and Food Sciences Travel Award for enabling me to do a secondment in Prof Corby Kistler's lab in the USA. All the results presented in chapter III were produced during this secondment.

I also want to thank Prof Corby Kistler for inviting me to do the secondment in his lab and for funding all lab and operating expenses during that time. I also want to thank him for this great opportunity to work on this exciting project. In addition, I want to thank Dr Marike Boenisch for the excellent supervision and support during my secondment in the USA.

My acknowledgements also go to Virginia Nink from the Queensland Brain Institute for performing the Fluorescence Activated Cell Sorting in Chapter I.

I want to thank the whole QBP CSIRO Agriculture and Food team for all their support and for welcoming me in their team.

Finally, I want to thank my family, my partner and my friends for their great support.

Keywords

toxin production, fluorescence activated cell sorting (facs), camp, super resolution structured illumination microscopy (sim), organized smooth endoplasmic reticulum (oser), toxisomes, cytokinin, fusatin, fungal plant pathogen, secondary metabolism

Australian and New Zealand Standard Research Classifications (ANZSRC)

ANZSRC code 060199: Biochemistry and Cell Biology not elsewhere classified, 50%

ANZSRC code 060505: Mycology, 40%

ANZSCR code 060408: Genomics, 10%

Fields of Research (FoR) Classification

FoR code: 0601, Biochemistry and Cell Biology, 50%

FoR code: 0604, Genetics, 10%

FoR code: 0605, Microbiology, 40%

Table of contents

Figure and table index

Figure index

Table index

Abbreviations

A	adenine
AA	amino acid
Arg	arginine
ATP	adenosine triphosphate
bp	base pairs
C	cytosine
cAMP	cyclic 3’,5’-adenosine monophosphate
DON	deoxynivalenol
dpi	days past inoculation
EMS	ethyl methanesulfonate
ER	endoplasmic reticulum
F	phenylalanine
FAC1	*Fusarium graminearum* adenylyl cyclase
FACS	Fluorescence Activated Cell Sorting
FCK1	*Fusarium pseudograminearum* cytokinin biosynthesis enzyme
FRET	Fluorescence Resonance Energy Tranfer
HMR1	3-hydroxy-3- methylglutaryl -CoA-reductase
HMS1	3-hydroxy-3- methylglutaryl CoA synthase
HPLC	high-performance liquid chromatography
L, Leu	leucine
G	guanine
GFP	green fluorescent protein
Gly	glycine
Gln	glutamine
GPCR	G-protein coupled receptor
MAPK	mitogen activated protein kinase
MAPKK	mitogen activated protein kinase kinase
MAPKKK	mitogen activated protein kinase kinase kinase
MM	minimal media
PCR	polymerase chain reaction
Phe	phenylalanine

Δ*pks12*	knockout mutant of the polyketide synthase *PKS12* that catalyses the condensation of one acetyl-CoA and six malonyl-CoA to form the red pigment nor-rubrofusarin
P, Pro	proline
S, Ser	serine
R	arginine
REMI	restriction enzyme-mediated integration
RFP	red fluorescent protein
SIM	Structured Illumination Microscopy
SNP	single nucleotide polymorphism
T	thymine
Trp	tryptophan
TRI1	cytochrome P450 monooxygenase involved in trichothecene biosynthesis
TRI4	cytochrome P450 monooxygenase involved in trichothecene biosynthesis
TRI5	trichodiene synthase, first essential enzyme in DON biosynthesis
WT	wild type

1 Literature Review

1.1 *Fusarium*: an uncontrolled major threat for agriculture

Fusarium head blight (FHB) and *Fusarium* crown rot (FCR) impose a major threat to international agriculture with annual losses of AUD$100 million in Australia (Murray and Brennan, 2010, 2009) and up to US$2.7 billion losses during the head blight epidemic in the US in 1998-2000 (McMullen et al., 1997; Nganje et al., 2002). FHB is considered one of the most serious diseases of wheat crops throughout the world (Gilbert and Haber, 2013). The most common cause of FHB throughout Europe, America and Asia is the fungal pathogen *Fusarium graminearum* (Dublin et al., 1997; McMullen et al. 1997; O'Donnell et al. 2004). FCR can be caused by different *Fusarium* species (Smiley et al., 2009), but *F. pseudograminearum* is the most common cause of FCR in Australia and a major cause in Africa, North America and Asia (Bentley et al., 2006; Burgess et al., 2001; Smiley and Patterson, 1996; van Wyk et al., 1987). Exacerbating the problem is the fact that Fusaria produce a range of mycotoxins, such as fusarins, zearalenone and the trichothecenes nivalenol and deoxynivalenol (DON) during plant infection (Desjardins, 2006). The trichothecene mycotoxins inhibit protein biosynthesis and thus are toxic for plants, as well as for humans and animals that consume grain from infected plants (Desjardins et al., 2003). Therefore many countries, including the whole of Europe and the USA, apply regulatory limits to DON levels in food supplies.

To date there is no single effective control strategy for FHB (Gilbert and Haber, 2013). Therefore, combinations of different strategies have to be applied. Though FHB disease outbreaks cannot be prevented, lower disease severity, lower DON contaminations and higher yields can be achieved with a combination of intensive tillage, the most resistant cultivars, avoiding consecutive wheat or maize rotations and the application of azole fungicides at the right timing (Beyer et al., 2006; McMullen et al., 2008). Growers have to avoid using fields in which wheat had been planted the previous two years, because these contain increased *F. graminearum* inoculum levels (Guo et al., 2010), as the fungus survives the winter on the crop residues left in the fields. To better preserve the soil, reduce water usage, soil erosion, fuel usage and labour, farmers are moving away from intensive tillage to reduced tillage or conservation tillage since 1997 (Conservation Technology Information Centre, 1989-2004). However, reduced tillage and conservation tillage leave more crop residue on the soil surface of the fields and thus result in higher *F. graminearum* inoculum

levels in the fields than intensive tillage (Guo et al., 2010). Another limitation of current control strategies is that only a few partially resistant lines are known and these have poor agronomic and quality traits (Comeau et al., 2011). Fungicides are expensive, have negative effects on the environment and often show inconsistent results in field trials (Heier et al., 2005; Hollingsworth et al., 2006). Non-pathogenic bacteria, fungi and yeasts are being investigated as biocontrol agents against FHB. However, so far they can only be used in combination with fungicides to reduce the amounts of fungicides used, but not replace them (Palazzini et al., 2007; Xue et al., 2009; Zhang et al., 2007). Thus, it is important to understand how toxin production is regulated in *F. graminearum* in order to develop better control strategies and secure the production of mycotoxin-free food and feed.

1.2 *F. graminearum* infection mechanisms during head blight

During the infection of crop plants like wheat, *F. graminearum* switches between different lifestyles allowing specific developmental and metabolic adaptations, including the production of toxins, during specific infection stages which facilitates effective and successful plant infection and colonisation. Figure 1.1 (modified from Trail, 2009) illustrates the life and infection cycle that *F. graminearum* undergoes during the infection of wheat plants in a crop field. Infection is usually initiated by contaminated crop residues left in the fields after harvesting, on which the fungal inoculum can survive for up to two years (Summerell and Burgess, 1988). Macroconidia, vegetative fungal spores on the crop residues, can infect the new growing plants through rain splash dispersion. The fungus can also reproduce sexually through the development of perithecia that produce ascospores. These are forcibly discharged, resulting in airborne spores that spread the infection across the whole plant including the flowers, where they cause head blight. Flower infection is first initiated through invasion of the anthers by degeneration of tissue or through natural openings (reviewed in Bushnell et al. 2003).

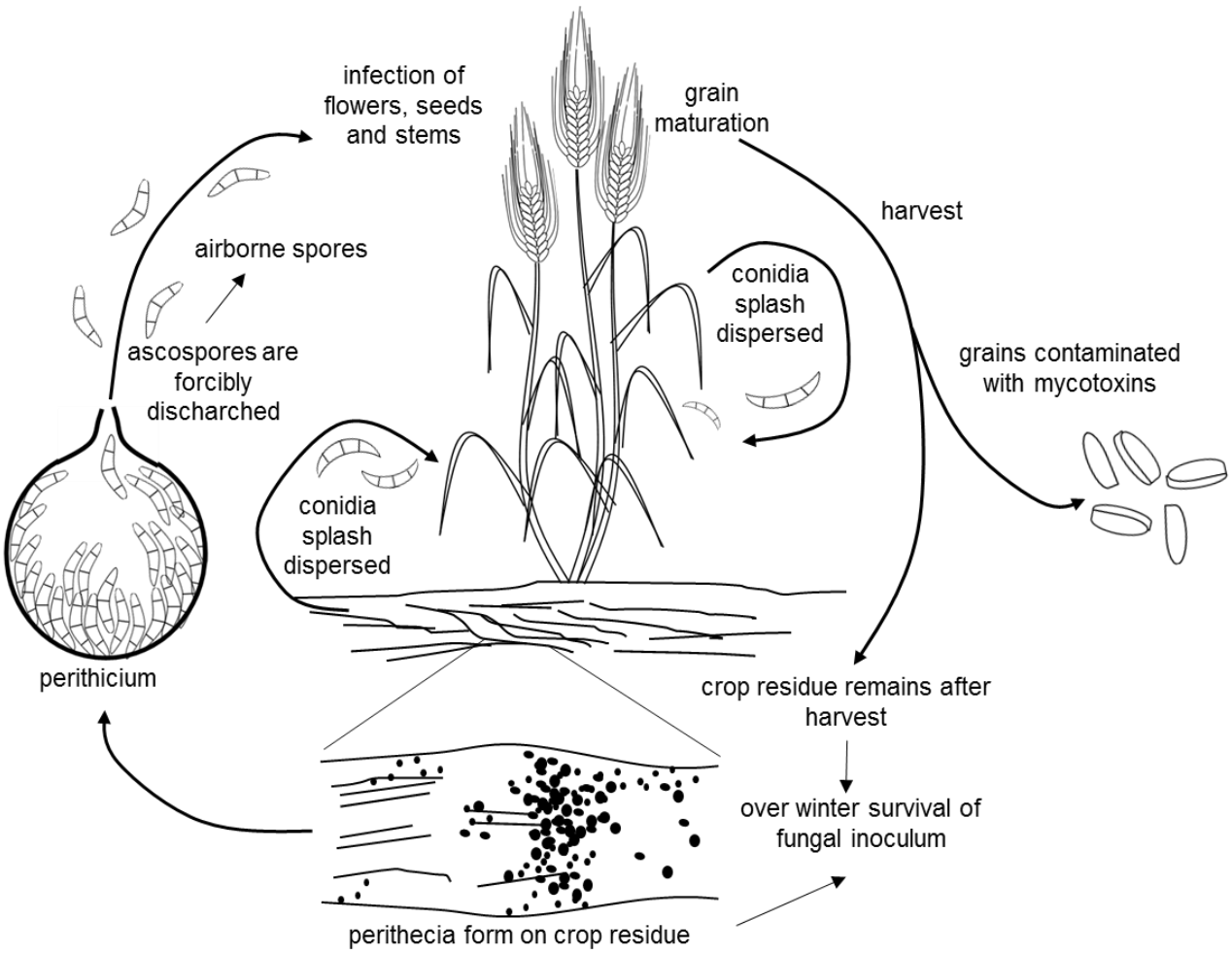

Figure 1.1. Life and infection cycle of *F. graminearum* on wheat (modified from Trail, 2009).

Many reports describe an initial biotrophic phase, during which the fungal hyphae grow only in the apoplast without penetrating the host plant cells (Brown et al., 2010; Bushnell et al., 2003; Guenther and Trail, 2005; Jansen et al., 2005; Rittenour and Harris, 2010; Trail, 2009). However, Jansen et al. (2005) could not identify any initial biotrophic phase, because even during initial infection stages host cells were penetrated and cell death was induced. Brown et al. (2010) also described that during early infection stages the hyphae in the infection centre already resembled a necrotrophic lifestyle, whereas the hyphae at the infection front still appeared to grow biotrophically in the apoplast. Nevertheless, supporting an initial biotrophic lifestyle is the fact, that the fungus produces only minimal amounts of toxins during the early infection stage (Gardiner et al., 2010).

Detailed microscopic analysis of infected floret organs described three infection stages (Boenisch and Schäfer, 2011). During the first stage runner hyphae colonize the plant surface, forming a homogenous hyphal network. Short infection hyphae penetrate epidermal

cells, but DON production is not induced yet and no necrosis can be observed. In the second stage, the hyphae start to branch extensively and foot structures, lobate appressoria and infection cushions are developed and necrotic lesions start to form in the plant tissue. During this second stage, DON production is induced in infection hyphae, lobate appressoria and infection cushions. However, DON production is not required for the development of these structures and necrotic cells could also be found underneath these infection structures in a mutant unable to produce DON (Boenisch and Schäfer, 2011). As the infection progresses, necrotic lesions spread further throughout the plant tissue and aerial hyphae, as well as spores, are developed. DON production is not induced in this third and final infection stage. DON production is not only induced in specific hyphae, but also by specific plant tissue. During floret infection DON biosynthesis is induced during the infection of the developing kernel and later especially once the fungus reaches the wheat rachis (Jansen et al., 2005). Indeed, DON production is required for the fungus to overcome the rachis barrier and spread from the initially infected floret (Jansen et al., 2005; Maier et al., 2006). Once the infection spreads across the wheat heads, the fungus also colonizes the seeds, resulting in the contamination of the grains with DON and yield losses.

Post-harvest the plant stubble is left in the field to conserve the soil and reduce water loss. However, stubble of infected plants might carry perithecia or macroconidia that can survive the winter. In the next season the whole infection cycle starts again. In addition, not only wheat plants are infected by *F. graminearum*, but also barley and maize can be colonized by the fungus, causing head blight and cob or ear rot respectively.

1.3 *F. pseudograminearum* infection mechanisms during crown rot

During FCR, the emerging shoot, crown and stem base are infected by soil borne spores from contaminated stubble or plant residue (Burgess et al., 2001). During *F. pseudograminearum* infection of wheat seedlings, hyphae spread across the coleoptile edge onto the leaf sheath, but hyphae can also penetrate the coleoptile spreading to the inner surface of the coleoptile from which they can directly penetrate the leaf sheath epidermis (Knight and Sutherland, 2013). In contrast, FHB is initiated through the infection of flowers where anthers are penetrated through natural openings or the degeneration of tissue (Burgess et al., 2001). Thus, the fungus needs to move down the stem after flower infection during FHB, in order to overwinter on the stubble (Summerell and Burgess, 1988), whereas the fungus spreads up the stem during FCR.

During FCR, leaf sheaths are mainly penetrated through stomata (Knight and Sutherland, 2013). Within the leaf sheath, hyphae grow inter- and intracellularly and cells are penetrated by either swollen hyphae or by septate foot-shaped appressoria (Knight and Sutherland, 2013). Hyphae re-emerge from stomata and spread across and infect younger leaf sheaths underneath (Knight and Sutherland, 2013). After the initial infection, *F. pseudograminearum* then grows in the pith parenchyma to colonise the stem (Mudge et al., 2006). Both *F. graminearum* and *F. pseudograminearum* produce DON during wheat stem base infection, however similar to wheat head infection, DON is not required for the initial infection, but rather for the spread of the fungus through the stem (Bai et al., 2002; Jansen et al., 2005; Mudge et al., 2006; Powell et al., 2017). As the infection progresses, necrosis of the crown and stem base develop and under drought conditions 'whiteheads' can develop, as the heads die prematurely, due to impeded water transport caused by the necrosis in the crown and stem (Burgess et al., 2001). In contrast to 'whiteheads', blighted heads during FHB are directly infected by the fungus (reviewed in Bushnell et al. 2003). In addition, *F. graminearum* and *F. pseudograminearum* can also infect wheat heads causing FHB after stem base infection of young seedlings (Mudge et al., 2006).

1.4 The *Fusarium* family, their toxins and other secondary metabolites

F. graminearum belongs to the *Fusarium* genus of filamentous fungi in the *Ascomycota* phylum. The *Fusarium* genus includes more than one hundred species, e.g. *F. avenaceum*, *F. crookwellense*, *F. culmorum*, *F. equiseti*, *F. langsethiae*, *F. oxysporum*, *F. poae*, *F. pseudograminearum*, *F. sambucinum*, *F. sporotrichioides*, *F. tricinctum* and *F. verticillioides* (O'Donnell et al., 2013). Most of the afore mentioned *Fusarium* species are plant pathogens and many infect plants of economic importance such as wheat, barley, maize, rice, oats, coffee, banana, legumes and potatoes (Booth, 1971; De Nijs et al., 1996). Some species can cause opportunistic infections in humans, for example on nails, however, critical infections only occur in immune-deficient humans, caused by species like *F. oxysporum* or *F. verticillioides* (Howard, 2002).

Of the above mentioned species *F. crookwellense*, *F. culmorum*, *F. equiseti*, *F. poae*, *F. pseudograminearum*, *F. sambucinum* and *F. sporotrichioides* can produce trichothecenes, like *F. graminearum* (De Nijs et al., 1996). Each *Fusarium* species can usually produce more than one of the occurring trichothecenes, like DON, nivalenol, T-2 toxin, calonectrin, neosolaniol, scirpenetriol, sporotrichiol, isotrichodermin and

trichothecolone and most of these trichothecenes also occur in different derivates. In addition to trichothecene toxins, *Fusarium* species can also produce two other major classes of mycotoxins, fumonisins and zearalenones, as well as further minor toxins like beauvericin, fusaproliferin, fusarins and moniliformin (Desjardins, 2006). Despite this great variety of *Fusarium* species and the great variety of toxins produced by them, *F. graminearum* producing trichothecenes like DON is the most common cause of wheat and barley head blight epidemics and human and animal toxicoses due to ingestion of contaminated grains (O'Donnell et al., 2004). However, *F. culmorum*, *F. poae*, *F. pseudograminearum*, and *F. avenaceum* may also be associated with FHB, kernel blight and related diseases throughout the world (Trail, 2009).

Apart from toxins, Fusaria can produce a wide range of other secondary metabolites. Sieber et al. (2014) predicted 67 secondary metabolite gene clusters in *F. graminearum*, of which the function of only 12 is known. In addition, there are 114 predicted cytochrome P450 monooxygenase enzymes in the *F. graminearum* genome and as these enzymes are known to be involved in many known biosynthesis pathways, there might be even more yet unknown secondary metabolite gene clusters (Sieber et al., 2014). Many of the secondary metabolite biosynthesis gene clusters are shared amongst the different Fusarium species, though some are also exclusive to certain species. E.g. out of the 67 predicted secondary metabolite gene clusters in *F. graminearum*, 57 orthologs can be found in the closely related *F. pseudograminearum*. However, a recently described novel secondary metabolite gene cluster for the biosynthesis of the cytokinin fusatin in *F. pseudograminearum* does not exist in *F. graminearum*, but is present in *F. oxysporum*, *F. fujikuroi* and *F. verticillioides*. As examples, the biosynthesis of fusatin and DON will be explained in more detail below.

1.5 Cytokinin biosynthesis in *F. pseudograminearum*

Fusatin is a novel cytokinin-like compound, which has been discovered recently by Sørensen et al. (2017). *F. pseudograminearum* produces the cytokinins fusatin, fusatinic acid, 8-oxo-fusatin, cis-zeatin and trans-zeatin via two different biosynthesis pathways. In the tRNA pathway cis-zeatin is produced via the degradation of prenylated-adenine moieties. Fusatin, fusatinic acid and trans-zeatin are synthesized by FCK1 and FCK2, which are encoded in a small cytokinin gene cluster consisting of *FCK1-4*. FCK1 contains two catalytic domains, one is homologous to the catalytic domain of the *Arabidopsis* gene lonely

guy LOG1 and the other is an isopentyl-transferase. In plants these activities are encoded in separate proteins (Kakimoto, 2001; Kurakawa et al., 2007; Takei et al., 2001).

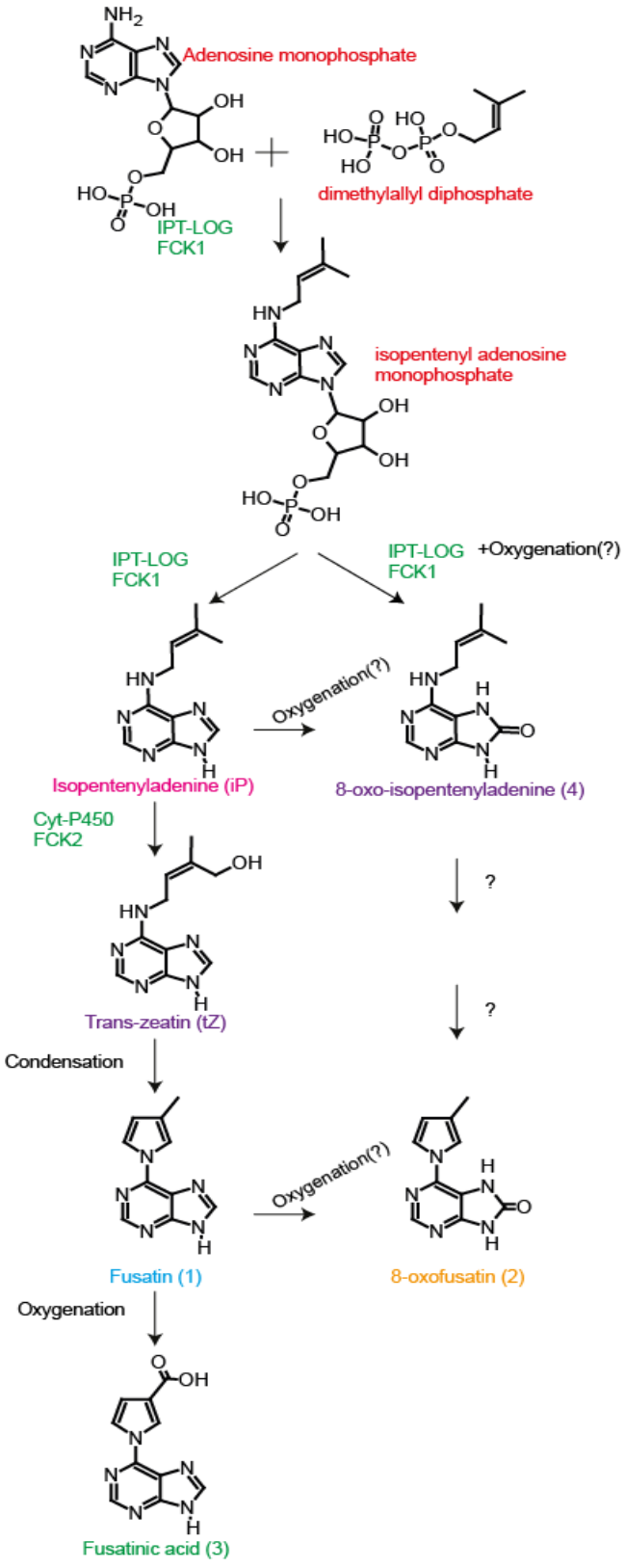

Figure 1.2. Fusatin biosynthetic pathway.

In *F. pseudograminearum* FCK1 prenylates adenosine monophosphate and dimethylallyl diphosphate to form isopentenyl adenosine monophosphate (Figure 1.2). The second active site of FCK1 then removes the phosphoribose to form isopentenyladenine or 8-oxo-isopentenyladenine. 8-oxo-isopentenyl-adenine is then converted to 8-oxo-fusatin by yet unknown mechanisms. Isopentenyladenine is converted to trans-zeatin by the cyotchrome P450 monooxygenase FCK2. Through condensation trans-zeatin can then be converted to fusatin, which in turn can be converted to either fusatinic acid or 8-oxo fusatin by oxygenation by yet unknown mechanisms.

The function of the other members of the cytokinin gene cluster, FCK3 and FCK4, is still unknown, but their knockouts each resulted in increased production of cytokinins and thus they could be involved in the downstream production of yet unknown compounds. FCK3 contains a putative glycosyl transferase domain and FCK4 a putative alcohol acetyltransferase domain.

The function of the *Fusarium* cytokinins is still unknown, but the expression of *FCK1*, *FCK2* and *FCK3* is highly induced in *F. pseudograminearum* during barley and *Brachypodium* infection and the *Fusarium* cytokinins accumulate in infected wheat heads in concentration levels similar to those of physiologically active plant cytokinins (Sørensen et al., 2017). In addition, *Fusarium* cytokinins can activate cytokinin signalling of an *Arabidopsis* cytokinin receptor *in vitro* and fusatinic acid activates cytokinin signalling in *Brachypodium* (Sørensen et al., 2017). The potential function of the *Fusarium* cytokinins and the regulation of the cytokinin gene cluster will be further analysed here in Chapter IV.

1.6 DON biosynthesis in *F. graminearum*

The biosynthesis pathway of DON in *Fusarium* has been intensively researched and, as such, is known in great detail (reviewed in Desjardins 2006). Figure 1.3 (modified from Alexander et al. 2009) illustrates the chemical reactions and the respective catalizing enzymes in the DON, nivalenol or T-2 toxin biosynthesis.

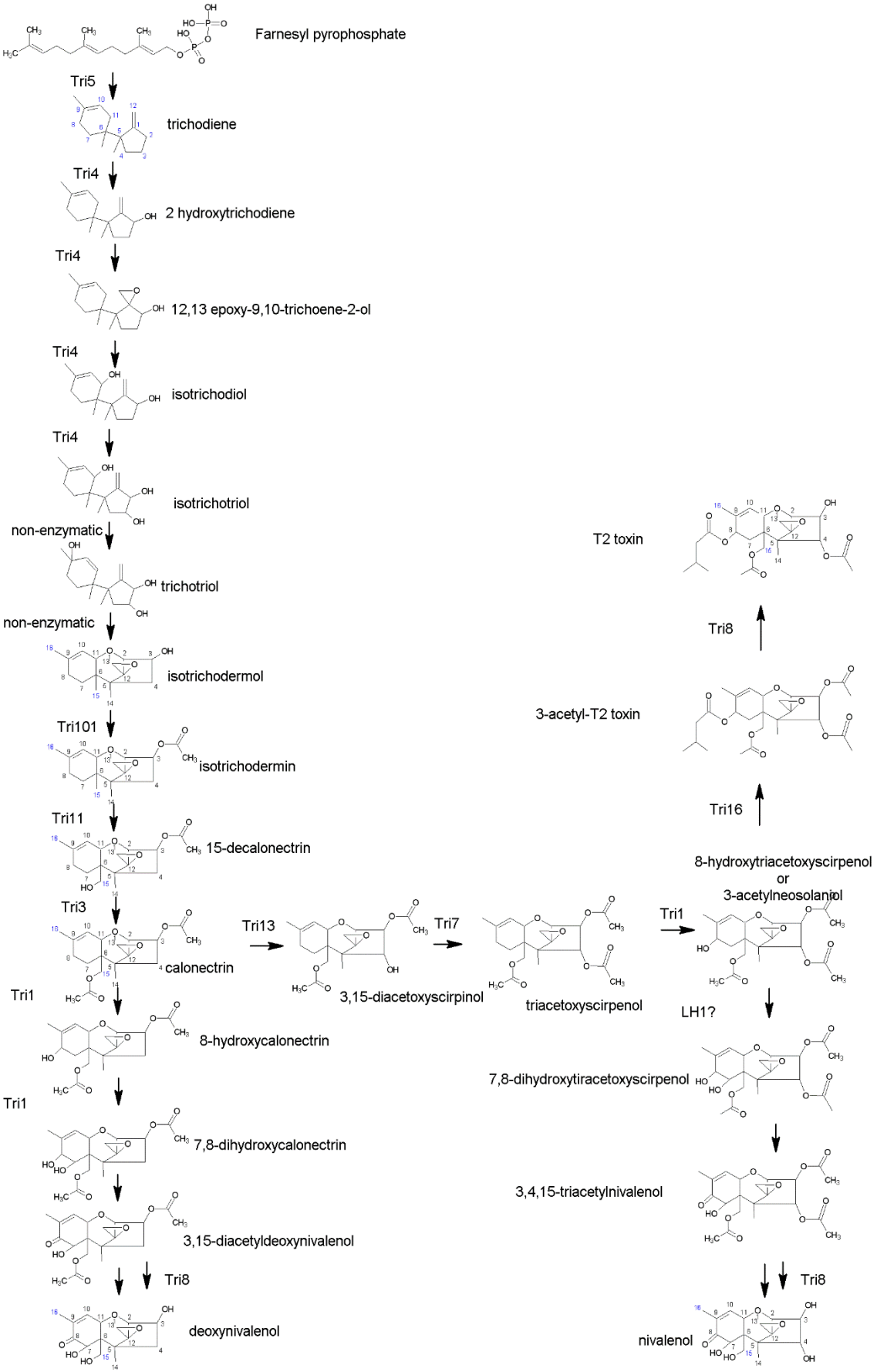

Figure 1.3. *Fusarium* T-2 toxin, DON and nivalenol biosynthesis pathways including the respective catalysing enzymes (modified from Alexander et al., 2009).

The first essential enzyme in the DON biosynthesis pathway in *Fusarium* spp. is the trichodiene synthase TRI5 (Hohn & VanMiddlesworth 1986). It catalyses the sesquiterpene cyclisation of the 15 carbon farnesyl pyrophosphate to trichodiene (Hohn and Beremand, 1989). Following the trichodiene formation are a number of oxygenations and additions and removals of ester groups catalysed by four cytochrome P450 monooxygenases, TRI4, TRI11, TRI13 and TRI1 and four acetyltransferases TRI3, TRI101, TRI7 and TRI16, and the esterase TRI8 (shown in Figure 1.3 (modified from Alexander et al. 2009) and reviewed in Desjardins 2006). Although different *Fusarium* species produce different trichothecenes, most cyclizations and oxygenations in the trichothecene biosynthesis are shared between *F. culmorum*, *F. graminearum*, *F. sambucinum* and *F. sporotrichioides*. However, the synthesis pathways become specific for the respective toxin after the 11th step, the synthesis of calonectrin, resulting in the formation of nivalenol/DON by *F. culmorum*/*F. graminearum* or of T-2 toxin by *F. sambucinum*/*F. sporotrichioides* (Desjardins, 2006).

The genes encoding the afore mentioned trichothecene biosynthesis enzymes are highly conserved across different *Fusarium* species and are all organised at three genomic locations in the *TRI1-TRI16* two gene cluster on chromosome 1, the 12 gene core *TRI5* cluster on chromosome two and *TRI101* at a single gene locus (reviewed in Alexander et al. 2009). The arrangement of the different genes is shown in Figure 1.4 (modified from Alexander et al. 2009). Within the *TRI5* gene cluster are also the *TRI9* and *TRI14* genes, whose function is not yet known (Brown et al., 2002, 2001; Dyer et al., 2005).

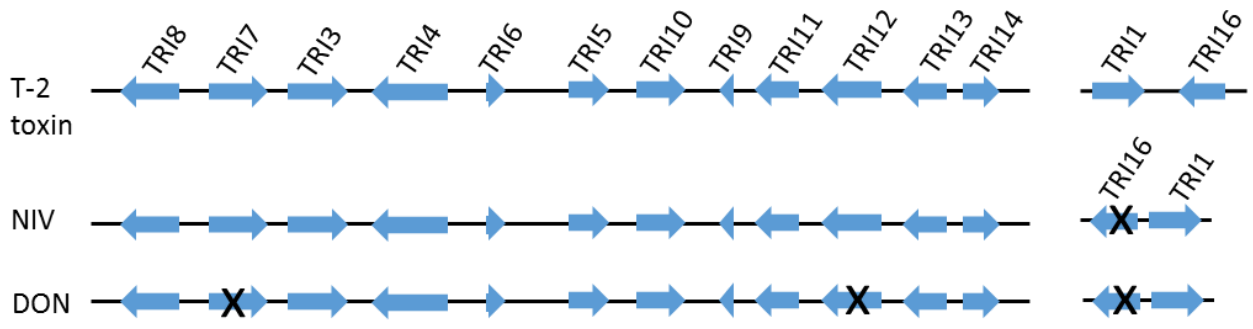

Figure 1.4. *Fusarium* trichothecene biosynthesis enzyme gene clusters: *TRI5* 12 gene cluster and *TRI1-TRI16* two gene cluster (modified from Alexander et al., 2009). The x indicates genes lost in the respective clusters.

The expression of the above mentioned DON synthesis enzymes, as well as the isoprenoid biosynthetic gene for farnesyl pyrophosphate synthetase, is regulated by the transcription

factors TRI6 and TRI10 (Hohn et al., 1999; Peplow et al., 2003; Proctor et al., 1995b; Seong et al., 2009). In addition, a transcription factor with negative regulatory activity, TRI15, was identified, which is encoded on chromosome three, unlike the *TRI5* gene cluster, which is on chromosome two (Alexander et al., 2004). *TRI15* is believed to encode a negative regulatory transcription factor, because it is similar to known zinc finger transcription factors, but it is not essential for toxin production and it is up regulated, when the activating transcription factors TRI6 and TRI10 and DON synthesis enzymes, like TRI5, are down regulated (Alexander et al., 2004). A further member of the *TRI5* gene cluster is *TRI12*, which encodes a potential trichothecene efflux pump with 14 predicted transmembrane spanning regions (Alexander et al., 1999; Wuchiyama et al., 2000). TRI12 is required for auto-tolerance of *F. graminearum* to growth inhibition under toxin production inducing conditions (Menke et al., 2012).

1.7 DON inhibits cytosolic as well as mitochondrial protein biosynthesis

The trichothecene DON can be considered as a host-non-specific effector as it affects plant cells as well as mammalian cells (Kazan et al., 2012). It inhibits protein biosynthesis *in vitro* in mammals and induces programmed cell death and strong immune responses in both plants and mammals (Desmond et al., 2008; Nishiuchi et al., 2006; Pestka, 2010). These effects are mediated by interaction of DON with the ribosome and phosphorylation of ribosome associated mitogen-associated protein kinases (MAPK), which trigger immune responses including programmed cell death (Bae et al., 2010; Bae and Pestka, 2008; Zhou, 2003). However, the afore mentioned inhibition of cytosolic translation may not be the main cause of DON toxicity as recent studies in yeast showed that DON directly inhibits mitochondrial translation and that yeast cells lacking normal functioning mitochondria were resistant to otherwise lethal doses of DON (Bin-Umer et al., 2011, 2014; McLaughlin et al., 2009).

1.8 Trichothecene production is complexly regulated by several abiotic factors and many genes in *F. graminearum*

During infection, the fungus is not constitutively producing DON, but rather only in the second stage of infection, after initial colonization of the host (Boenisch and Schäfer, 2011). Accordingly, toxin production needs to be tightly regulated to coincide with the successful

development of the appropriate cellular structures and the right infection stage. The fungus does not produce DON under standard *in vitro* growth conditions either, but only in specific toxin production inducing media (Miller et al., 1983; Miller and Blackwell, 1996; Miller and Greenhalgh, 1985). In these media specific carbon sources, amino acid nitrogen sources and yet unknown components of yeast extract are required for the induction of DON production. However, the actual direct inducing agent in those media has not been identified. Therefore, it is essential to understand which signals activate toxin production and how the signalling pathway is regulated. The following Table 1.1 (modified from Kazan et al. 2012) lists all reported inducers and repressors of trichothecene biosynthesis in *F. graminearum.*

Table 1.1. Summary of inducers and repressors of trichothecene production in *F. graminearum* (modified from Kazan et al. 2012).

Regulatory compound	Mode of action	Reference
Polyamines	Activate *TRI* gene expression and toxin biosynthesis	Gardiner *et al*. 2009a
Sugars (sucrose, 1-kestose and nystose)	Activate *TRI4* and *TRI5* expression and DON and 3ADON biosynthesis	Jiao *et al*. 2008
Reactive oxygen (e.g. H_2O_2)	Activates *TRI* gene expression and toxin biosynthesis	Audenaert *et al*. 2010; Ponts *et al*. 2006; 2007
Cinnamic-derived acids and phenolic acids	Ferulic acid and coumaric acid activates DON biosynthesis	Ponts *et al*. 2011
Cobalt chloride	Induces *TRI4* and *TRI6* expression and DON biosynthesis	Tsuyuki *et al*. 2011
Warm temperature (e.g. 25 °C)	Induces trichothecene production	Kokkonen *et al*. (2010)
pH	Low pH activates *TRI* gene expression and toxin biosynthesis	Gardiner *et al*. 2009b; Merhej *et al*. 2011
Magnesium ions	Repress *TRI5, TRI6* and *TRI12* expression and toxin biosynthesis	Pinson-Gadais *et al*. 2008
Salt (NaCl) in culture	Represses DON biosynthesis	Ochiai *et al*. (2007)
Precocenes and piperitone from the essential oils of *Matricaria recutita* and *Eucalyptus dives*	Represses *TRI4, TRI5, TRI6* and *TRI10* expression and DON biosynthesis	Yaguchi *et al*. 2009
Ferulic acid	Represses *TRI5* expression and DON biosynthesis	Boutigny *et al*. 2009

As DON production seems to be highly condition specific, it is likely that the fungus can perceive plant derived signals to determine the right timing of induction. Therefore, various plant defence molecules have been explored for their effects on trichothecene production in *Fusarium*. Reactive oxygen species like H_2O_2 activate DON production (Audenaert et al., 2010; Ponts et al., 2007, 2006). *Fusarium* induces H_2O_2 production in infected wheat plants (Desmond et al., 2008; Zhou et al., 2005) and reactive oxygen species are one of the first defence responses produced by plants (Kachroo et al., 2003; Repka, 1999). However, the levels of DON production and DON synthesis enzyme induction triggered by reactive oxygen species are not significant when compared to the amounts of DON produced during plant infection (Gardiner et al., 2009a). Further, another pro-oxidant compound, paraquat, represses trichothecene production (Ponts et al., 2006).

Several other potential positive regulators of trichothecene synthesis are known, including sucrose, cinnamic-derived acids and phenolic acids, like ferulic acid, cobalt chloride and warm temperatures of 25°C, which similar to ROS are also only weak inducers (Jiao et al., 2008; Kokkonen et al., 2010; Ponts et al., 2011; Tsuyuki et al., 2011). However, ferulic acid can also repress DON production (Boutigny et al., 2009). Further repressors of trichothecene production are, precocenes and piperitone from essential oils of *Matricia recutita*, magnesium ions and NaCl (Ochiai et al., 2007; Pinson-Gadais et al., 2008; Yaguchi et al., 2009).

The first described effective *in vitro* inducers of trichothecene production in *F. graminearum* are reduced nitrogen sources like arginine, agmatine or putrescine (Gardiner, et al. 2009a). These were the first substances which induced levels of DON production *in vitro* comparable to the levels produced by the fungus during plant infection (Gardiner, et al. 2009a). In addition, Gardiner et al. (2009a) also showed that in contrast to reduced nitrogen sources, oxidized nitrogen sources like sodium nitrate repress DON production. The afore mentioned activating reduced amines accumulate in plants during final infection stages coinciding with increased DON production by *F. graminearum* (Gardiner et al., 2010). Consistently, the biosynthesis of polyamines is increased in plants during the induction of defence responses (Haggag and Abd-El-Kareem, 2009; Walters, 2002). However, the exact mechanism of how reduced amines activate DON production is still not known. They do not serve as direct synthesis precursors, as the DON molecule does not contain any nitrogen, neither does nitrogen seem to be directly required for the synthesis. In addition, it takes up to 48h from the application of the reduced amines until the first detectable induction of DON biosynthesis

proteins both on mRNA and protein expression level (Gardiner, et al. 2009a). Thus, it still remains to be revealed how reduced amines are perceived as activating signals, which signalling cascade they trigger and what the final direct endogenous DON production activating signal is.

Gardiner et al. (2009b) reported that a reduction of pH during the consumption of the reduced amines by the fungus could contribute to the DON production inductive effects of amines, like arginine or putrescine. After 24h putrescine is completely consumed by the fungus and as the putrescine is consumed by the fungus the extracellular pH of the medium is lowered. Coinciding with lower pH values (pH 2-3) DON synthesis enzymes such as TRI5 are expressed and DON can be detected in the medium. Accordingly, acidic pH plays a regulatory role in toxin production. It not only induces, but is also required for DON production. Hence, pH seems to be able to override inducing or repressing effects of different nitrogen sources on DON production (Gardiner, et al. 2009b). However, the induction of DON production by amines is not only due to the decrease of the pH of the medium. This was shown in an experiment by Gardiner et al. (2009), in which the fungus produced more DON with agmatine as the sole nitrogen source than with glutamine at the same pH. Thus amines and pH synergistically induce DON production.

Fungi adapt to different pHs through a highly conserved regulatory transcription factor PacC whose activity represses low pH responsive genes during high pH conditions and the inactivation of PacC at low pHs allows the expression of low pH responsive genes (reviewed in Peñalva et al. 2008). In *F. graminearum*, the DON production inducing effects of low pH conditions seem to be mediated by the *PacC* homologue *FgPac1*, because a ∆*Fgpac1* knockout mutant induced DON production earlier under acidic conditions and a constitutively active *FgPac1*^{c} mutant repressed DON production (Merhej et al., 2011).

Another regulatory pathway that controls DON production is cyclic 3',5'-adenosine monophosphate (cAMP) signalling (Bormann et al., 2014; Park et al., 2012; Yu et al., 2008). cAMP was the first second messenger to be discovered and thus cAMP signalling has been extensively studied in mammals and yeast (Hanoune and Defer, 2001; Hoffman, 2005; Kronstad et al., 1998; Palecek et al., 2002). Extracellular signals are perceived via membrane associated receptors, which heterotrimeric G-proteins are attached to. Upon activation the G-proteins dissociate into an α-monomer and a β-γ dimer. The α-subunit can activate the adenylyl cyclase which converts ATP to cAMP and pyrophosphate. cAMP can

activate cAMP dependent protein kinases, which in turn can activate a large number of downstream effectors (Li et al., 2007).

G-proteins can also activate mitogen-activated protein kinase (MAPK) signalling cascades that involve the sequential phosphorylation of MAPK kinase kinase (MAPKKK), to MAPK kinase (MAPKK), to MAPK. Accordingly, many proteins, such as transcription factors and other regulatory proteins, can be phosphorylated and thus regulated by the activated terminal MAPK (Bardwell, 2005). The *F. graminearum* adenylyl cyclase FgAC1 is essential for DON production, as the Δ*Fgac1* knockout mutant was unable to produce DON (Bormann et al., 2014). However, it is not yet fully understood which role G proteins play in the regulation of DON production in *F. graminearum*. In contrast to the Δ*Fgac1* knockout, mutants of G-protein α and β subunits (GPA1 & GPB1), as well as knockout mutants of regulators of G protein signalling (FlbA & RgsA), exhibited increased DON production (Park et al., 2012; Yu et al., 2008). Different MAPK, such as MAP1, MGV1, Os2 and its corresponding MAPKK Os5 and MAPKKK Os4 have been identified, which are involved in the regulation of DON production, as the loss of those results in reduced DON production (Hou et al., 2002; Ochiai et al., 2007; Urban et al., 2003; Van Thuat et al., 2012).

A phenome-based functional analysis by Son et al. (2011) has identified a great number of transcription factors, which influence the production of DON. The transcription factor AreA, which is a global nitrogen regulator in filamentous fungi (Yin and Keller, 2011), is essential for DON production (Min et al., 2012). The velvet complex, which is conserved throughout various genera of filamentous fungi as a regulator of development and metabolism, is also a positive regulator of DON production in *F. graminearum* (Jiang et al., 2012, 2011a; Kim et al., 2013; Lee et al., 2012; Merhej et al., 2012). Chromatin modifications mediated by HDF1 and HEP1 also positively regulate DON production (Li et al., 2011; Reyes-Dominguez et al., 2012). Further proteins ranging from lyases, to lipases and phosphatases have also been reported as positive regulators and are summarized in Table 1.2.

Table 1.2. Summary of genes influencing DON production. Genes, whose knockout results in loss of DON production, indicating that they are essential, are in black. Potential positive regulators, whose knockout leads to reduced DON production are highlighted in green. Potential negative regulators, whose knockout results in increased or earlier DON production are indicated in red.

Gene – encoded protein	DON production in knockout mutant	Regulatory mechanism	Reference
AC1 – adenylyl cyclase	completely lost	signalling	(Bormann et al., 2014)
AreA – transcription factor	completely lost	transcription	(Min et al., 2012)
ACL1 & *ACL2* – ATP citrate lyase	reduced	metabolic flux alterations	(Son et al. 2011a)
HMR1 – HMG-CoA reductase	reduced (truncated mutant)	metabolic flux alterations	(Seong et al., 2006)
ERG4 – sterol C-24 reductase	reduced	metabolic flux alterations	(Liu et al., 2013)
AMT1 – protein arginine methyltransferase	reduced	pleiotropic effects	(Wang et al., 2012)
Atg15 - autophagy-like lipase	reduced	pleiotropic effects	(Nguyen et al., 2011)
Ptc3 – type 2C protein phosphatase	reduced	pleiotropic effects	(Jiang, et al. 2011b)
Rrg1 – putative response regulator, potentially upstream of Os2	reduced	pleiotropic effects	(Jiang, et al. 2011c)
Tri12 – major facilitator super family protein, potentially trichothecene exporter	reduced	pleiotropic effects	(Menke et al., 2012)
BDM1 - phosducin-like protein, involved in G-protein signalling	reduced	signalling	(Horevaj and Bluhm, 2012)
MAP1 – MAPK	reduced	signalling	(Urban et al. 2003)
MGV1 – MAPK	reduced	signalling	(Hou et al., 2002)

Os2 - MAPK, *Os4* - MAPKKK, *Os5* - MAPKK	reduced *in vitro*	signalling	(Ochiai et al., 2007)
Os2 – MAPK	reduced *in planta* increased *in vitro*	signalling	(Van Thuat et al., 2012)
StuA – transcription factor	reduced	transcription	(Lysøe et al., 2011)
ZIF1 – b-ZIP transcription factor	reduced	transcription	(Wang et al., 2011)
Fgp1 – Wor1 like protein	reduced	transcription	(Jonkers et al., 2012)
VeA – part of velvet complex	reduced	transcription	(Jiang et al., 2011a; Merhej et al., 2012)
VelB – part of velvet complex	reduced	transcription	(Jiang et al., 2012; Lee et al., 2012)
LaeA – nuclear global regulator, interacting with the velvet complex	reduced	transcription through chromatin modification	(Kim et al., 2013)
HEP1 – heterochromatin protein	reduced	transcription through chromatin modification	(Reyes-Dominguez et al., 2012)
HDF1 – histone deacetylase	reduced	transcription through chromatin modification	(Li et al., 2011)
CID1 – cyclin C-like gene	reduced	regulating activity of RNA ploymerase	(Zhou et al., 2010)
TOP1 – topoisomerase 1	reduced	relaxes super coiled DNA	(Baldwin et al., 2010)
FGL1 – secreted lipase	increased	pleiotropic effects	(Voigt et al., 2005, 2006)
FGSG_00007 – cytochrome P450 monooxygenase	increased	potentially metabolic flux	(Gardiner et al., 2009b)
FGSG_10397 – potential terpene cyclase	increased	potentially metabolic flux	(Gardiner et al., 2009b)
GPA1 & *GPB1* – G protein α & β subunit	increased	signalling	(Yu et al., 2008)
FlbA & *RgsA* - regulators of G protein signalling	increased	signalling	(Park et al., 2012)
PAC1 – pH regulatory factor	induced earlier	transcription	(Merhej et al., 2011)

In summary, there are a great number of abiotic factors and regulatory mechanisms which influence DON production (Figure 1.5). Most of these regulators not only influence the production of DON, but also developmental programs required for pathogenicity of *F. graminearum* and for vegetative or sexual production (reviewed in Geng et al. 2014). Accordingly, the production of DON in *F. graminearum* is very complexly regulated by a great range of proteins. However, a detailed understanding of the mechanisms of how these proteins mediate the regulatory effects on DON production and the structure and interplay of the signalling cascades and regulatory pathways is still lacking.

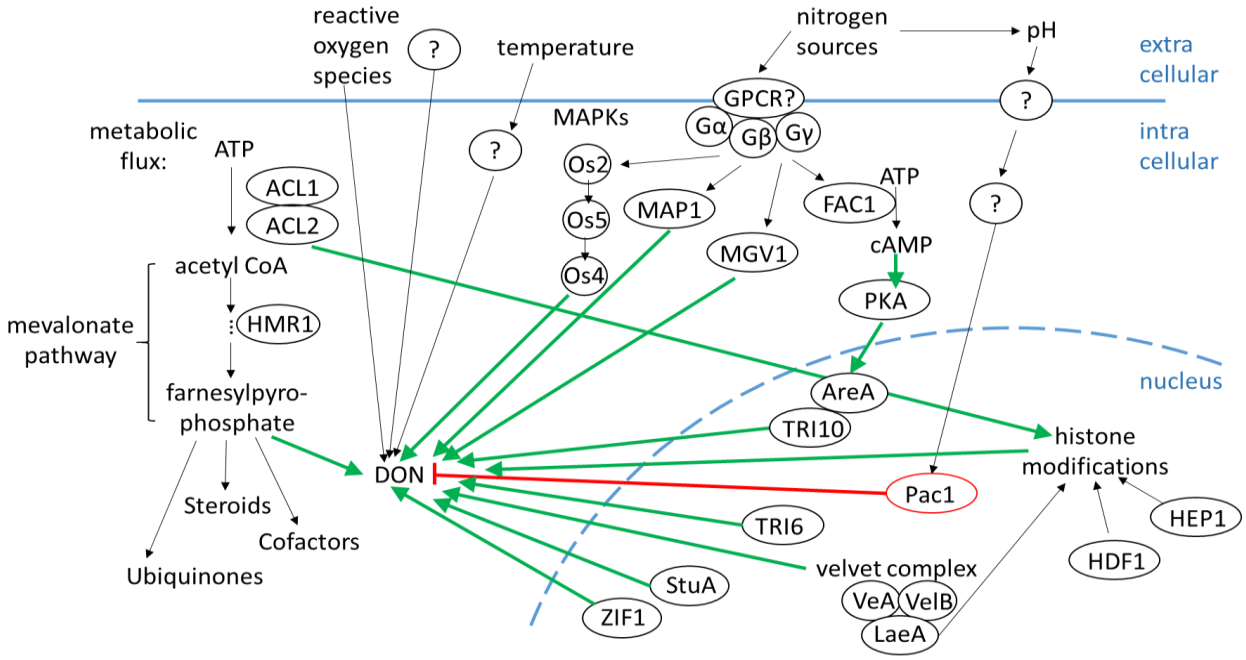

Figure 1.5. Hypothetical scheme of different regulatory mechanisms influencing DON production. DON production is complexly regulated through a number of abiotic factors, like for example reactive oxygen species, temperature, nitrogen sources, pH and potentially yet unknown factors. These extracellular factors regulate DON production through a number of different signalling pathways, like for example cAMP signalling and MAP kinase signalling. Most signalling pathways alter transcription through histone modifications or transcription factors. In addition, metabolic flux alterations also influence DON production, for example through availability of precursors required for DON production.

1.9 Objectives: Regulation and cell biology of secondary metabolites in *F. graminearum* and *F. pseudograminearum*

1.9.1 Development of a high throughput mutant screen to identify regulators of toxin production in *F. graminearum*

The characterization of many secondary metabolites (or gene clusters suspected of producing secondary metabolites) is hindered, because they cannot be produced *in vitro.* Therefore, the first objective of this thesis was to develop a high throughput mutant screen to identify mutants over-producing a desired secondary metabolite. Such a screen has applicability to both increasing amounts of the compounds e.g. for compound characterisation as well as the identification of key regulators of production of the compound.

1.9.2 How is DON production regulated in *F. graminearum?*

DON is an important virulence factor in the economically important crop diseases *Fusarium* head blight and *Fusarium* crown rot. The production of DON is differentially regulated during different infection stages as well as during the infection of different plant tissues. However, it is not yet fully understood how DON production is regulated in the fungus. Therefore, the second objective was to perform the above mentioned mutant screen with a DON production reporter strain to identify regulators of DON production.

1.9.3 How is DON production coordinated on a cellular level in *F. graminearum?*

Recent results by Boenisch et al. (2017) revealed that *F. graminearum* develops complex ER proliferations in DON producing cells, at which DON biosynthesis enzymes are localized. However, TRI5, which catalyses the first DON biosynthesis step, is localized in the cytosol and thus the question arises, how toxin production is coordinated between the ER and the cytosol. Therefore, the third objective was to analyse the localization of the cytosolic TRI5-GFP with structured illumination super resolution microscopy. As microscopic analyses usually only provide qualitative results, an additional objective was to develop a quantification system, which would allow statistical analyses of localization patterns of cytosolic proteins from microscopic images.

1.9.4 How is the *F. pseudograminearum* cytokinin-like compound fusatin regulated *in vitro* and where/when is it expressed during infection?

The function of the recently discovered novel *F. pseudograminearum* cytokinin fusatin is still unknown. Therefore, the first part of the fourth objective was to analyse the regulation of fusatin production by different nitrogen sources, as well as the influence of these different growth conditions on DON production. To further characterize fusatin production, the second part of this objective was to determine the subcellular localization of the fusatin biosynthesis enzyme FCK1. In addition, to get a better understanding of the potential function of *F. pseudograminearum* cytokinins during plant infection, the third part of this objective was to determine when and where fusatin is produced during wheat seedling infection.

2 High-throughput FACS-based mutant screen identifies a gain-of-function allele of the *Fusarium graminearum* adenylyl cyclase causing deoxynivalenol over-production

Ailisa Blum[a,b], Aurélie H. Benfield[a], Jiri Stiller[a], Kemal Kazan[a,d], Jacqueline Batley[b,c], Donald M. Gardiner[a]

[a] CSIRO Agriculture, Queensland Bioscience Precinct, 306 Carmody Road, St Lucia, Brisbane, Queensland 4067, Australia

[b] School of Agriculture & Food Sciences, University of Queensland, St Lucia, Brisbane, Queensland 4072, Australia

[c] School of Plant Biology, University of Western Australia, Crawley, Western Australia 6009, Australia

[d] Queensland Alliance for Agriculture & Food Innovation (QAAFI), University of Queensland, St Lucia, Brisbane, Queensland 4067, Australia

Abstract

Fusarium head blight and crown rot, caused by the fungal plant pathogen *Fusarium graminearum,* impose a major threat to global wheat production. During the infection, plants are contaminated with mycotoxins such as deoxynivalenol (DON), which can be toxic for humans and animals. In addition, DON is a major virulence factor during wheat infection. However, it is not fully understood how DON production is regulated in *F. graminearum*. In order to identify regulators of DON production, a high-throughput mutant screen using Fluorescence Activated Cell Sorting (FACS) of a mutagenized *TRI5-GFP* reporter strain was established and a mutant over-producing DON under repressive conditions identified. A gain-of-function mutation in the *F. graminearum* adenylyl cyclase (FAC1), which is a known positive regulator of DON production, was identified as the cause of this phenotype through genome sequencing and segregation analysis. Our results show that the high-throughput mutant screening procedure developed here can be applied for identification of fungal proteins involved in diverse processes.

Keywords

Gibberella zeae, DON, trichothecene, Fluorescence Activated Cell Sorting, flow cytometry, cAMP

2.1 Introduction

Crop diseases caused by *Fusarium* species are a major threat to global wheat production. Fusarium head blight (FHB) epidemics and the chronic crown rot (FCR) problem can cause up to AUD$ 100 million annual losses in Australia (Murray and Brennan, 2010, 2009) and FHB reportedly causes up to US$ 2.7 billion losses in the United States of America (Nganje et al., 2002). In addition to yield reductions, the contamination of the infected plants, including the grains, with mycotoxins produced by the fungus is a major issue particularly with FHB (Desjardins et al., 2003). Worldwide, the mycotoxin deoxynivalenol (DON) is the most common contaminant of wheat, barley and corn (Jelinek et al., 1989; The World Health Organization, 1992). The DON producing fungus *Fusarium graminearum* is the most common causative agent of FHB epidemics and subsequent human and animal toxicoses (O'Donnell et al., 2004). In *F. graminearum* DON is a major virulence factor towards wheat, and is essential for the spread of the disease from the infection site (Jansen et al., 2005; Proctor et al., 1995a). The biosynthesis of DON from farnesyl pyrophosphate is catalysed by trichothecene biosynthesis enzymes encoded by several *TRI* genes (reviewed in Desjardins, 2006). The trichodiene synthase TRI5 catalyses the first essential step of DON biosynthesis (Hohn and Vanmiddlesworth, 1986). *F. graminearum* specifically induces DON production *in planta*, which is associated with the formation of infection structures (Boenisch and Schäfer, 2011). However, it is not yet fully understood how this specific induction is regulated in the fungus. As there is no single effective control strategy against *F. graminearum* to date (Gilbert and Haber, 2013), a better understanding of the regulatory mechanisms of toxin production is crucial for the development of improved disease control strategies.

A number of DON biosynthesis inducers such as reactive oxygen species (Audenaert et al., 2010; Ponts et al., 2006, 2007), sugars (Jiao et al., 2008; Miller and Greenhalgh, 1985; Miller et al., 1983), cinnamic-derived acids and phenolic acids (Ponts et al., 2011), cobalt chloride (Tsuyuki et al., 2011) and warm temperatures (Kokkonen et al., 2010; Miller et al., 1983) have been identified. Reduced nitrogen sources such as the amines putrescine and arginine in combination with a low pH are also excellent *in vitro* inducers of DON production (Gardiner et al., 2009a, 2009c; Merhej et al., 2011). Putrescine and arginine accumulate in *F. graminearum* infected wheat heads (Gardiner et al., 2010) and their biosynthesis is known to be upregulated in plants during defence responses (Haggag and Abd-El-Kareem, 2009; Walters, 2002). However, it is not understood how amines induce DON production in the

fungus. Nitrogen is not required for DON biosynthesis; so it is unlikely that amines serve as precursors. In addition, it is likely that amines do not directly induce DON production, as it takes approximately 48 hours between the application of amines and the actual induction of DON production in the fungus (Gardiner et al., 2009a).

The global nitrogen regulatory transcription factor AreA is an essential regulator of DON production (Giese et al., 2013; Min et al., 2012). AreA in turn might be regulated by cAMP-PKA signalling (Hou et al., 2015). Generally, protein kinase A (PKA) is activated by cyclic 3',5'-adenosine monophosphate (cAMP) produced by adenylyl cyclases, which are regulated by G-proteins (Li et al., 2007). In *F. graminearum* G-protein α and β subunits (GPA1 & GPB1) and regulators of G protein signalling (FlbA & RgsA) are negative regulators of DON production, whereas the adenylyl cyclase FAC1 is an essential positive regulator of DON production (Bormann et al., 2014; Park et al., 2012; Yu et al., 2008). Despite the identification of different regulators of DON production, relatively little is known about the underlying signalling mechanisms that induce or repress DON production and how these different regulators might be interconnected.

Mutant analysis is an essential tool to identify novel regulators or key components of signalling pathways. However, forward genetic screens in *F. graminearum* are inefficient. Thus, it is essential to screen large numbers of individuals to identify potential mutants presenting a phenotype of interest. Here, we present a novel mutant screening method for *F. graminearum* spores using Fluorescence Activated Cell Sorting (FACS) to identify and isolate mutants with altered DON biosynthesis. The usefulness of this approach is demonstrated by the identification and characterization of a DON over-production mutant (called *g8*) which is shown to be a gain-of-function allele of the *F. graminearum FAC1* gene encoding adenylyl cyclase.

2.2 Material and methods

2.2.1 Culture conditions

To either induce or repress DON production, the fungus was grown in minimal media with either 5 mM arginine (Arg) or 5 mM sodium nitrate ($NaNO_3$) as the sole nitrogen source respectively. The media was slightly modified from Correll et al. (1987) and contained the following ingredients per litre: 30 g sucrose, 1 g KH_2PO_4, 0.5 g $MgSO_4.7H_2O$, 0.5 g KCl, 10 mg $FeSO_4.7H_2O$, 200 µL of trace element solution (per 100 mL, 5 g citric acid, 5 g

$ZnSO_4.7H_2O$, 0.25 g $CuSO_4.5H_2O$, 50 mg $MnSO_4.H_2O$, 50 mg H_3BO_3, 50 mg $NaMoO_4.2H_2O$) adjusted to pH 6.5 with NaOH.

For spore production the respective strains were grown in liquid CMC media (Cappellini and Peterson, 1965) by shaking at 26°C under fluorescent white and blue lights, except for the mutant screen during which DON production repressing media was used.

2.2.2 EMS mutagenesis

F. graminearum spores of the *TRI5-GFP* reporter strain ($2x10^6$) were washed twice in 0.1 M sodium phosphate buffer (pH 7.4) and resuspended in 500 µL of that buffer before 30 µL ethyl methanesulfonate (EMS) was added. A similar sample was treated the same way without the addition of EMS as a negative control. The samples were incubated gently rolling at room temperature. After 30 min, 530 µL 8% sodium thiophosphate was added to quench the EMS. The samples were washed twice in 0.1 M sodium phosphate buffer. A dilution series of aliquots of the EMS treated sample, as well as the negative control, were plated out to determine the kill rate of the EMS treatment. This analysis showed that over 99% of all spores were killed by EMS.

2.2.3 FACS

Spore sorting was performed with a FACSAria Cell Sorter (BD Bioscience, San Jose, CA, USA) using a 100 µm nozzle. A 488 nm laser was used to excite GFP in the spores and emission was detected with a 530/30 nm bandpass filter. To determine the background GFP levels, untreated *TRI5-GFP* spores that had been cultured the same way as the EMS treated spores were first analysed with the flow cytometer. These GFP levels were then considered background GFP levels and the cut-off for GFP positive spores in the EMS treated sample was set well above these background levels. Only spores with GFP values higher than 10 000 were considered GFP positive. In the untreated *TRI5-GFP* spore population only one out of 30 000 spores was GFP positive. Thus these settings allowed a high cut-off for the selection of potential mutant candidates.

2.2.4 TRI5-GFP induction assays

The assays were performed in 96-well plates with 10^4 spores per well in 100 µL minimal media (see section 2.2.1) with either Arg or $NaNO_3$ as the sole nitrogen source. The

inoculated 96-well plates were cultured in the dark at 28°C without shaking. GFP intensity and optical density at 405 nm (OD405), to determine growth rates, were measured every hour using an EnSpire plate reader from Perkin Elmer (Waltham, MA, USA). GFP signals were quantified from the top with an excitation wavelength of 488 nm, an emission wavelength of 509 nm and a measurement height of 7 mm. In each well, five measurements in different positions were taken and averaged. In addition, three biological replicates were measured per sample. The first reading was subtracted as baseline and GFP values normalized by OD405, but only if the OD405 was greater than 0.5 absorbance units, to avoid artificially high values.

2.2.5 DON quantification

The levels of DON secreted by the fungus were quantified in liquid culture in the 96-well plates. The AgraQuant® ELISA DON Kit (Romer Labs, Union, MO, USA) was used for quantification and the resulting DON levels normalized by the fungal dry weight of each respective sample. Three biological replicates were quantified per sample.

2.2.6 Whole genome sequencing and sequence data analyses

The libraries for the Illumina HiSeq sequencing were prepared with the TruSeq DNA Sample Preparation kit and sequencing was performed with 100 bp paired end reads with ~400 bp inserts at ~25-fold coverage. The obtained whole genome sequencing data derived from the mutant and the parental *TRI5-GFP* strain were aligned to the CS3005 (the WT strain used to create the *TRI5-GFP* reporter) reference genome (Gardiner et al., 2014) using the 'biokanga align' program (http://sourceforge.net/projects/biokanga/) treating read pairs as single ended reads. A maximum of five aligner induced substitutions (i.e. difference compared to the reference) per 100 bp were allowed. As biokanga align uses an exhaustive search procedure and discards reads that mapped to more than one location, the differences between the reads and reference were rarely this high. Identification of single nucleotide polymorphisms (SNPs) was performed using the 'biokanga snpmarkers' program with a minimum coverage of four reads per loci for both the parental strain and mutant read alignments to the CS3005 genome. Identified SNPs were further filtered for high confidence SNPs using a custom perl script with a minimum score of 80%. This score is derived from biokanga snpmarkers output and is the percentage of reads that covers that locus having that base call. In practice, most identified SNPs had scores of 100%. Manual inspection of

high confidence SNPs in coding regions was used to determine if they caused an amino acid change or generated a stop codon in the predicted protein. Sequence reads from the *TRI5-GFP* and *g8* mutant strains are available from the NCBI sequence read archive as part of BioProject PRJNA294990.

2.2.7 Backcrossing and genotyping

The *g8* mutant was crossed to a strain lacking the polyketide synthase responsible for aurofusarin biosynthesis (*Δpks12*). This strain was derived from the same parental strain (CS3005) as the *TRI5-GFP* strain (see Table 2.1 for a summary of the fungal strains used in this study). Crossing was performed on carrot agar plates (Klittich and Leslie, 1987) as described elsewhere (Bowden and Leslie, 1999). Ascospores were harvested from the Petri plate lid and spread on to ½ PDA plates containing 50 mg L^{-1} G418 and 200 mg L^{-1} hygromycin. Germinating spores were individually picked under a dissecting microscope onto double antibiotic selection plates. Nineteen individuals of the *g8* x Δ*pks12* progeny were phenotyped using the TRI5-GFP induction assay described in section 2.4 and also genotyped using the FAC1f/FAC1r and TRF1f/TRF1r primer pairs (Table 2.2) amplifying ~400 bp region around the respective SNPs in *FAC1* and *TRF1*.

2.2.8 cAMP quantification

Freeze-dried hyphae were used for cAMP quantification with the Cyclic AMP EIA Kit from Cayman Chemicals (Ann Arbor, MI, USA). For this, the fungus was grown in 96 well plates for three days in 100 µL minimal media with either Arg or $NaNO_3$ as sole nitrogen sources at 28°C in the dark without shaking, similar to the TRI5-GFP assay conditions. The samples were extracted in trichloroacetic acid according to the tissue sample protocol in the kit. Six biological replicates were quantified per sample.

2.2.9 Fungal strains

The *TRI5-GFP* reporter strain (Table 2.1), which encodes *GFP* as a C-terminal fusion to *TRI5* separated by four glycine residues, plus the hygromycin resistance gene *hph* with the *TrpC* promoter was constructed as follows. The 3' end of *TRI5* (978 bp) up to but not including the stop codon was amplified from CS3005 gDNA using primers TRI5pYES2F and TRI5RV (see Table 2.2 for a full list of primers used in this study). The reverse primers

included sequence to encode four glycines as a linker between *TRI5* and *GFP*. A *GFP-SV40* terminator-*TrpC* promoter-*hph* was generated by first cloning PCR amplified *GFP-SV40* terminator (primers GFPfKpnI and GFPrSacI) into pPZPHyg (*Hin*dX) (Elliott and Howlett, 2006) and then subsequently amplified as a single fragment (GFPFW and HYGRV2) up to but not including the stop codon from *hph*. The sequence downstream of the *TRI5* coding sequence was used as the *hph* terminator to allow targeting of the vector into the native *TRI5* locus. This fragment (1289 bp including the stop codon) was amplified using primers TRI5utrF2 and TRI5pYES2R. All products were amplified using Phusion DNA polymerase (Thermo Fisher Scientific, Waltham, MA, USA) according to the manufacturer's instructions with the following reaction specific conditions: all reactions were performed with 10% DMSO and with an annealing temperature of 55°C for the first 5 cycles followed by annealing at 65°C for 30 subsequent cycles. Extension was performed for 2 minutes. Each primer used for fragment amplification contained at least 15 bp of sequence (30 bp of total overlap) at the 5' end to allow yeast mediated homologous recombination of the fragments into a *Hin*dIII/*Xba*I linearized pYES2 with yeast transformation as described elsewhere (Kettle et al., 2015). Transformation of the isolate CS3005 was conducted as previously described (Desmond et al., 2008).

The vector for deletion of the *polyketide synthase 12* (*PKS12*) was constructed by amplifying 1014 bp of sequence immediately upstream of the *PKS12* coding sequence (PKS12pYES2F and PKS12_5RV) from isolate CS3005, a *gpdA* promoter-*npt* cassette including the stop codon (gpdAneoFW and gpdAneoRV) from pAN9.1 (Gardiner et al., 2009b) and 1644 bp of sequence immediately downstream of the *PKS12* stop codon (PKS12_3FW and PKS12pYES2R). All primers contained a minimum of 15 bp of sequence at the 5' end to allow yeast mediated homologous recombination to assemble the fragments (minimum total overlap between PCR products was 30 bp). Transformants were screened using a triplex PCR assay (FgPKS12KOscrF, FgPKS12KOscrR, gpdAr2), in which the absence of the wild type band (432 bp product) and presence of the vector band (677 bp product) was taken as evidence for successful gene disruption.

Table 2.1. Fungal strains used in this study.

Strain	Background	Transgene	Mutations (gene, base, aa)	Resistance
TRI5-GFP	CS3005	*proTRI5::TRI5-GFP*	none	Hygromycin
g8	*TRI5-GFP*	*proTRI5::TRI5-GFP*	*FGSG_01234,* C4321T, P1441S *FGSG_08713*, C1194T, F398L	Hygromycin
Δpks12	CS3005	*proPKS12::gpda*	knockout of *PKS12*	G418
g8.1-20	*g8* x *Δpks12*	*proTRI5::TRI5-GFP, proPKS12::gpda*	*FGSG_01234,* C4321T, P1441S *FGSG_08713*, C1194T, F398L	Hygromycin, G418

Table 2.2. Primers used in this study.

Primer name	Sequence 5'-3'	Use
TRI5pYES2F	CTGTAATACGACTCACTATAGGGAATATTAAGC TTAAACAATCGTTGGCATGGTT	Amplification of *TRI5* coding sequence for reporter strain construction
TRI5RV	GCTCACCATACCTCCGCCACCCTCCACTAGCT CAATTGA	
GFPFW	CTAGTGGAGGGTGGCGGAGGTATGGTGAGCA AGGGCGAG	Amplification of *GFP* and *hph* for reporter strain construction
HYGRV2	ACTCGCCTTCGGTTATTCCTTTGCCCTCGGACG AGTGCT	
TRI5utrF2	CCGAGGGCAAAGGAATAACCGAAGGCGAGTTT GGAAGTA	Amplification of *TRI5* 3' downstream region for reporter strain construction
TRI5pYES2R	GTGACATAACTAATTACATGATGCGGCCCTCTA GAAGCCGAAGTGTGATTCATCC	
GFPfKpnI	AATGGTACCATGGTGAGCAAGGGC	Amplification of *GFP* for creation of *GFP* and *hph* containing construct
GFPrSacI	GGCGAGCTCATACATTGATGAGTTTG	
PKS12pYES2F	CTGTAATACGACTCACTATAGGGAATATTAAGC TTGCCATCGTTGACAAATTCCT	*PKS12* knockout 5' flank
PKS12_5RV	TTTTGGTTACGCCGTTGATGGGGTCATGTTGAA TGAACT	
gpdAneoFW	AACATGACCCCATCAACGGCGTAACCAAAAGT CACACAA	*PKS12* knockout antibiotic cassette
gpdAneoRV	CCCTCTCCATCGTGTTCAGAAGAACTCGTCAAG AAGGCG	
PKS12_3FW	GACGAGTTCTTCTGAACACGATGGAGAGGGCT GTTTGTG	*PKS12* knockout 3' flank
PKS12pYES2R	GTGACATAACTAATTACATGATGCGGCCCTCTA GATCTTTGACAGATGCCGAGTG	
FgPKS12KOscrF	ATCCGAATGCCGTCTAACAC	Primers for screening for successful deletion of *PKS12*
FgPKS12KOscrR	GTCGGCAAAGTTTGGAAAAA	
gpdAr2	GAGCTCACGAGTTCGTCACA	
FAC1f	CGGCAACAGGTTTACCAACT	*FAC1* genotyping
FAC1r	CAGATGCTCGTGCTTACCAA	
TRF1f	CGGAGTAGGGAAATGGACAA	*TRF1* genotyping
TRF1r	CCGTTTCTTTGGTCTGGAAA	

2.3 Results

2.3.1 Reporter strain construction

To conduct a forward genetic screen for altered DON production a toxin-production reporter strain was constructed. We previously demonstrated that fluorescence signal from a *TRI5-promoter-GFP* (*proTRI5::GFP*) strain was an excellent indicator of *TRI5* expression and hence DON production (Gardiner et al. 2009a). However, the *proTRI5::GFP* strain previously constructed was designed with two copies of the *TRI5* promoter, making this strain unsuitable for sexual crosses as duplicated sequences are expected to promote repeat induced point mutations in *F. graminearum* (Cuomo et al 2007). To avoid this potential problem, a strain was constructed whereby *GFP* was inserted as a translational fusion to the carboxy-terminal end of *TRI5*. To determine correct insertion of the transforming DNA and ensure that it is a single copy insertion, whole genome sequencing of three transformants was conducted and one of these was shown to contain a single insertion at the desired location (Figure S1 and Table S1). The selected *TRI5-GFP* strain does not show any obvious growth defects (Figure S2C) and vegetative and sexual spore production appear normal compared to the CS3005 progenitor strain (data not shown). In addition, the *TRI5-GFP* translational reporter strain shows similar patterns of TRI5 inducibility by different nitrogen sources as the previously published *proTRI5::GFP* transcriptional reporter strain and also similar levels of DON production as *proTRI5::GFP* and the progenitor CS3005 strain (data not shown). Thus, the *TRI5-GFP* strain fulfils all requirements for an appropriate reporter strain.

2.3.2 FACS allows high-throughput screening of millions of spores in a few hours

Fluorescence Activated Cell Sorting (FACS) has the potential to efficiently screen a population of mutated spores for phenotypes of interest. In human cell cultures for example, FACS is commonly used to screen and isolate large numbers of cells. Flow cytometers create fine droplets, each of which contains only one cell. This allows the analysis of individual cells in a large population for cell size, density and fluorescence intensities. In addition, flow cytometers can sort cells with predefined features individually into plates. In this study, this technology was applied to ethyl methanesulfonate (EMS) treated spores of a *F. graminearum TRI5-GFP* reporter strain. The screen was performed to identify mutants with constitutive DON production under repressive conditions.

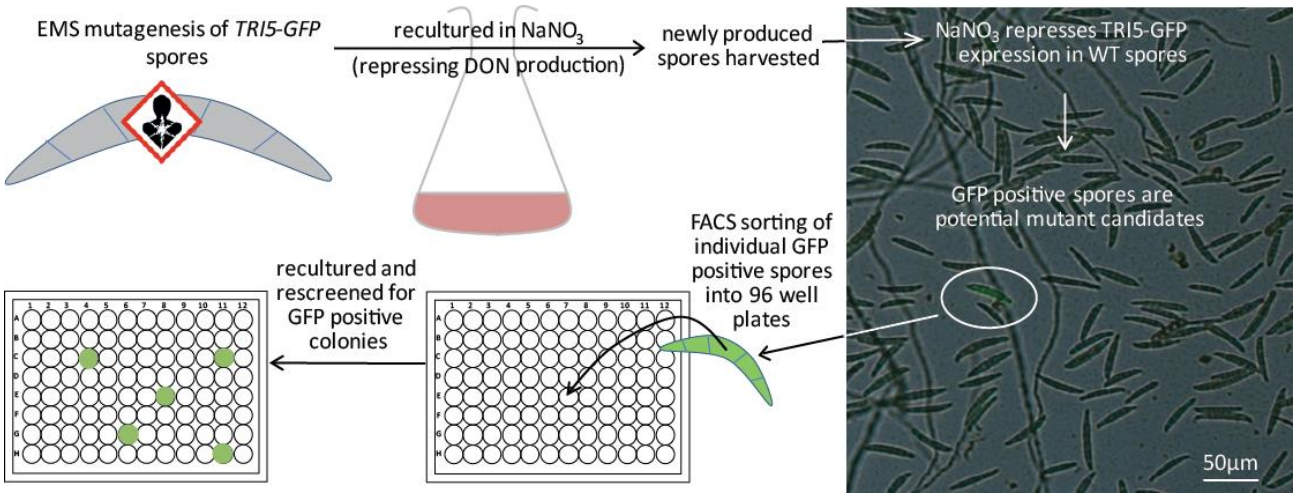

Figure 2.1. Workflow of the screen to isolate DON production mutants. *TRI5-GFP* spores were mutagenized using EMS and recultured under DON repressive conditions with $NaNO_3$ as sole nitrogen source until they re-sporulated. These newly produced spores were analysed by Fluorescence Activated Cell Sorting (FACS) using a flowcytometer. As $NaNO_3$ represses DON production, TRI5-GFP expression is low in un-mutagenized spores, but is detectable only in mutants with misregulated toxin production. FACS was used to sort only those few GFP positive spores individually into 96-well plates containing defined media with $NaNO_3$ as sole nitrogen source. The single spores in the 96-well plates were recultured and rescreened to exclude false positives and confirm mutant candidates.

Figure 2.1 illustrates the procedure employed to identify mutants with constitutive DON production. Mutagenized spores were cultured under DON repressive conditions at 26°C under fluorescent white and blue lights until they re-sporulated. Under these conditions, *TRI5* is not typically expressed and any GFP positive spores were thus potential mutants in DON regulatory pathways. To determine an appropriate fluorescence threshold above which to collect spores, we first analysed the distribution of fluorescence signals from a population of non-mutagenized *TRI5-GFP* spores grown under the same DON repressive conditions (Figure 2.2 A). The majority of these spores exhibited low fluorescence signals up to 1000 relative fluorescence units (RFU) (Figure 2.2 A, gate P1). A smaller sub-population showed GFP signals between 1000 RFU and 10 000 RFU (Figure 2.2 A, gate P2) and only one spore out of 30 000 exhibited a fluorescence signal greater than 10 000 RFU (Figure 2.2 A, gate P3, arrow). Presumably this is due to natural variation in TRI5 expression or possibly spontaneous mutation. Thus the threshold for the selection of GFP positive spores from the EMS-treated sample was set at 10 000 RFU.

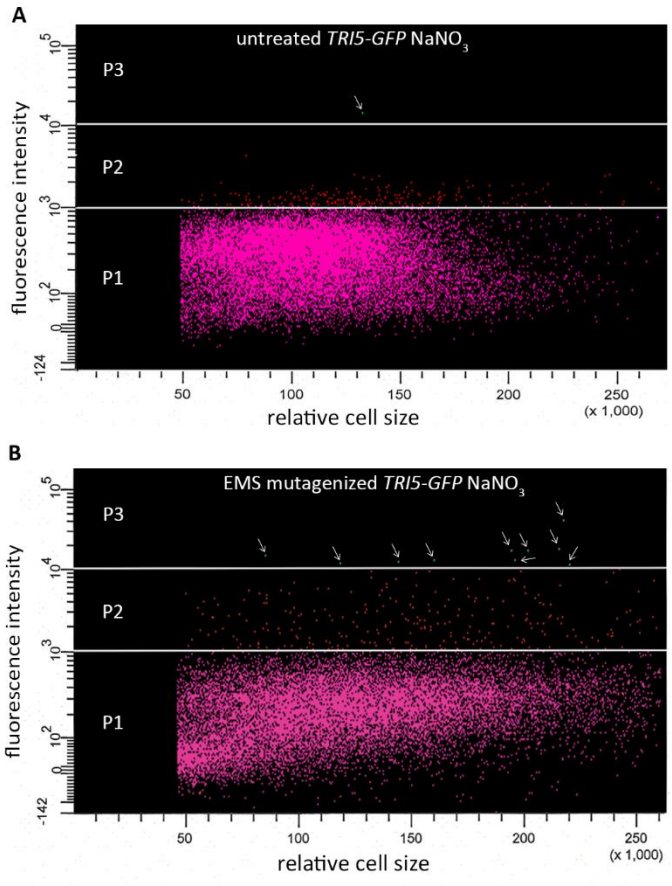

Figure 2.2. Fluorescence activated cell sorting gating. Gate P1 (pink) and P2 (red) show the GFP background levels of spores. Gate P3 (green) represents GFP positive spores with GFP signals greater than 10 000 RFUs. **A** In the untreated *TRI5-GFP* sample grown in $NaNO_3$ only one spore was considered GFP positive out of a population of 30 000. **B** In the EMS treated *TRI5-GFP* sample an increase of the GFP signals could be observed within the P2 gate as well as in the numbers of GFP positive spores (P3). These GFP positive spores (P3) were sorted individually into the 96-well plates. Arrows indicate GFP positive spores.

In the EMS-treated samples, compared to the non-treated controls, there were substantially more spores with fluorescence levels between 1000 and 10 000 (Figure 2.2 B, gate P2) and also more GFP positive spores with fluorescence signals above 10 000 RFU (Figure 2.2 B, gate P3, arrows). Out of a population of 30 000 spores, 14 exhibited signals above 10 000 RFU. Nevertheless, the GFP positive spores only made up 0.1% of the whole population of the EMS-treated spores. Using the 10 000 RFU cut off, GFP positive spores were recovered into 96-well plates containing DON repressive media. These plates were recultured at room temperature and rescreened for TRI5-GFP expression in hyphae using a fluorescence plate reader. Positive samples were subcultured for an additional round of screening for the final selection of putative mutants. In total, 950 mutant candidates were sorted into 96 well plates

during the flow cytometry step. Out of these, 15 were confirmed as mutants showing TRI5-GFP overexpression under repressive conditions in the following two rounds of screening using the fluorescence plate reader. This makes a final rate of 0.00075% of mutant candidates showing the phenotype of interest out of a population of $2x10^6$ spores. This low identification rate emphasizes the importance of using a high-throughput mutant screening method such as the FACS. However, this mutant recovery rate may be an under-estimate as the FACS-based screen selects for spores with elevated TRI5-GFP expression and the confirmatory plate-based screen primarily measures fluorescence from hyphae; so only mutants with elevated TRI5-GFP expression in both of these developmental states were recovered at the end.

2.3.3 DON production is induced under repressive conditions in the *g8* mutant

One strong mutant identified through the above screen was named *g8* (*gain-of-induction 8*). To further characterize the *g8* mutant, the TRI5-GFP expression was quantified in a time course experiment. Under DON repressive conditions ($NaNO_3$), TRI5-GFP was expressed up to 50 times higher in the *g8* mutant than in the parental *TRI5-GFP* strain, even though *g8* showed a slightly reduced growth rate (Figure S2 C). In comparison, these two strains showed similar expression values under DON inductive conditions at 3dpi (Arg) (Figure 2.3 A). The *TRI5-GFP* over-expression phenotype was consistently observed in other assay formats, including 6 well plate liquid cultures and on solid media (Figure S2).

In addition, the levels of DON production were quantified to determine if the increased TRI5-GFP levels in the *g8* mutant under DON repressive conditions resulted in increased DON production. As expected, the parental *TRI5-GFP* strain produced only low (0.07 µg DON per mg hyphae) levels of DON under repressive conditions (Figure 2.3 B). In contrast, the *g8* mutant produced approximately 25 times more DON (1.83 µg DON per mg hyphae) than the *TRI5-GFP* parent under the same experimental conditions. Even under DON inductive conditions, significantly higher amounts of DON were produced by the *g8* mutant (Figure 2.3 B).

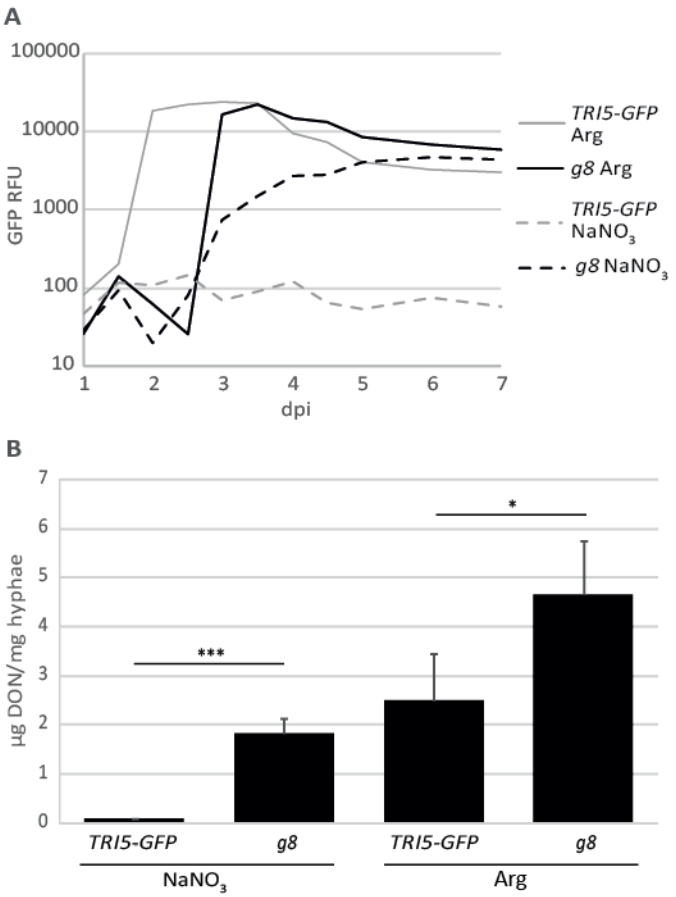

Figure 2.3. TRI5-GFP expression (A) and DON production (B) in the *g8* mutant and the *TRI5-GFP* parent under repressive ($NaNO_3$) and inductive (Arg) conditions. Strains were grown for seven (**A**) or four (**B**) days. Asterisks indicate statistically significant differences with *, $p<0.05$; ***, $p<0.0005$ (Student's t-test), dpi = days post inoculation.

The above experiments were conducted using macroconidia produced in liquid cultures, and no obvious alterations in conidia production or morphology were observed in g8 (data not shown). In addition, as the forward screen procedure involved a re-culturing and subsequent harvest of macroconidia for cell sorting, there was an inherent selection against mutants impaired in sporulation. Together these observations suggest *g8* has a relatively normal sporulation ability.

2.3.4 The *g8* mutant develops toxin-production-specific cellular structures under toxin production repressive conditions

Previous studies by Menke et al. (2012) have shown that *F. graminearum* develops specific subapical ovoid cell structures and highly branched thick coralloid hyphae under toxin production inductive conditions *in vitro*. These cellular structures are similar to

infection-related cellular structures observed in *in planta* studies (Boddu et al., 2006; Ilgen et al., 2009; Jansen et al., Kistler and Broz, 2015; Pritsch et al., 2000; 2005; Rittenour and Harris, 2010;). Hyphal development of the *g8* mutant under DON inductive and repressive conditions in comparison to the *TRI5-GFP* parental strain was microscopically analysed, to see if the *g8* mutant, apart from over-producing DON, also develops toxin-production-specific structures under repressive conditions.

Under DON repressive conditions ($NaNO_3$), only low background TRI5-GFP levels could be observed from the parental strain, as expected. These were mainly in vesicular structures (Figure 2.4 A, closed arrow) and almost all hyphae appeared to have a similar morphology in the *TRI5-GFP* strain. Only few isolated hyphae were slightly thickened (not shown), although even these were still thinner than the coralloid hyphae (Figure 2.4 C, closed arrow) observed under DON inductive conditions. In contrast, strong vesicular (Figure 2.4 B, closed arrow) and also cytoplasmic (not shown) TRI5-GFP signals could be observed in thickened coralloid hyphae (Figure 2.4 B, closed arrow) of the *g8* mutant under DON repressive conditions. The coralloid 10-20 µm wide hyphae of *g8* were twice as thick as the 'normal' hyphae observed in the *TRI5-GFP* parental strain under repressive conditions (Figure 2.4 A). These thinner 'normal' hyphae could still be observed in the *g8* mutant under repressive conditions, with the majority of them being GFP negative (Figure 2.4 B). Thus, the TRI5-GFP over-production phenotype of the g8 mutant occurs heterogeneously within an individual fungal culture which is not unexpected as a similar observation is made in the *TRI5-GFP* strain under inductive conditions and suggests other control mechanisms are acting to keep *TRI5* expression in check.

Under DON inductive conditions (Arg), the *TRI5-GFP* parental strain exhibited strong vesicular (Figure 2.4 C, closed arrow) and cytoplasmic (Figure 2.4 C, open arrow) TRI5-GFP signals in thickened coralloid hyphae (Figure 2.4 C, closed arrow) and also in bulbous ovoid cell structures (Figure 2.4 C, open arrow). The *g8* mutant exhibited similar strong vesicular (Figure 2.4 D, closed arrow) and cytoplasmic (not shown) GFP signals in thickened coralloid hyphae (Figure 2.4 D, closed arrow) under inductive conditions. These coralloid hyphae were similar to those observed under repressive conditions (Figure 2.4 B, closed arrow), but were more abundant under inductive conditions.

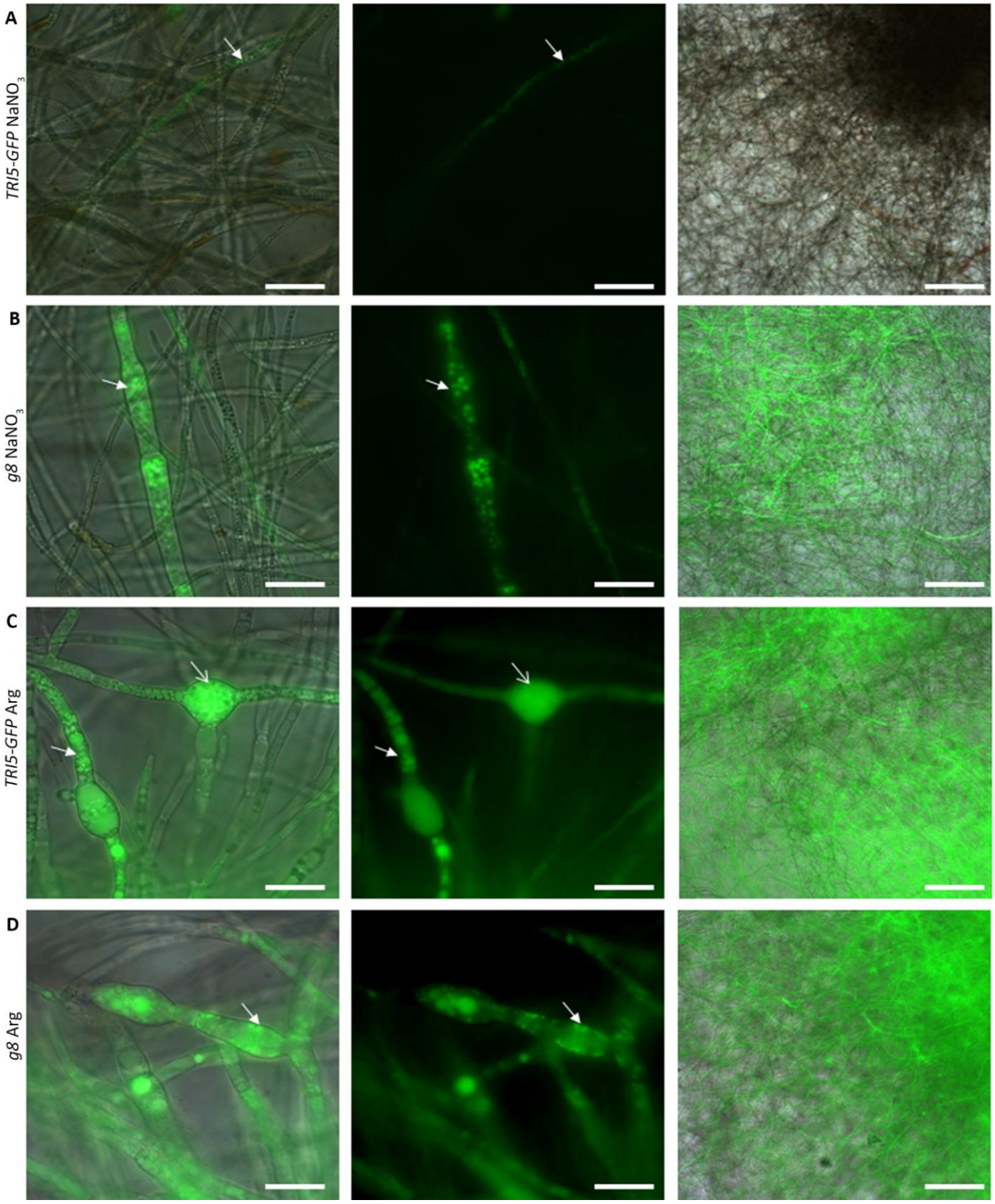

Figure 2.4. Microscopic analysis of TRI5-GFP induction and hyphal development under DON production inductive and repressive conditions in the *g8* mutant and the *TRI5-GFP* parental strain. The strains were grown from spores in 96-well plates in DON production repressive ($NaNO_3$) and inductive (Arg) conditions for three days. The left column shows bright field and GFP merged images, the middle GFP and the right column shows merged images of an overview of the mycelia in lower resolution. The scale bars represent 20 µm in the left and middle columns and 200 µm in the right column. The closed arrows indicate TRI5-GFP positive vesicular structures (**A**-**D**) in bulbous hyphae (**B**-**D**) and the open arrow in **C** indicates cytoplasmic TRI5-GFP signals in an ovoid cell.

Figure S3 further illustrates the higher abundance of the coralloid hyphae vs normal hyphae in *g8*. Nevertheless, bulbous ovoid cells could only be observed rarely in the *g8* mutant, whereas such cells were quite abundant in the *TRI5-GFP* parent under inductive conditions. Accordingly, the toxin over-production phenotype observed under repressive conditions in the *g8* mutant correlates with a developmental switch to toxin-production-specific cellular structures. However, the mutation in *g8* may also affect the complete differentiation of these structures.

2.3.5 The *g8* mutant carries mutations in two genes

To identify potential causal mutations that may be responsible for the *g8* DON over-production phenotype, the whole genome of the *g8* mutant was sequenced. Five high confidence single nucleotide polymorphisms (SNPs) were identified by comparing reads derived from the parental strain and *g8* after alignment to the *F. graminearum* CS3005 genome. However, only two out of the five SNPs were in coding regions. These two mutations resulted in amino acid changes in the coding region of *TRF1* (*FGSG_08713*) (not shown) and *FAC1* (*FGSG_01234*) (Figure 2.5), respectively. The mutation in *TRF1*, which encodes a telomere binding protein, results in an amino acid change from phenylalanine to a leucine at position 398. This mutant allele is hereafter termed $TRF1^{F398L}$. The mutation in *FAC1*, which encodes an adenylyl cyclase, changes proline at position 1441 to a serine. This allele is hereafter termed $FAC1^{P1441S}$.

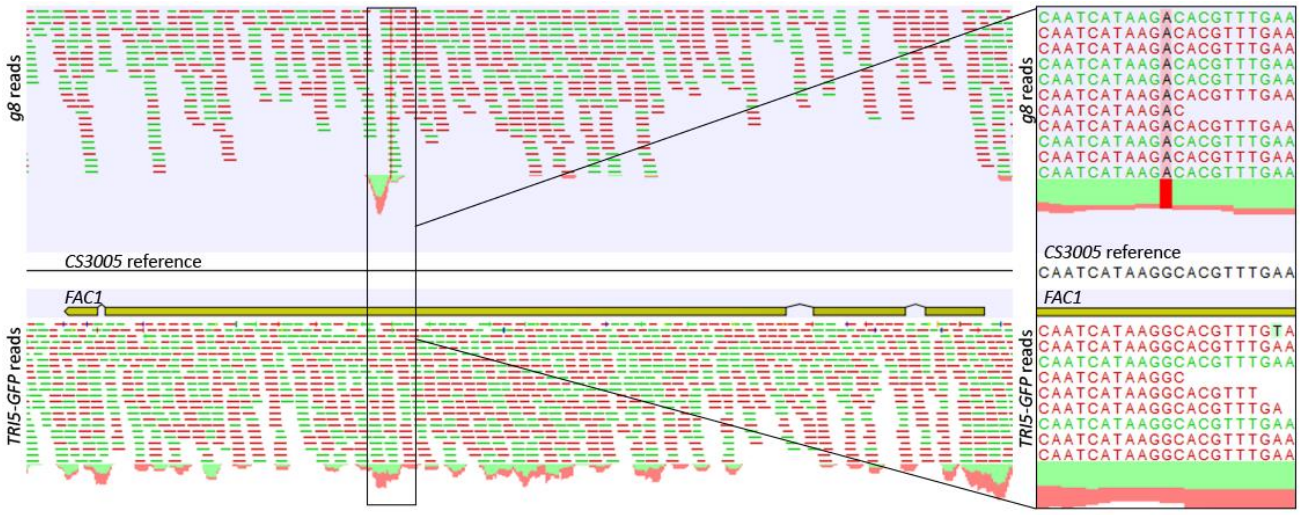

Figure 2.5. Alignment of whole genome sequencing data of *g8* mutant and *TRI5-GFP* parental strain to CS3005 wild type *F. graminearum*. The SNP in *FAC1* in *g8* is highlighted in red in the box. Green and red lines represent forward and reverse reads.

2.3.6 DON over-production in *g8* is caused by a gain-of-function mutation in *FAC1*

Segregation analysis was performed to determine which mutation was responsible for the altered regulation of DON production in *g8*. To this end, the *g8* mutant was crossed with a Δ*pks12* strain, lacking the aurofusarin pigment in the same CS3005 genetic background as the *TRI5-GFP* reporter strain. The use of the Δ*pks12* mutant allows both phenotypic as well as antibiotic selection for recombinants. As *F. graminearum* is homothallic, selection for recombinants on dual antibiotics is essential for this analysis. Given the success of sexual crosses with g8 and the resultant production of ascospores, the g8 mutant appears to have normal sexual reproduction capabilities.

The resulting progeny were phenotyped for TRI5-GFP expression and genotyped at the *TRF1* and *FAC1* loci identified in the genome sequencing. Eleven out of 19 progeny, namely *g8.1-7*, *g8.9-10*, *g8.12* and *g8.16* exhibited the mutant TRI5-GFP expression phenotype under DON repressive conditions (Figure 2.6) which is not significantly different from expected segregation ratios ($\chi^2 = 0.47$ *p*-value 0.49). Under the same conditions, the other eight progeny, namely *g8.11, g8.13-15* and *g8.17-20* expressed low TRI5-GFP levels similar to those found in the parental *TRI5-GFP* strain. Genotyping of the progeny around the SNP loci of *FAC1* revealed cosegregation of the $FAC1^{P1441S}$ allele with the mutant TRI5-GFP over-production phenotype (Figure 2.6). Likewise, all progeny carrying the wild type *FAC1* allele exhibited parental-like TRI5-GFP expression levels. In contrast, the $TRF1^{F398L}$

mutation did not segregate with the TRI5-GFP expression phenotype. Therefore, the *FAC1*^{P1441S} allele is the most likely cause of the TRI5-GFP over-expression and DON over-production in the *g8* mutant.

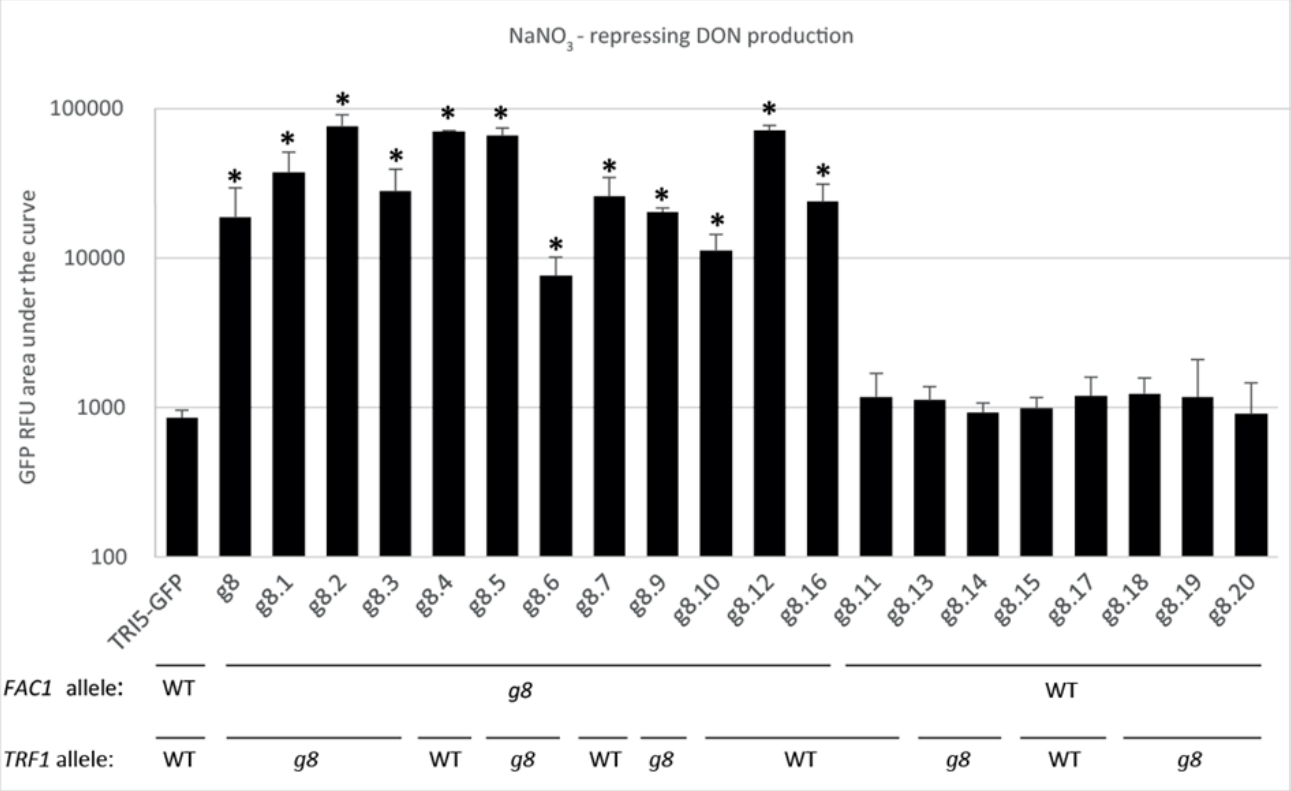

Figure 2.6. TRI5-GFP expression in the parental *TRI5-GFP* strain, *g8* mutant and progeny from a *g8*×*Δpks12* 'backcross' under DON production repressive conditions. Cumulative TRI5-GFP expression is presented from a seven day time course**.** All 11 individual progeny carrying the mutant *FAC1*^{P1441S} allele showed a statistically significantly over-induction of TRI5-GFP compared to the unmutated *TRI5-GFP* parent when grown under DON production inhibiting conditions with NaNO3 as sole nitrogen source. Asterisks indicate $p \leq 0.05$ (Student's t-test) compared to *TRI5-GFP* strain.

FAC1 has already been reported as a regulator of DON production by Hu et al. (2014) and Bormann et al. (2014). However, in these studies, the Δ*fac1* knock-out mutant was unable to produce DON. As the *FAC1*^{P1441S} allele identified in the current study causes over-production of DON, this suggested that the mutation was a gain-of-function allele. As the adenylyl cyclase converts ATP to cAMP, this mutation may also have an effect on cAMP levels. To address this possibility, cAMP levels were quantified in the *g8* mutant under DON repressive conditions and compared to the *TRI5-GFP* strain under repressive and inductive conditions. cAMP levels were determined after three days of culture at a time when

TRI5-GFP expression is maximal. Under DON repressive conditions, the *g8* mutant produced approximately 50% more cAMP than the parental *TRI5-GFP* strain (*p*-value = 0.03) (Figure 2.7). The cAMP levels of the parental *TRI5-GFP* strain were also quantified under DON inductive conditions. A two-fold difference in cAMP levels was observed for this strain between the repressive and inductive conditions. Thus, the 1.5-fold increase in cAMP observed in the *g8* mutant compared to the parental strain under repressive conditions is likely to be biologically relevant. Furthermore, the cAMP levels observed mirrored the DON measurements for these same genotype/treatment combinations where the parental strain produced less DON under repressive conditions than the *g8* mutant (Figure 2.7, Figure 2.3 B).

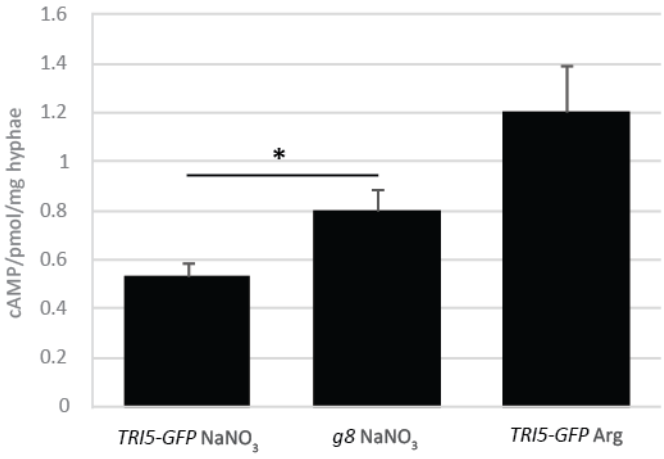

Figure 2.7. Quantification of cAMP in hyphae of the *g8* mutant vs the *TRI5-GFP* parent. The *g8* mutant strain was grown under DON production repressive ($NaNO_3$) conditions and the unmutated *TRI5-GFP* strain under repressive ($NaNO_3$) as well as under inductive (Arg) conditions for three days. The asterisk indicates a statistically significant difference with $p<0.05$ (Student's t-test).

2.4 Discussion

Herein the utility of FACS to facilitate high-throughput mutant screens for fungi has been demonstrated. Recently, Vlaardingerbroek et al. (2015) reported the use of FACS to select fungal transformants in *F. oxysporum* using fluorescent proteins as selection marker instead of an antibiotic resistance gene. In the mutant screen presented here, the combination of the *TRI5-GFP* reporter strain with DON repressive growth conditions and the high-throughput capabilities of FACS using a flow cytometer allowed unparalleled efficiency

to identify potential mutants. In a similar approach, Huang et al. (2015) used UV radiation to create a mutant library of yeast (*Saccharomyces cerevisiae*) cells, which they then encapsulated individually with a reporter compound to perform fluorescence activated droplet sorting. They identified eight clones with a total of 330 mutations. We identified a similar number of mutants in *F. graminearum*, but with less mutations. This might be due to the fact that the screen was conducted with diploid *S. cerevisiae* cells in contrast to the haploid spores used here. Huang et al.(2015) also used a different mutagen, which may have been more effective than EMS. Other effective mutagens, which have previously been used with considerable success in fungi are gene tagging by direct DNA transfer (Seong et al., 2005), restriction enzyme mediated integration (REMI) (Brown et al., 1998), *Agrobacterium* mediated T-DNA (Li et al., 2005) and transposon insertions (Firon et al., 2003). However, in some cases, these mutagens can induce chromosomal rearrangements and/or multiple insertions (Brown et al., 1998; Chung et al., 2003), causing difficulties in determining the causative mutation behind an observed phenotype (reviewed in Weld et al., 2006). Here EMS treatment only resulted in low mutagenesis rates, however the inherently high-throughput nature of FACS allowed successful identification of mutants of interest out of a large population. Under these circumstances, the low mutagenesis rate makes the identification of the causative mutation easier in comparison to more effective mutagenesis approaches, such as REMI or transposons.

The *g8* mutant identified here clearly over-produces TRI5-GFP under normally repressive conditions in comparison to the *TRI5-GFP* strain. This TRI5-GFP over-production is reflected in an equivalent DON over-production. Gardiner et al. (2009a) previously showed that *GFP* expression from a transcriptional *proTRI5::GFP* reporter strain correlated with DON levels produced by the fungus. In this study, a translational fusion was inserted into the native *TRI5* locus in the *TRI5-GFP* strain, which also appears to show a correlation between GFP signals and DON levels. In addition, microscopic analysis showed that the *g8* mutant exhibited strong TRI5-GFP signals in thickened coralloid hyphae under repressive conditions similar to those only observed under inductive conditions in the *TRI5-GFP* parental strain. These toxin-production-specific structures, as described by Menke et al. (2012), developed in the mutant under repressive conditions, but their complete differentiation was impaired, even under inductive conditions.

Whole genome sequencing and segregation analysis revealed that the *FAC1*^{P1441S} mutation in the *F. graminearum* adenylyl cyclase, which synthesizes the secondary messenger cAMP

(Bormann et al., 2014), was responsible for the TRI5-GFP over-induction phenotype of *g8*. *FAC1* has previously been reported as a positive regulator of DON production based on the inability of Δ*fac1* knock-out mutants to produce DON (Bormann et al., 2014; Hu et al., 2014). The Δfac1 knock-out mutant characterised by Bormann et al., 2014 was non-pathogenic on wheat, but fully virulent on maize, indicating the importance but also the complexity of cAMP signalling during fungal pathogenesis. It is likely that the mutant *FAC1* allele identified here is a gain-of-function allele, given that this mutation has resulted in a DON over-production phenotype rather than loss-of DON production. In addition, the development of toxin-production-related structures under repressive conditions also indicates a gain of function *FAC1* allele, because the Δ*fac1* knock-out mutant was not able to develop these at all. Indeed, this was confirmed by the observation of increased cAMP levels in the *g8* mutant under repressive conditions compared to the *TRI5-GFP* strain. Although the cAMP level in the *g8* mutant was only 50% higher than in the parental strain, such increase is likely to be biologically relevant as there was only a two-fold difference in cAMP levels between repressive and inductive conditions for the parental *TRI5-GFP* strain. In addition, the cAMP levels observed in the parental and *g8* strains reflected the DON levels observed. That is both the DON and cAMP levels in the mutant under repressive conditions were higher than those in the *TRI5-GFP* strain under repressive conditions, but lower than those observed in the *TRI5-GFP* strain under inductive conditions. In addition, toxin-production-specific structures are developed in the *g8* mutant under repressive conditions, but their complete differentiation is impaired. This suggests that there are other regulatory mechanisms controlling the development of toxin-production-specific structures and DON production. These additional regulatory mechanisms cannot fully compensate the *FAC1* gain-of-function allele, but still restrict the development of toxin-production-specific structures and keep DON production below levels observed under inductive conditions. For example, further inducers might be required to fully activate FAC1 to produce higher cAMP levels. The cAMP levels within a cell are also regulated by phosphodiesterases (PDEs) (Ma et al., 1999; Riley and Barclay, 1990). These have been described in *F. solani*, where the PDEs control cAMP levels through degradation (Bagga and Straney, 2000). To our knowledge, *F. graminearum* PDEs have not been functionally characterised, but three genes related to cyclic-nucleotide PDEs are annotated in the genome, namely *FGSG_03661*, *FGSG_06914* and *FGSG_06633* (Cuomo et al., 2007; Güldener et al., 2006; Wong et al., 2011). Hence PDEs might be more active in the *g8* mutant to allow a higher turnover of the increased cAMP levels.

Domain analyses show that the mutation in the *FAC1*^{P1441S} allele causes an amino acid change at the end of the leucine rich repeat domain located between the putative substrate binding site and the putative active site of the FAC1 protein. The FAC1 gain-of-function could be caused by an increase in catalytic activity, increase in the activity of a positive regulatory site or via the loss-of-function of a negative regulatory site of the protein. The amino acid change from proline to serine, lacking the rigid cyclic structure, could also potentially cause a structural change in the protein by bringing the substrate binding domain and catalytic domain closer and thus increasing cAMP production efficiency. In a constitutively active mutant of the *Dictyostelium* adenylyl cyclase, a mutation in the first cytoplasmic loop was thought to bring this domain closer to the second cytoplasmic loop, which might mimic activation by G proteins (Parent and Devreotes, 1996). Similarly, Hatley et al. (2000) created constitutively active mammalian adenylyl cyclase mutants through single amino acid substitutions, which increased the interaction of the two cytosolic domains of the adenylyl cyclase responsible for the catalytic activity (Tang and Gilman, 1995). One of those mutants, namely P1015Q has a similar amino acid change to our FAC1^{P1441S} gain-of-function allele, from a rigid proline to a non-polar glutamine (Hatley et al., 2000). Thus the change from proline to a non-polar serine in FAC1^{P1441S} could potentially cause similar structural changes, which increase the interaction between the substrate binding domain and the catalytic domain. Alternatively, as leucine rich repeats are often involved in protein-protein interactions, the mutation in *FAC1*^{P1441S} presented here could cause a structural change, normally induced by the binding of an activator, or alternatively prevent the binding of a negative regulator of the adenylyl cyclase. Further research is required to distinguish between these possibilities.

Known regulators of adenylyl cyclase, such as heterotrimeric G-protein subunits (Park et al., 2012; Yu et al., 2008), are possible candidates through which altered regulation could act. cAMP produced by the adenylyl cyclase can activate the PKA subunits CPK1 and CPK2, which in turn activate regulators through phosphorylation (Li et al., 2007). The expression of essential DON biosynthesis and transport genes *TRI5, TRI6* and *TRI12* was reduced in a Δ*cpk1* knockout, indicating a regulation of DON production through cAMP-PKA signalling (Hu et al., 2014). The *F. graminearum* global nitrogen regulator AreA carries a conserved putative PKA phosphorylation site and could thus be activated by CPK1 and CPK2 (Hou et al., 2015). The activated AreA could then regulate DON production through TRI10, one of the key transcription factors of the *TRI* cluster; with which AreA has been shown to interact (Hou et al., 2015; Peplow et al., 2003; Seong et al., 2009).

In summary, we have demonstrated the effectiveness of FACS-assisted mutant screening as a step towards dissecting an important aspect of fungal biology. In theory, this methodology could be applied to screen for gain- as well as for loss-of-function mutations in any gene for which a suitable reporter strain is available. For example, an unknown metabolite gene cluster could be tagged with a reporter gene, mutagenized and mutants altered in producing the metabolite of interest could be identified. This may have applications in drug discovery and production in fungi. Even if no reporter strain is available, the single cell sorting function of flow cytometers can be combined with more efficient mutagens like REMI or transposons to individually sort the mutagenized spores, circumventing one of the most time consuming steps in forward mutant screens.

2.5 Supplementary material

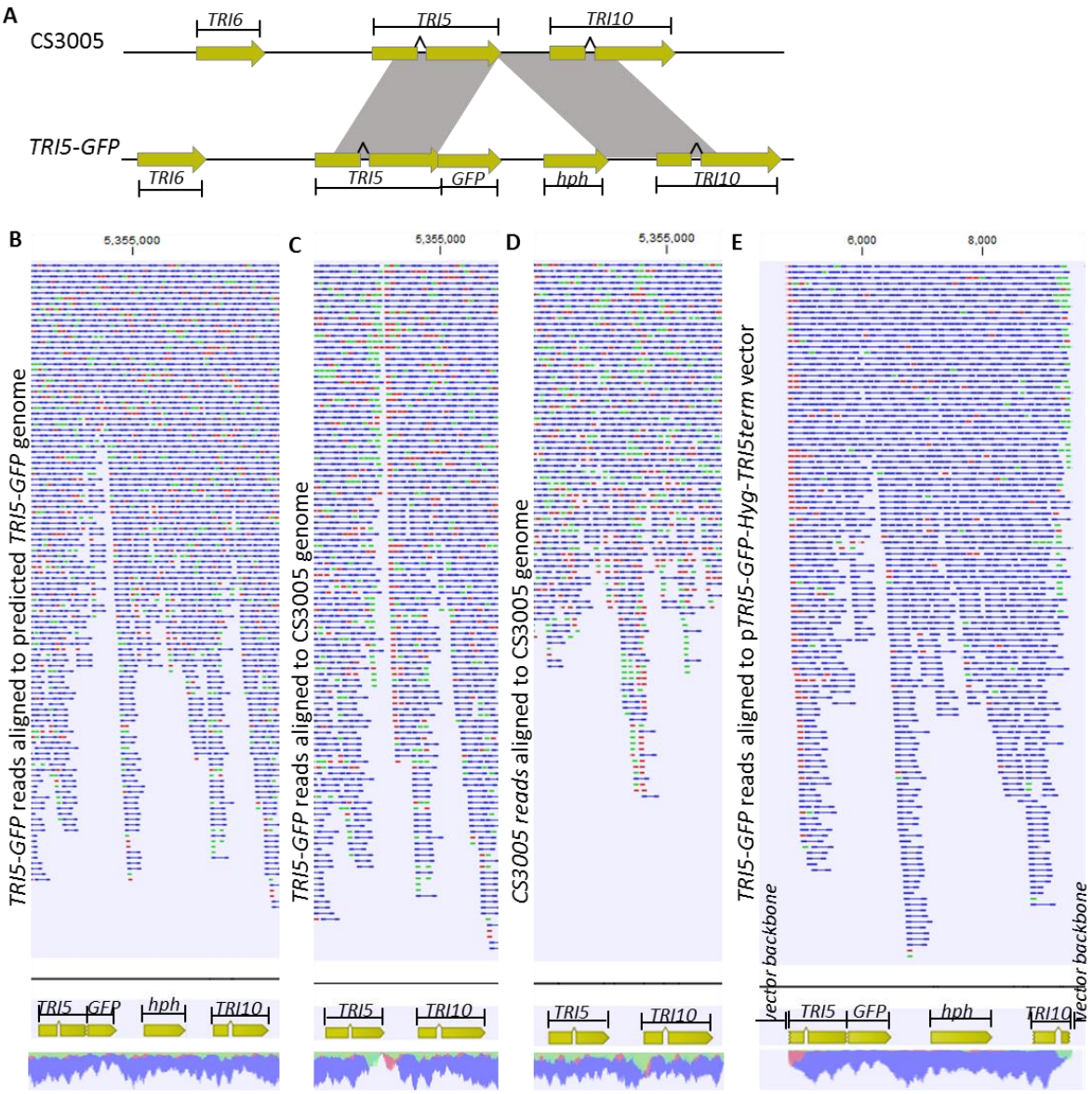

Figure S1. WT and transgene *TRI5* locus and analysis of whole genome sequencing data. (**A**) scheme of the WT CS3005 and the transgene *TRI5-GFP TRI5* locus. The grey projections indicate the homology regions of the vector used for the homologues recombination. (**B**–**E**) The horizontal blue lines represent paired reads and the red and green lines unpaired reads. The same colour code applies to the read coverage graphs below the gene diagrams. The *TRI5-GFP* reads map gaplessly to the predicted *TRI5-GFP* genome (**B**), confirming the whole desired insert has been integrated at the desired site. In contrast, there is a clear gap and an abundance of broken read pairs at the 3′ end of *TRI5* when the *TRI5-GFP* reads are mapped to the CS3005 genome, confirming that there is no WT *TRI5* allele without *GFP* left in the *TRI5-GFP* strain (**C**). CS3005 reads map gaplessly to the CS3005 genome (**D**), showing that the gap in **C** is not due to an error in the CS3005 genome. When *TRI5-GFP* reads are mapped to the plasmid sequence used in transformation (**E**) a gapless coverage across the desired insert can be observed with broken pairs at the extremities of the homology flanks as expected without reads mapping into the vector backbone from the insert.

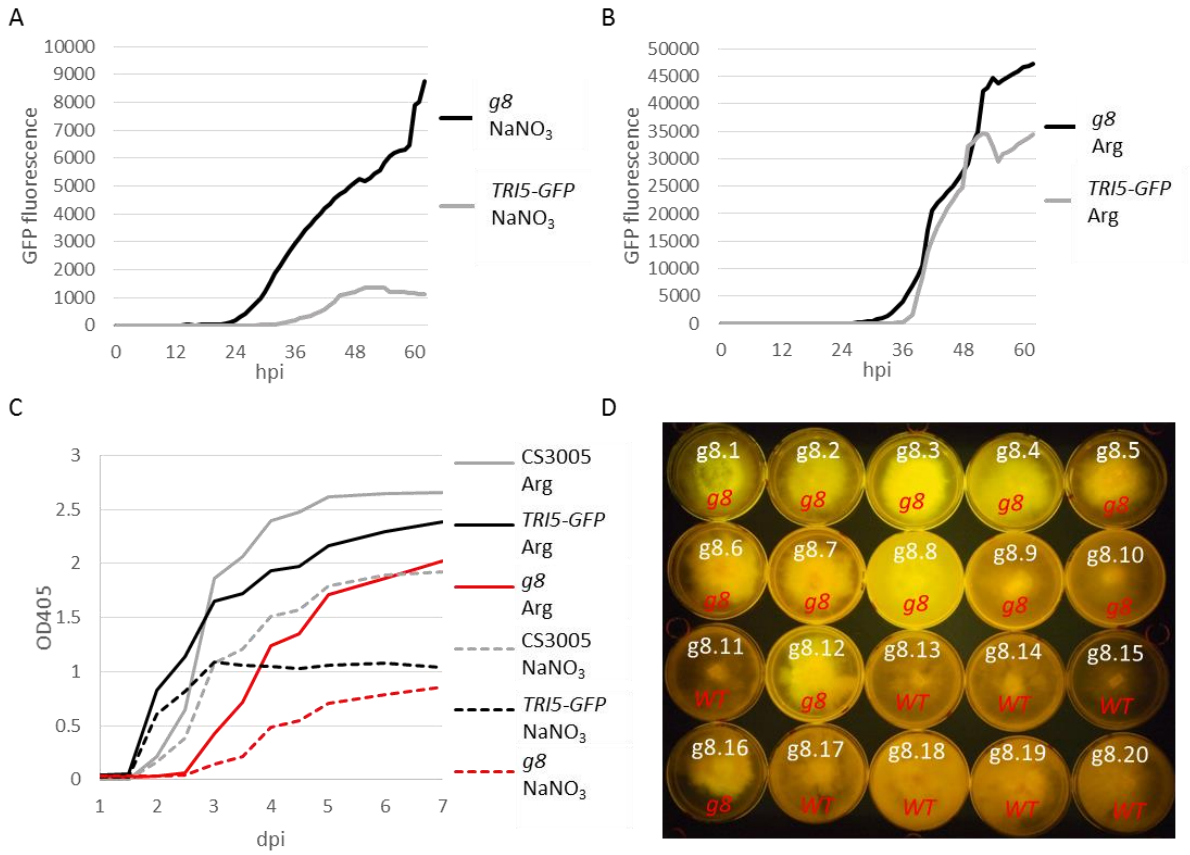

Figure S2. *g8* phenotype in different culture conditions. (**A** and **B**) TRI5-GFP fluorescence signals from *TRI5-GFP* and *g8* spores grown for four days in minimal media in six well plates with either $NaNO_3$ (**A**) or Arg (**B**) as sole nitrogen sources. (**C**) Relative growth (OD405) of CS3005, *TRI5-GFP* and *g8* spores grown for seven days in minimal media with either $NaNO_3$ or Arg as sole nitrogen sources (data from the same experiment presented in (Figure 2.3). **D** TRI5-GFP expression of *g8.1-20* progeny grown on minimal media agar plates with $NaNO_3$ as sole nitrogen source, visualised on a transilluminator (Clare Chemical Research). The white labelling indicates the progeny number and the red labelling if they carry the *g8 FAC1* or the *WT FAC1* allele.

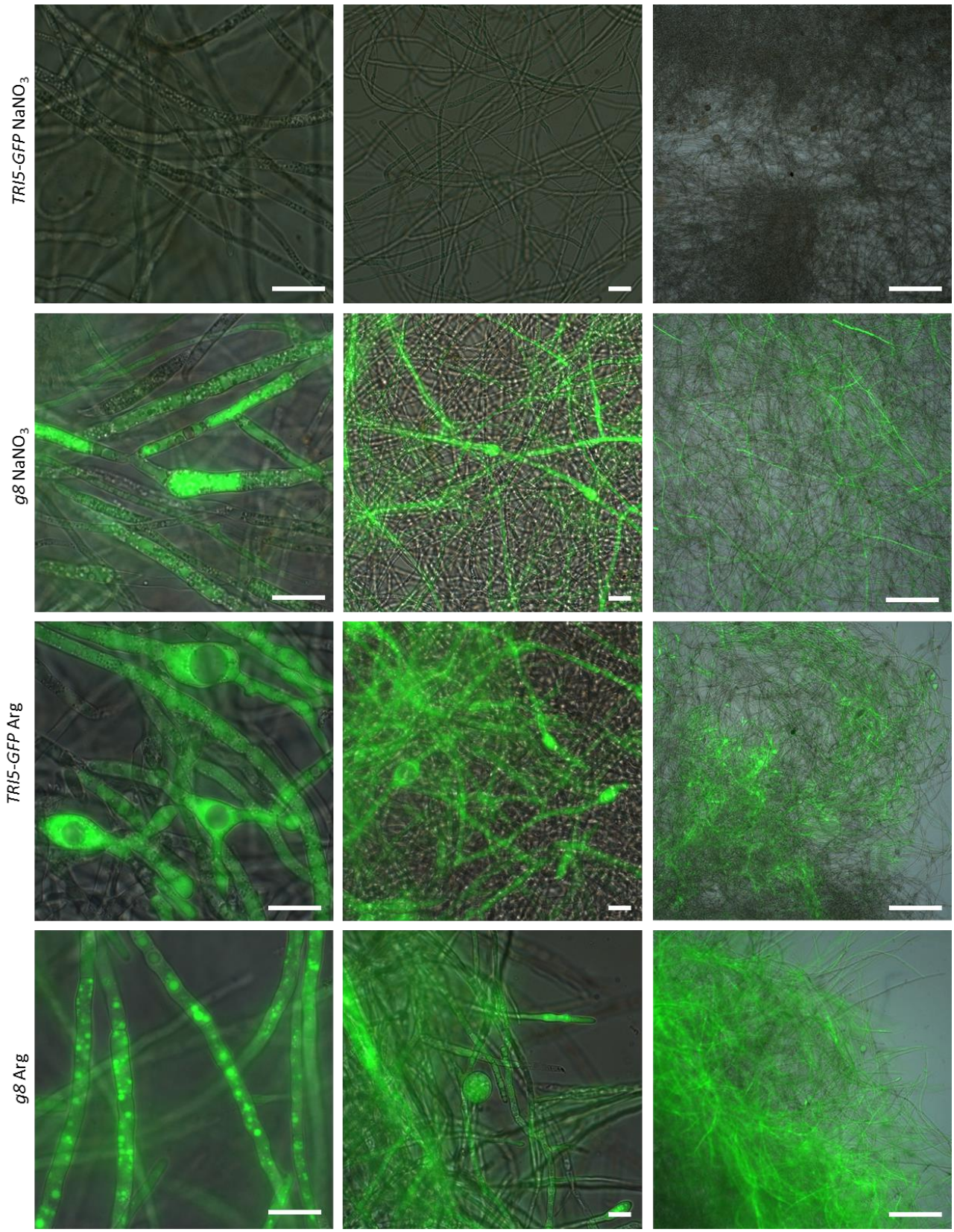

Figure S3. Microscopy of *TRI5-GFP* and *g8* grown under repressive ($NaNO_3$) and inductive (Arg) conditions. *TRI5-GFP* or *g8* spores were grown in 96 well plates for three days with either $NaNO_3$ or Arg as sole nitrogen sources. All images are merged images of DIC and GFP images. The white scale bars represent 20 µm in the first two columns and 200 µm in the third column.

Table S 1. Read coverage of the insert of three different *TRI5-GFP* transformants normalized by the average whole genome coverage (30 (*TRI5-GFP.1*), 44 (*TRI5-GFP.2*), 46 (*TRI5-GFP.3*)). *TRI5-GFP.1* is the *TRI5-GFP* reporter strain used in these studies.

Whole genome normalized coverage (total coverage)	5'homology flank	GFP-hph	3'homology flank
TRI5-GFP.1	0.9 (27)	0.7 (21)	1.0 (30)
TRI5-GFP.2	1.8 (77)	0.7 (31)	1.9 (83)
TRI5-GFP.3	2.7 (124)	1.4 (63)	3.0 (137)

3 The cytosolic trichodiene synthase TRI5 clusters around ER proliferations in nanoscale zones of the cytosol during deoxynivalenol production in *Fusarium graminearum*

Abstract

The production of the mycotoxin deoxynivalenol (DON) in *Fusarium graminearum* has been extensively studied due to its agronomic importance. The underlying genetics and enzymology are mostly known, but until recently the cell biology of toxin production had not been explored. Recent studies revealed that *F. graminearum* develops smooth endoplasmic reticulum (ER) proliferations (toxisomes) when it produces toxin and that two DON biosynthesis enzymes localize to these structures. However, the first DON biosynthesis enzyme TRI5 is localized in the cytosol, which raises the question how the toxin biosynthesis is coordinated between the cytosol and the ER. Here, super resolution structured illumination microscopy (SIM) was used to investigate this question. SIM indicated an accumulation of the cytosolic TRI5 around the toxisomes. Accordingly, a quantification system was developed to allow statistical analysis of fluorescence intensities of cytosolic proteins around toxisomes. The analyses of 91 toxisomes showed that the cytosolic TRI5-GFP accumulates significantly around toxisomes, whereas another fluorescently tagged cytosolic enzyme, which is part of the mevalonate pathway that feeds into toxin production, did not show any significant clustering. These results show that the cytosolic TRI5-GFP is not randomly distributed throughout the cytosol, but rather accumulates in nanoscale zones around toxisomes, where other DON biosynthesis enzymes are localized. These 250 nm zones are just above the resolution limit of 200 nm of conventional microscopy and thus the analysis was only possible due to the increased resolution of SIM.

3.1 Introduction

Fusarium graminearum synthesises the toxin deoxynivalenol (DON) during plant infection. DON is a major virulence factor during wheat infection (Jansen et al., 2005; Proctor et al., 1995a) and also the most common contaminant of wheat, maize and barley worldwide (Jelinek et al., 1989; The World Health Organisation, 1992). The *TRI* gene cluster encodes the biosynthesis enzymes which are required for the complex trichothecene biosynthesis

pathway which converts farnesyl pyrophosphate into DON (reviewed in Desjardins, 2006). During axenic culture, DON biosynthesis can be induced or repressed by growing the fungus in minimal media with specific nitrogen sources, e.g. putrescine induces DON production and sodium nitrate represses it (Gardiner et al., 2009a). Although, the genetics and enzymology behind DON production are known, nothing has been elucidated about the cell biology until recently.

Novel insights into the cell biology behind DON production by Menke et al. (2013) and Boenisch et al. (2017) showed that *F. graminearum* develops subcellular structures, called toxisomes, when it produces toxin *in vitro* as well as during plant infection. Menke et al. (2013) had described these subcellular structures as toxisomes in accordance to the aflatoxisomes, which *Aspergillus parasiticus* develops during aflatoxin production (reviewed in Roze et al., 2011). In *A. parasiticus* aflatoxin biosynthesis starts in peroxisomes and continues in the specialized aflatoxisomes which develop through the fusion of peroxisome and mitochondria derived vesicles with cytoplasm-to-vacuole transport vesicles and secretory vesicles (reviewed in Roze et al., 2011). In contrast, these *F. graminearum* toxisomes were shown to be smooth endoplasmic reticulum (ER) proliferations (Boenisch et al., 2017), also known as Organized Smooth ER (OSER) (Snapp et al., 2003). Transmission electron microscopy, as well as ER staining in living hyphae, showed that the toxisomes can only be found during toxin production inducing conditions, whereas the ER exhibits a fine reticulate network during toxin production repressing conditions (Boenisch et al., 2017). The *F. graminearum* toxisomes are similar to OSER previously described e.g. in mammalian hepatocytes grown in nutrient replete conditions. In contrast, the reticulate non proliferated ER structures observed under toxin production repressing conditions are similar to those observed in fasted mammalian hepatocytes (Fawcett, 1955).

The DON biosynthetic enzymes TRI1 and TRI4, as well as TRI14 (whose function is unknown), localize to these smooth ER proliferations (Boenisch et al., 2017). TRI1 and TRI4 are both cytochrome P450 monooxygenases which catalyse the eleventh and twelfth and the second through fifth DON biosynthesis steps respectively (reviewed in Desjardins, 2006). However, TRI5 which catalyses the first DON biosynthesis step, is localized in the cytosol (Blum et al., 2016; Boenisch et al., 2017). This raises the question how the toxin biosynthesis is coordinated between the cytosol and the smooth ER proliferations. To address this question, the localization of TRI5 and TRI4 were analysed using super resolution structural illumination microscopy (SIM).

In comparison to the resolution limits of conventional microscopy of about 250 nm in the x and y direction and >450-700 nm in the z direction, 3D SIM enables a resolution of about 100 nm in the x and y direction and about 400 nm in the z direction (reviewed in Galbraith and Galbraith, 2011). During SIM the whole field of view will be excited, however with a grid in front of the laser, which generates a striped pattern of light (Gustafsson, 2000). Together with the spatial pattern of the sample an interference pattern is created. For every image, fifteen individual images will be obtained, for which the grid will always be slightly rotated, to obtain a set of images with different interference patterns. Accordingly, the pattern of the grid can be mathematically removed from the images, as its exact light pattern is known. This mathematical processing and the following reconstruction of the single image out of the fifteen images enables a twofold resolution increase.

Here, the analysis of toxin producing *TRI5-GFP* hyphae with SIM indicated a potential gradient of the cytosolic TRI5-GFP enriched around the toxisomes. Accordingly, a quantification system was developed which allows statistical analysis of localization patterns of proteins in nanoscale subcellular regions. This analysis showed a significant accumulation of TRI5 in the cytosol directly around toxisomes, whereas another cytosolic protein, HMS1 predominantly accumulated in the cytosol apart from toxisomes.

3.2 Material and Methods

3.2.1 Culture conditions

To induce DON production, the fungus was grown in minimal medium with 5 mM putrescine as the sole nitrogen source. The medium was slightly modified from Correll et al. (1987) and contained the following ingredients per litre: 30 g sucrose, 1 g KH_2PO_4, 0.5 g $MgSO_4.7H_2O$, 0.5 g KCl, 10 mg $FeSO_4.7H_2O$, 200 µL of trace element solution (per 100 mL, 5 g citric acid, 5 g $ZnSO_4.7H_2O$, 0.25 g $CuSO_4.5H_2O$, 50 mg $MnSO_4.H_2O$, 50 mg H_3BO_3, 50 mg $NaMoO_4.2H_2O$) adjusted to pH 6.5 with NaOH. The fungus was grown in 5 ml of the inducing medium in 10 ml tubes, shaking in the dark at 25°C.

For spore production, the respective strains were grown in liquid CMC medium (Cappellini and Peterson, 1965) by shaking at 25°C under fluorescent white and blue lights.

3.2.2 Fungal strains

All fungal strains used in this study have been kindly provided and generated by Karen Broz (USDA, St. Paul, USA), Marike Boenisch (USDA, St. Paul, USA) and John Menke (USDA, St. Paul, USA). The strains carry C-terminal translational GFP or RFP fusions, which are under the control of the native promoters (Table 3.1).

Table 3.1. Fungal strains used in this study.

Strain	Background	Transgene	Reference
TRI5-GFP/ TRI4-RFP	PH-1 (NRRL 31084)	Translational *TRI5-GFP* and *TRI4-RFP* fusions	Boenisch et al., 2017
HMS1-GFP/ TRI4-RFP	PH-1 (NRRL 31084)	Translational *HMS1-GFP* and *TRI4-RFP* fusions	Crossing of *HMS1-GFP* (Broz, unpublished) and *TRI4-RFP* (Menke et al., 2013) strains
TRI5-GFP/ HMS1-RFP	PH-1 (NRRL 31084)	Translational *TRI5-GFP* and *HMS1-RFP* fusions	Crossing of *TRI5-GFP* (Boenisch et al., 2017) and *HMS1-RFP* (Broz, unpublished) strains

The *TRI5-GFP/TRI4-RFP* strain was created previously as described in Boenisch et al. (2017). An *HMS1-GFP* strain had been generated by transformation of a fusion PCR construct into protoplasts as described before (Menke et al., 2013). This *HMS1-GFP* strain had then been crossed with the previously published *TRI4-RFP* strain (Menke et al., 2013) to generate the double tagged *HMS1-GFP/TRI4-RFP* strain. The crossing procedure is described in detail in Boenisch et al. (2017). An *HMS1-RFP* strain had been generated by transformation of a fusion PCR construct into protoplasts as described previously (Menke et al., 2013). This *HMS1-RFP* strain had then been crossed with the previously published *TRI5-GFP* strain (Boenisch et al., 2017) to generate the double tagged *TRI5-GFP/HMS1-RFP* strain.

3.2.3 Super resolution microscopy

Structured Illumination Microscopy (SIM) was performed for the super resolution microscopy with wet mount samples of live liquid fungal cultures. These were imaged using a Nikon Ti-E microscope equipped with a Nikon structured illumination system, an Andor DU-897 X-8444 camera and an Apo TIRF 100x Oil DIC N2 (NA: 1.49 refractive index: 1.515) objective. For the detection of GFP signals a 488 nm laser was used for excitation and emission was detected at 525 nm. For the detection of RFP signals a 561 nm laser was used for excitation and emission was detected at 600 nm. Z-stacks were acquired in 0.2 µm steps using 3D SIM acquisition mode. Hyphae were mounted on glass slides (Gold Seal Plain Microslides) and covered with high precision 18x18 mm glass coverslips with a thickness of 170 nm ± 5 µm (Marienfeld Superior). Z stacks were reconstructed with the following settings of the Nikon NIS Elements AR software (Low contrast off; contrast 0.50; apodization 0.50; Width3DFilter 0.10; optimize on).

3.3 Results

3.3.1 The cytosolic TRI5-GFP shows a range of different localization patterns around toxisomes, but often clusters and co-localizes with toxisome margins

To get a better understanding of how toxin production is organised between the cytosolic TRI5 and the ER (toxisome) localised TRI4, a double tagged *TRI5-GFP/TRI4-RFP* strain was analysed using SIM. The higher resolution revealed a potential clustering of the cytosolic TRI5-GFP around the TRI4-RFP positive toxisomes, as indicated by the arrows in Figure 3.1 A and B. Most hyphae showed a clustering of TRI5-GFP with some co-localization at the TRI4-RFP positive toxisomes, similar to that shown in Figure 3.1 A. In some hyphae, strong co-localization of the clustering TRI5-GFP signals with all TRI4-RFP positive toxisomes could be observed (Figure 3.1 B). However, rarely some hyphae also showed more evenly distributed cytosolic TRI5-GFP signals, without distinct clustering or co-localization at the toxisomes (Figure 3.1 C). Thus, even though TRI5-GFP seemed to cluster around the toxisomes in most hyphae, there appeared to be a range of different localisation patterns varying from cell to cell.

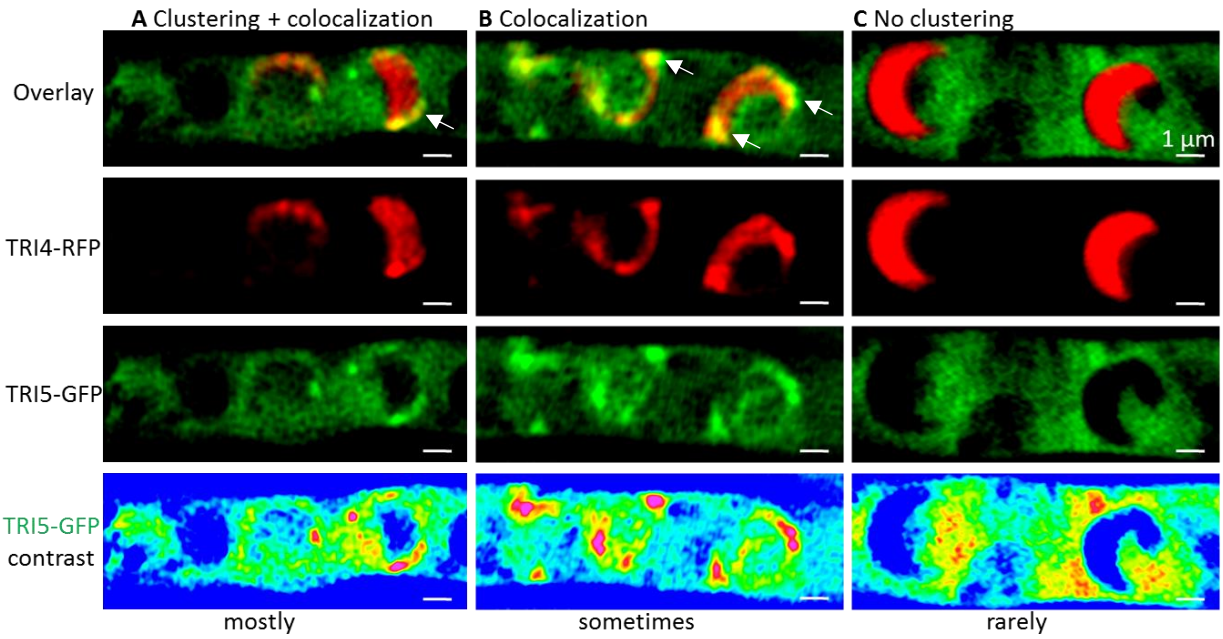

Figure 3.1. Super resolution microscopy images showing the different localization patterns of TRI5-GFP around TRI4-RFP labelled toxisomes. *TRI5-GFP/TRI4-RFP* strain was grown in toxin production inducing medium for 48h. The arrows indicate TRI5-GFP clustering at TRI4-RFP positive toxisomes. The first row shows an overlay, the second row TRI4-RFP signals, the third TRI5-GFP signals and the last row the TRI5-GFP signal intensities, with low to high fluorescence intensities shown in a colour scale from blue to pink. The scale bars represent 1 µm.

3.3.2 TRI5-GFP co-localizing with toxisomes indicates a cytosolic network intruding into the toxisome

The TRI5-GFP signals co-localizing with TRI4-RFP toxisomes, exhibited interesting patterns. Accordingly, the SIM images of *TRI5-GFP/TRI4-RFP* were analysed in more detail. First, the displayed TRI5-GFP signals were limited to only show the strongest TRI5-GFP signals. In the hyphae, in which TRI5-GFP was co-localizing with TRI4-RFP toxisomes, the strongest TRI5-GFP signals were mostly associated with toxisomes and seemed to form a network around and partially also through the toxisome (Figure 3.2, A-C). As the single images only show one slice of a toxisome, whole Z-stacks of toxisomes were reassembled to show a 3D projection of the toxisome (Figure 3.2, D).

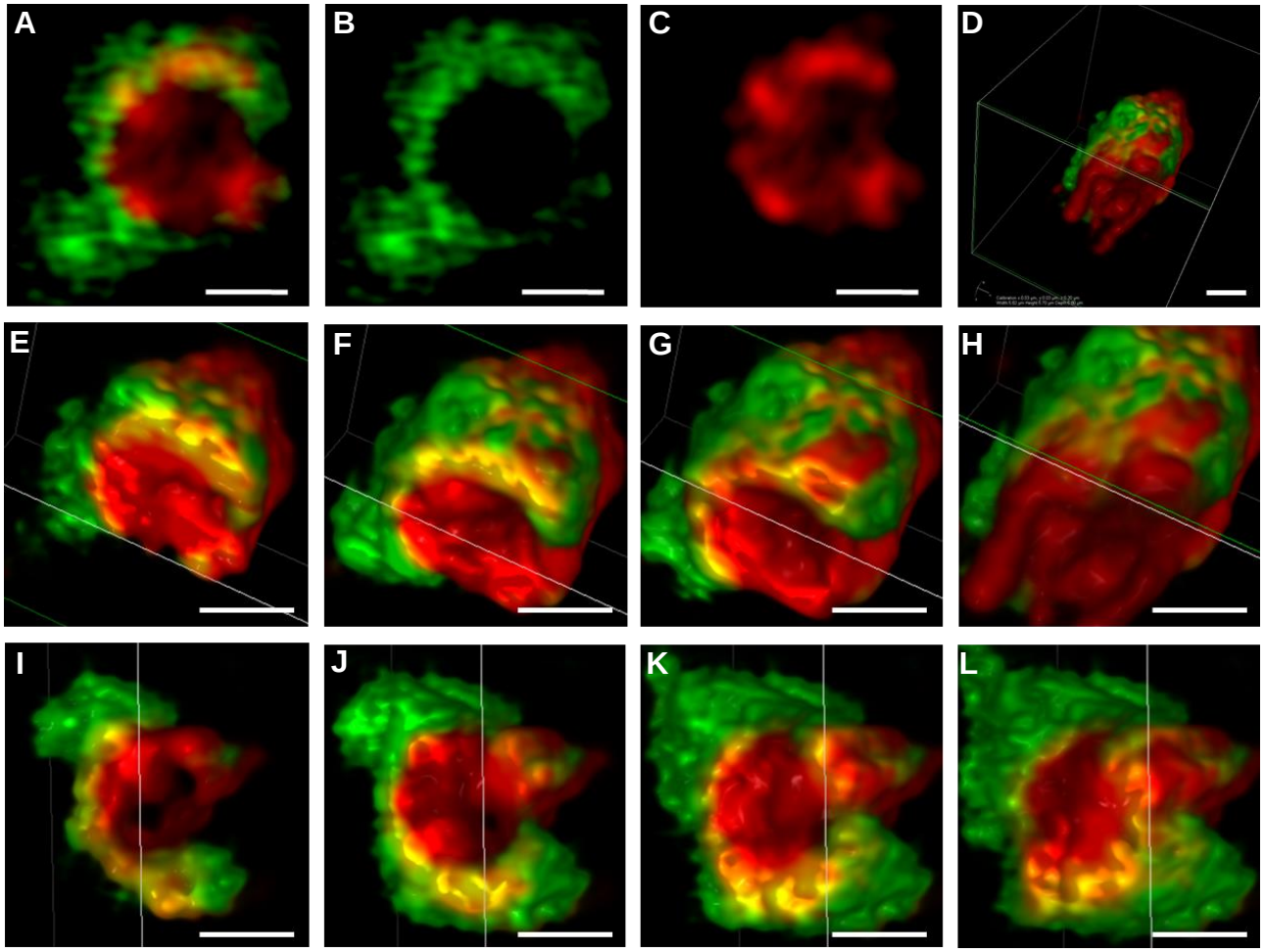

Figure 3.2. 3D volume shading of SIM showing clustering and co-localization of TRI5-GFP at a TRI4-RFP labelled toxisome. A-**C** show one layer of a Z-stack, whereas the first image shows an overlay, the second TRI5-GFP and the third TRI4-RFP. **D** shows a 3D volume shading reconstruction of the whole toxisome. **E**-**L** show a Z build-up of the toxisome, whereas the toxisome has been turned 180° in **I**-**L**. The TRI5-GFP signal display was limited to only display the strongest signals. The yellow signals indicate co-localization of TRI5-GFP and TRI4-RFP. The scale bars represent 1 µm. The fine white lines indicate the borders of the boundary box shown in **D**.

The 3D projection shows that the toxisomes seem to be formed by a complex ER network, which is surrounded by a complex network of cytosolic TRI5-GFP. The 3D projection was then sliced through the Z axis, which revealed irregular shaped “hollow”, i.e. fluorescently negative, spaces within the toxisome (Figure 3.2, E-L). In addition, the slices show how intimately the cytosolic TRI5-GFP network is wrapped around the toxisome. The TRI5-GFP intrusions throughout the toxisome can be observed irregularly throughout the whole length of the toxisome and thus seem to form a complex network through the whole toxisome.

3.3.3 HMS1-GFP also occasionally clusters and co-localizes around toxisomes, but less frequently than TRI5-GFP

To test if the above described clustering was a specific localization pattern of TRI5 or an artefact of SIM, the localization pattern of another cytosolic biosynthesis enzyme, namely HMG-CoA Synthase (HMS1) was analysed. HMS1 catalyses the condensation of acetyl-CoA with acetoacetyl-CoA forming 3-hydroxy-3-methylglutaryl-CoA (HMG-CoA) which is the second step of the mevalonate pathway. This pathway is an essential part of primary metabolism and produces farnesyl pyrophosphate which also feeds into various secondary metabolite pathways including the trichothecene pathway which produces DON.

The fluorescence signal from HMS1-GFP seemed to be evenly distributed throughout the cytosol without any obvious clustering around toxisomes in most cells, as shown in Figure 3.3, column A. However, while this was true for most cells, HMS1-GFP was also observed to cluster and co-localize at toxisomes in a few cells as indicated by the arrows in Figure 3.3 B and C. Thus, while there seemed to be a trend for a mostly even cytosolic localization pattern of HMS1-GFP, some cells showed different localization patterns, similar to the observations with TRI5-GFP.

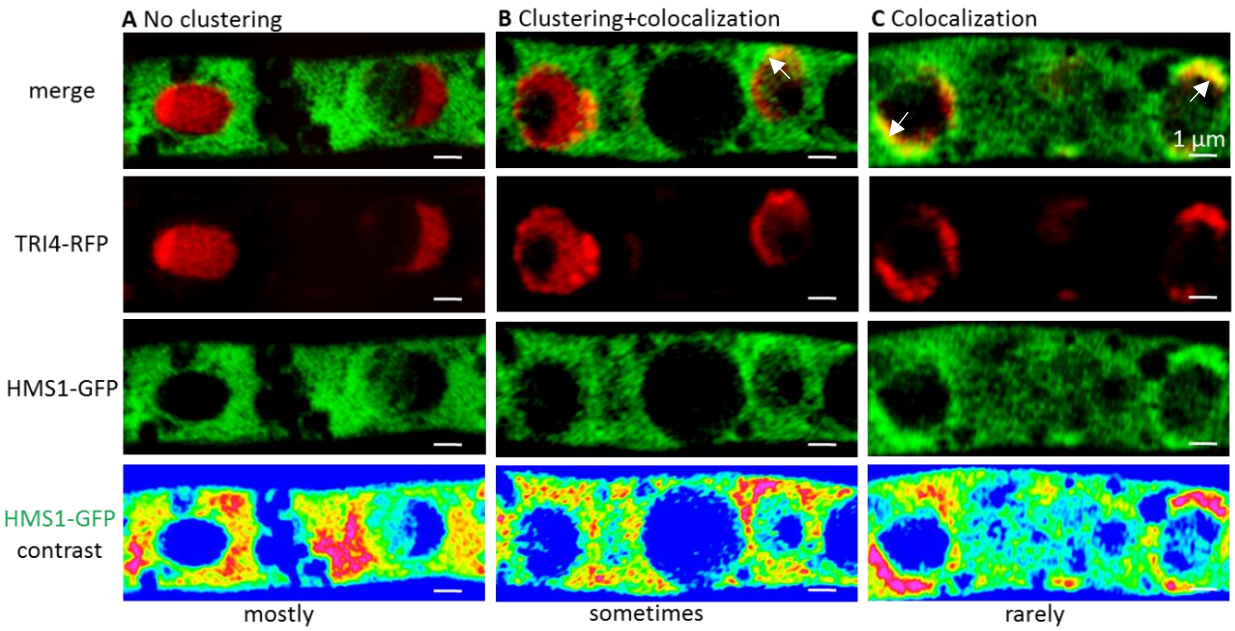

Figure 3.3. Super resolution microscopy images showing the different localization patterns of HMS1-GFP around TRI4-RFP labelled toxisomes. The *HMS1-GFP/TRI4-RFP* strain was grown in toxin inducing medium for 48h. The arrows indicate HMS1-GFP clustering at TRI4-RFP positive toxisomes. The first row shows an overlay, the second row TRI4-RFP signals, the third HMS1-GFP signals and the last row the HMS1-GFP signal intensities, with low to high fluorescence intensities shown in a colour scale from blue to pink. The scale bars represent 1 µm.

3.3.4 TRI5-GFP clusters at toxisomes more frequently than HMS1-RFP, when both are expressed in the same strain

The different localization patterns of TRI5-GFP and HMS1-GFP described above had been observed in separate strains, each with TRI4-RFP tagged toxisomes. Therefore, the different ratios of clustering and non-clustering localization patterns of TRI5-GFP and HMS1-GFP could be due to different cells being imaged in the different strains. To rule out the possibility that different hyphae at possibly different metabolic stages were imaged in the separate strains, a *TRI5-GFP/HMS1-RFP* strain was created that allowed SIM imaging of TRI5-GFP and HMS1-RFP in the same hyphae. Similar to the previous results, TRI5-GFP seemed to cluster around toxisomes more often than HMS1-RFP when they were expressed in the same cells, as shown in Figure 3.4 A. In this *TRI5-GFP/HMS1-RFP* strain the toxisomes can only be identified by the characteristic crescent-shaped non-fluorescent silhouette in the TRI5-GFP and HMS1-RFP cytosolic signals. The intensity displays of the fluorescence signals shown in the bottom two rows of Figure 3.4 A highlight that the strongest TRI5-GFP signals are mainly localized around the toxisome silhouette, indicating the clustering of TRI5-GFP. In contrast, the strongest HMS1-RFP signals did not seem to be spatially associated with the toxisome. On the other hand, in some cells TRI5-GFP and HMS1-RFP both clustered around toxisomes (Figure 3.4 B) and in rare cases clustering of neither of the two proteins could be observed (Figure 3.4 C). In summary, SIM analysis of the *TRI5-GFP/HMS1-RFP* strain showed a trend that TRI5-GFP clusters more often around toxisomes than HMS1-RFP, which is consistent with the previous observations of TRI5-GFP and HMS1-GFP in different strains (Figure 3.1, Figure 3.3).

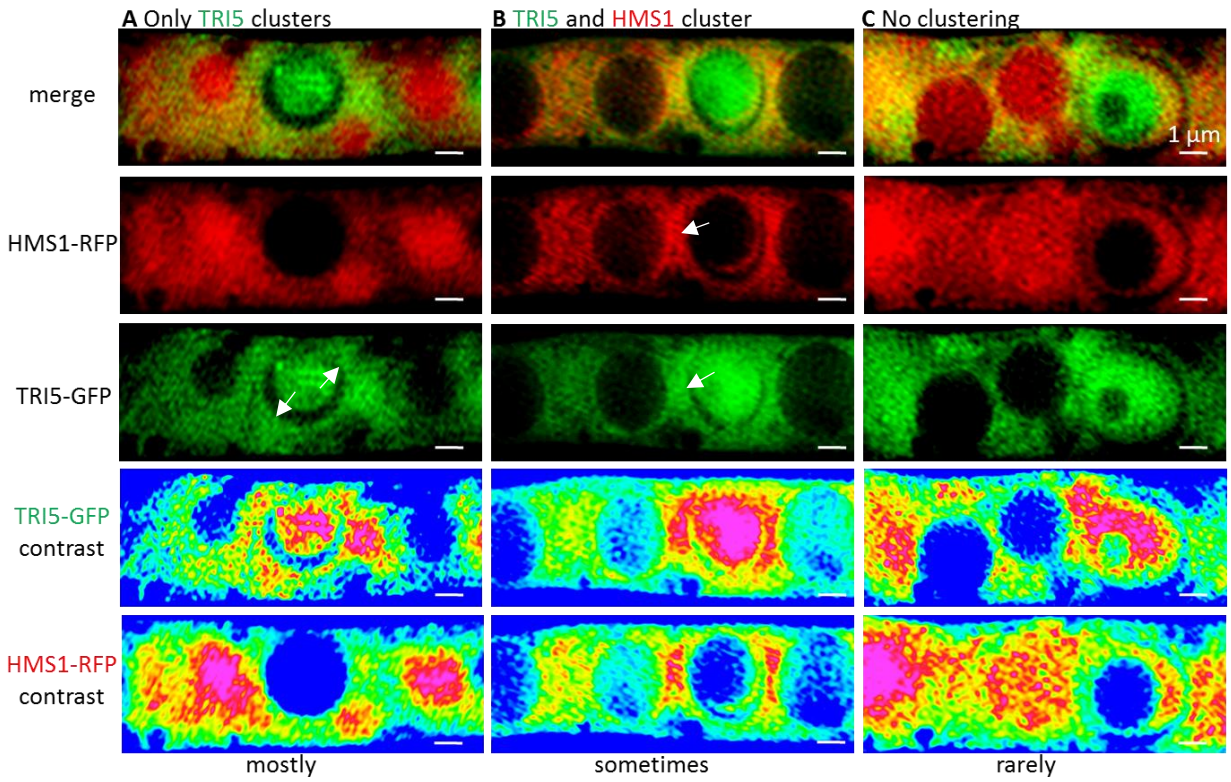

Figure 3.4. Super resolution microscopy images showing the different localization patterns of co-expressed TRI5-GFP and HMS1-RFP. *TRI5-GFP/HMS1-RFP* strain was grown in toxin production inducing medium for 48h. The arrows indicate TRI5-GFP or HMS1-RFP clustering at toxisome silhouettes. The first row shows an overlay, the second row HMS1-RFP signals, the third TRI5-GFP signals, the fourth row the TRI5-GFP signal intensities and the last row the HMS1-GFP signal intensities, with low to high fluorescence intensities shown in a colour scale from blue to pink. The scale bars represent 1 µm.

3.3.5 Quantification of fluorescence signals along 250 nm vectors confirms clustering of cytosolic TRI5-GFP around toxisomes

Although the qualitative image analysis suggested frequent clustering of TRI5-GFP around toxisomes, the situation was complex. As such, a system was developed to quantify the fluorescence signal differences of TRI5-GFP or HMS1-GFP around toxisomes in comparison to the average cytosolic signals. As shown in Figure 3.5, the fluorescence signals of TRI5-GFP and HMS1-GFP were quantified in the 250 nm toxisome-cytosol interface and in the 250 nm toxisome periphery (Figure 3.5 A, blue lines). For both TRI5-GFP and HMS1-GFP the highest signals that could be found in the two areas were quantified. These signals were then normalised by the average cytosol signals per 250 nm in the same cell and in the same Z section as the respective toxisome (Figure 3.5 B). Ten 250 nm cytosol regions were quantified and averaged within a 2500 nm zone, as indicated by the blue lines

in Figure 3.5 B. For these ten 250 nm measurements a 2500 nm cytosol region with the highest fluorescence signals was chosen to determine the respective average cytosol signals per 250 nm, for both TRI5-GFP as well as for HMS1-GFP. In this manner, the signal ratios of 91 toxisome-cytosol interfaces and 91 toxisome peripheries were quantified respectively for both TRI5 and HMS1 to sample representative fluorescence distribution patterns and to allow statistical analysis.

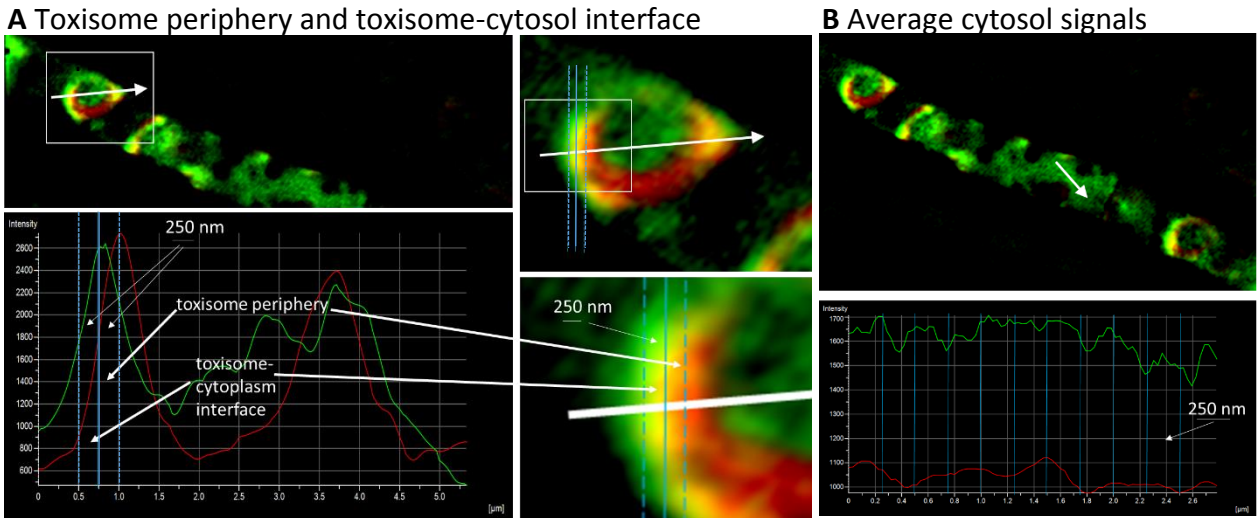

Figure 3.5. Quantification of fluorescence signals at 250 nm wide zones at the toxisome periphery and at the toxisome-cytosol interface. A Fluorescence signals of TRI5-GFP and HMS1-GFP were quantified in two, 250 nm zones around the toxisome. The zones quantified were the 250 nm inward from where the toxisome TRI4-RFP signals start increasing (the toxisome-cytosol interface) and the adjacent 250 nm of the toxisome periphery. **B** The respective signals from the two zones were each normalised by the average cytosol signals per 250 nm in the same cell and Z section.

The quantification of fluorescence in separate strains in which the toxisomes were marked with TRI4-RFP showed that the TRI5-GFP signals were on average about 29% higher at the periphery of toxisomes and about 10% higher at toxisome-cytosol interfaces compared to the cytosol (Table 3.2, grey rows). In contrast, HMS1-GFP signals were on average 17% lower at the periphery of toxisomes and 6% lower at toxisome-cytosol interfaces. These differences in the signal ratios of TRI5 and HMS1 were highly significant ($p<10^{-18}$ and $p<10^{-6}$). The higher signals of TRI5-GFP at toxisome peripheries compared to toxisome-cytosol interfaces were also statistically significant ($p<10^{-3}$). This also applied to the opposite effect observed with HMS1-GFP, where signals at toxisome peripheries were significantly lower compared to toxisome-cytosol interfaces ($p<10^{-6}$).

Table 3.2. Quantification of TRI5-GFP, HMS-GFP and HMS-RFP signals at toxisome borders. The grey rows show the results from the two separate *TRI5-GFP5/TRI4-RFP* and *HMS1-GFP/TRI4-RFP* strains and the white rows below the results from the *TRI5-GFP/HMS1-RFP* strain. A two tailed student's t-test type two was performed to determine, if the differences between TRI5 and HMS1 are significant with $p<10^{-6}$ indicating high statistical significance.

		Mean fold difference to average cytosolic signal	Standard deviation	Student's t-test p
Toxisome periphery	TRI5-GFP	1.286388596	0.398667	$7.77835x10^{-19}$
	HMS1-GFP	0.833909004	0.159573	
Toxisome-cytosol interface	TRI5-GFP	1.100409881	0.254216	$2.47071\ x10^{-7}$
	HMS1-GFP	0.941360074	0.123946	
Toxisome periphery	TRI5-GFP	1.018343108	0.139187	$1.42626\ x10^{-9}$
	HMS1-RFP	0.901071093	0.106485	
Toxisome-cytosol interface	TRI5-GFP	1.079027276	0.131922	$1.07135\ x10^{-7}$
	HMS1-RFP	0.97549623	0.120011	

The same quantitative analysis was also performed using the *TRI5-GFP/HMS1-RFP* strain. In this strain, both TRI5-GFP as well as HMS1-RFP could be quantified in the same cell at the same toxisome to exclude a bias in the analysis due to imaging cells in potentially different metabolic stages. As this strain was lacking a toxisome marker, the toxisome border was defined by the absence of fluorescence signals in the shape of a toxisome in the cytosolic TRI5-GFP and HMS1-RFP signals, as shown before in Figure 3.4. Similar to the results obtained from the separate strains, TRI5-GFP signals were on average higher in the two toxisome margin regions than in the cytosol, whereas HMS1-RFP signals were on average lower (Table 3.2, white rows).

At the toxisome periphery, TRI5-GFP signals were on average about 2% higher than in the cytosol and HMS1-RFP signals were about 10% lower. Again these differences between TRI5-GFP and HMS1-RFP were highly significant ($p<10^{-8}$). A similar localization pattern could be observed at the toxisome-cytosol interfaces, where TRI5-GFP signals were approximately 8% higher than in the cytosol and HMS1-RFP signals were about 2% lower.

The decreased differences of the TRI5-GFP signals between the toxisome peripheries and the cytosol were probably caused by the analysis technique, because toxisomes had been identified by their absence of signal in the cytosol for both TRI5-GFP and HMS1-RFP.

Therefore, the toxisome border region might have shifted towards the cytosol, which might decrease effects compared to measurements from the separate strains with the toxisome marker. However, due to this no toxisomes at which TRI5-GFP would have shown a strong co-localization were quantified, as the characteristic toxisome crescent silhouette would be masked by the strong TRI5-GFP signals. Nonetheless, although these potentially strongest signals of TRI5-GFP at the toxisome peripheries were not measured in this second quantification, the same trend could be observed with higher TRI5-GFP signals and lower HMS1-RFP signals at both toxisome margins compared to the cytosol, supporting the initial observations that TRI5 clusters around toxisomes.

In both the qualitative and quantitative analysis a range of different localisation patterns of both proteins could be observed in individual cells (Figure 3.1, Figure 3.3 and Figure 3.4). This is illustrated by the wide spread distribution of signal fold changes from well below one right through to signal fold changes well above one (Figure 3.6). Although, this range of localization patterns, i. e. the range of fold changes could be observed for both TRI5 and HMS1, the boxplots also show, that the TRI5 datasets are shifted towards signal fold changes greater than one. The notches in the boxplots of TRI5 and HMS1 are not overlapping within the two different toxisome margins, which indicates that not only the arithmetical means are significantly different to each other (as shown by the *p*-values), but also the medians are significantly different to each other. Taken together, the quantification system was able to reflect the range of different localization patterns of both cytosolic proteins TRI5 and HMS1, indicating that this is likely a dynamic process, but also demonstrated that TRI5-GFP clusters in the cytosol around toxisomes.

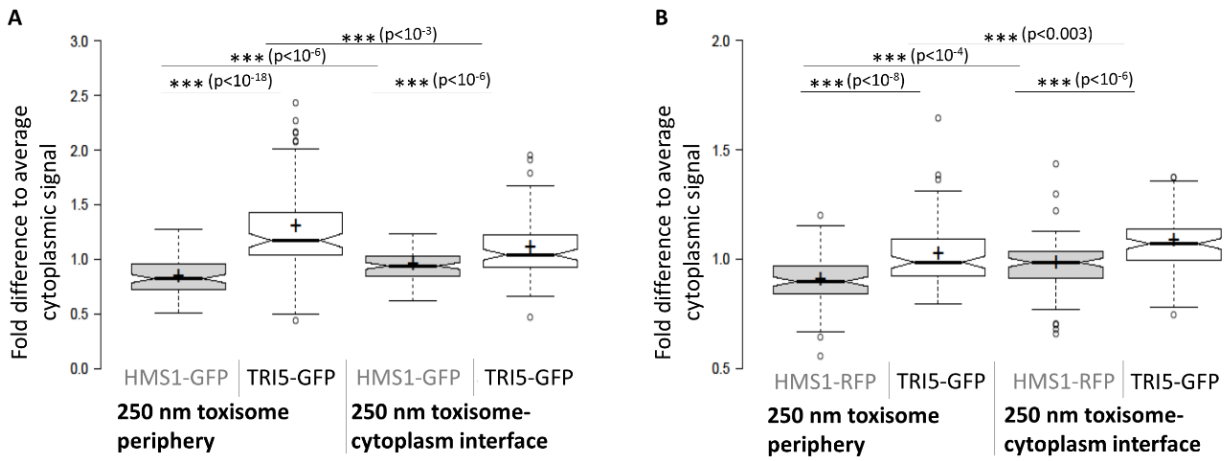

Figure 3.6. Quantification of TRI5-GFP and HMS1-GFP and -RFP signals around toxisomes. The box plots show the distribution of the normalised fluorescence signals in the toxisome peripheries and toxisome-cytosol interfaces quantified in the *TRI5-GFP/TRI4-RFP* and *HMS1-GFP/TRI4-RFP* strains (**A**) as well as in the *TRI5-GFP/HMS1-RFP* strain (**B**) with n=91. All strains were grown under toxin production inducing conditions for 48 h before they were imaged by super resolution microscopy. The notched boxes show the interquartile range (IQR), i.e. the middle 50% of the data, the bold band the median, the cross the mean, the whiskers the data points that are less than 1.5 x IQR away from the first or third quartile, according to Tukey, and the circles show the outliers. The notches represent the 95% confidence intervals (+/ 1.58 x IQR/sqrt(n)) of the medians, whereas non-overlapping notches indicate about 95% confidence that two medians differ. The asterisks indicate statistically significant mean differences with *** for p<0.005 (student's t-test type two with two tails).

3.3.6 TRI5-GFP is more likely to cluster around toxisomes when HMS1-RFP is also clustering around the same toxisome

Since both TRI5-GFP and HMS1-RFP sometimes appeared clustered around toxisomes and sometimes not, the question arose if their localization patterns were correlated, for example if TRI5-GFP would only cluster at toxisomes where HMS1-RFP would not cluster or vice versa. Qualitative analysis of the SIM images of the *TRI5-GFP/HMS1-RFP* strain did not show any clear trend. Accordingly, the quantitative dataset of the *TRI5-GFP/HMS1-RFP* strain (Figure 3.6 B) was tested for a statistical correlation between the signal ratios of TRI5-GFP and HMS1-RFP.

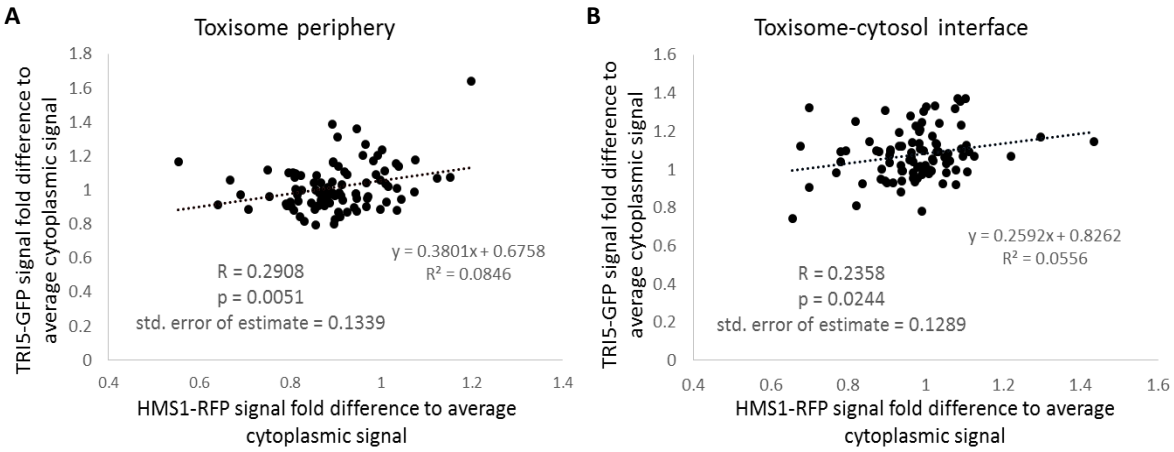

Figure 3.7. Scatter plots of TRI5-GFP and HMS1-RFP signal fold changes at toxisome peripheries and toxisome-cytosol interfaces. R shows the Pearson correlation coefficient and p the statistical significance of R in a two tailed students T-test of the 91 TRI5-GFP and HMS1-RFP signal fold differences to the average cytosol signals at toxisome margins (**A**) and cytosol margins around toxisomes (**B**).

As expected from the qualitative image analysis, the scatter plots of the TRI5-GFP and HMS1-RFP signal ratios did not show a strong correlation (Figure 3.7). However, there seems to be a weak, but statistically significant, positive correlation between the TRI5-GFP and HMS1-RFP signal ratios with a Pearson correlation coefficient of R = 0.29 (Figure 3.7 A) at the toxisome margin and R = 0.24 at the cytosol margin (Figure 3.7 B). So although HMS1-RFP does on average not cluster significantly at toxisome margins, it seems that when HMS1-RFP is clustering, TRI5-GFP is more likely to cluster around the same toxisome.

3.4 Discussion

Here, areas of soluble enzyme enrichment within the cytosol in toxin producing cells were identified. SIM, in combination with the quantitative signal analyses developed here, revealed and showed a statistically significant clustering of the cytosolic enzyme TRI5-GFP in 250 nm zones around toxisomes. The size of these cytosolic regions is close to the 200 nm resolution limit of conventional confocal microscopy. These findings raise a number of questions about the reasons for the different clustering behaviours of these two cytosolic enzymes which are from connected biosynthesis pathways and what function the clustering could have for the producing organism.

Why is TRI5 clustering around toxisomes?

The clustering of the cytosolic TRI5-GFP around the toxisomes might allow metabolite channelling from the cytosol to the toxisomes. Transmission electron microscopy had shown that there are thin cytosolic layers in between ER membrane stacks, which might allow a sequestration of potentially toxic intermediates (Boenisch et al., 2017). As TRI5 was not only clustering around the toxisomes, but also partially co-localising with them, TRI5 could potentially be localized in those thin cytosolic layers between the ER membrane stacks in the toxisomes. This theory is further supported by the network-like TRI5-GFP signals intruding throughout toxisomes, which have been shown here. In addition, the catalytic domain of the ER resident cytochrome P450 monooxygenases TRI1 and TRI4 is predicted to be on the cytosolic side. The transmission electron microscopy images of Boenisch et al. (2017) showed that the cytosolic layers were only about 10 nm wide. This narrow interface could bring cytosolic (TRI5) as well as ER resident (TRI1, TRI4) DON biosynthesis enzymes and intermediates into close proximity to allow efficient biosynthesis of DON.

Is there be a multi enzyme complex for DON biosynthesis?

The data presented above supports the possibility that DON biosynthesis enzymes, as well as in some cases a mevalonate pathway enzyme, are in relatively close proximity in toxin producing cells. Fluorescence Resonance Energy Transfer data (Broz, unpublished) confirmed a close proximity (≤10 nm) of TRI1, TRI4 and HMR1 (HMG (3-Hydroxy-3 methylglutaryl)-CoA reductase, catalysing the step after HMS1 in the mevalonate pathway). This could indicate a multi enzyme complex which facilitates metabolite channelling, not only within the DON biosynthesis pathway, but maybe even from a primary metabolite pathway, i.e. the mevalonate pathway to the secondary trichothecene biosynthesis pathway which produces DON. During aflatoxin production in *Aspergillus parasiticus*, metabolites are thought to be channelled through a multi enzyme complex formed by the first three aflatoxin biosynthesis enzymes (Watanabe and Townsend, 2002) and a potential further multi enzyme complex formed by at least four middle and late aflatoxin biosynthesis enzymes (Roze et al., 2011).

Could HMS1 be part of the potential multi enzyme complex?

A potential multi enzyme complex in *F. graminearum* including HMR1 could also explain, why HMS1 (part of the mevalonate pathway) is sometimes also clustering at toxisomes and why the TRI5-GFP and HMS1-RFP signals at toxisomes correlate positively. Expression data showed that genes encoding the biosynthesis enzymes of the mevalonate pathway are

also upregulated when toxin production is induced in *F. graminearum* (Broz, unpublished). However, they were upregulated 24 h earlier than the TRI genes. Hence, the prevalence of TRI5 clustering around the toxisomes and the more even cytosolic distribution of HMS1 may reflect the situation at this particular time point, namely 48 h after induction. Accordingly, HMS1 might be clustering around the ER at earlier time points before it is relocated to the general cytosol to allow the cytosolic TRI5 to cluster at the toxisome ER proliferations when the metabolism is shifting towards an increased DON biosynthesis. Hence, the different localization patterns of TRI5-GFP and HMS1-GFP and HMS1-RFP might reflect different metabolic stages of the respective cells. Taken together the data presented here and that of others suggests that there is a dynamic toxin biosynthesis multi enzyme complex at the interface of the cytosol and the toxisomes that likely includes primary metabolite pathway enzymes, but also that the resident proteins in that complex may change over time.

Is the multienzyme complex involved in the development of toxisomes?

In mammalian cells, yeast cells, as well as plant cells, smooth ER proliferations can be induced by overexpressing ER resident transmembrane proteins, like HMR1 (Gong et al., 1996; Ohkuma et al., 1995; Sandig et al., 1999; Snapp et al., 2003; Takei et al., 1994; Vergeres et al., 1993; Wright et al., 1990; Yamamoto et al., 1996). Thereby, the membrane insertion and retention mediating domains of ER resident proteins seem to induce the development of the smooth ER proliferations, as the C-terminal membrane anchor of HMR1 was already sufficient to induce these proliferations (Sandig et al., 1999). However, another report showed that the cytosolic HMR1 domain was also required for the formation of smooth ER proliferations (Profant et al., 1999). In accordance with this, Snapp et al. (2003) showed that dynamic low affinity interactions of ER resident proteins induce the development of organized smooth ER structures in mammalian cells. Thus, the potential DON-biosynthesis-multi-enzyme-complex itself could be inducing the formation of toxisomes through the high expression levels of the ER resident TRI1, TRI4 and HMR1 proteins, as well as through potential low affinity interactions between those biosynthesis enzymes.

Is subcellular partitioning a general phenomenon in fungal secondary metabolism?

Subcellular partitioning of toxin biosynthesis has been reported in other fungi, however in different cellular organelles than in *F. graminearum*. Instead of proliferating its ER to toxisomes, *Aspergillus parasiticus* develops toxisomes from peroxisomes and other vesicles (Roze et al., 2011). In *Penicillium chrysogenum* and *Aspergillus nidulans* the first penicillin biosynthesis enzyme is also localized in the cytosol like TRI5, but in contrast is also localized

at the vacuole and the final biosynthesis step is compartmentalized in peroxisomes (Müller et al., 1992; van de Kamp et al., 1999; van der Lende et al., 2002). Cyclosporine biosynthesis in *Tolypocladium inflatum* starts at the vacuolar membrane and is then compartmentalized in the vacuole (Hoppert et al., 2001). Thus, carbon flow during cyclosporine biosynthesis seems to be directed from the cytosol to the vacuolar lumen and during penicillin biosynthesis from the vacuole to the cytosol to peroxisomes (reviewed in Roze et al., 2011), whereas metabolite channelling seems to be directed from the cytosol to the ER in *F. graminearum*. In addition, the biosynthesis of another fungal secondary metabolite melanin is also compartmentalized (Upadhyay et al., 2016). In *Aspergillus fumigatus* and *A. nidulans* cytosolic enzymes involved in early steps of melanin biosynthesis are recruited to endosomes through a non-conventional secretory pathway, whereas late melanin enzymes accumulate in the cell wall (Upadhyay et al., 2016).

Taken together, different secondary metabolite biosynthesis pathways seem to be organised into different cellular organelles. Nevertheless, there may be a common need to compartmentalise different biosynthetic steps into different organelles, perhaps due to precursor availability, but also for self-protection from toxic intermediates. At the same time, the biosynthetic machinery needs to be in close association to allow efficient biosynthesis. In *F. graminearum* this is achieved through the co-localization of biosynthesis enzymes from different metabolic pathways at ER proliferations around which cytosolic biosynthesis enzymes from the same biosynthesis pathways are clustering. Thus, against the common first impression, that cytosolic enzymes are just randomly distributed throughout the cytosol, this study provides evidence that two cytosolic biosynthesis enzymes show statistically significant different distribution patterns around toxisomes. This highlights the complexity of secondary metabolism in filamentous fungi, as it involves e.g. in *F. graminearum* not only the regulation of biosynthesis gene clusters, but also subcellular reorganization of fundamental cellular organelles as well as the recruitment of cytosolic biosynthesis enzymes by yet unknown mechanisms.

4 Regulation of a novel cytokinin biosynthesis cluster in *Fusarium pseudograminearum*

Abstract

The Fusarium genus has the potential to produce a wide range of secondary metabolites of which only few have been characterized. Recently a novel gene cluster was discovered in *F. pseudograminearum,* which has the capability to produce a cytokinin-like metabolite named fusatin. It is structurally similar to plant cytokinins and can activate cytokinin signalling *in vitro* and in *Brachypodium*, however, nothing further is known about its function. Here, the induction of fusatin production was analysed *in vitro*. This revealed, that similar to deoxynivalenol (DON) production in *F. graminearum*, fusatin production can be induced *in vitro* by specific nitrogen sources. DON production was also induced in both *F. graminearum* and *F. pseudograminearum* in fusatin inducing conditions, however at lower levels compared to non-fusatin-inducing conditions. In addition, microscopic analyses of wheat seedlings infected with a fusatin reporter strain showed that *F. pseudograminearum* specifically induces fusatin production in hyphae, which are in close association with the plant, indicating a function of fusatin during infection.

4.1 Introduction

Like other Fusaria, *F. pseudograminearum* produces a wide range of secondary metabolites, for example the mycotoxin deoxynivalenol (DON). In the closely related *F. graminearum* DON is an important virulence factor during wheat infection and is required for the spread of the fungus from the infection site through the rachis to other florets (Jansen et al., 2005; Proctor et al., 1995a). The role of DON in *F. pseudograminearum* during crown rot is not as well understood, but DON seems to be required for the spread of the fungus from the crown and stem base to upper stem nodes (Mudge et al., 2006).

Other secondary metabolites produced by *F. pseudograminearum* are the polyketides zearalenone and fusarin and non-ribosomal peptides, like ferricrocin and fusarinine (reviewed in Hansen et al., 2015). Comparative genome analysis from the afore mentioned study identified 14 putative polyketide synthases (PKS) and 16 non-ribosomal peptide synthases (NPRS) in *F. pseudograminearum*, whereas only the products of 8 PKSs and of

4 NPRSs are known (Hansen et al., 2015). Thus, although not every PKS or NPRS might actually produce a product, there are still many secondary metabolites which have not been identified yet, especially considering that there are also other groups of secondary metabolites. Many of the PKSs and NPRSs are shared between different Fusaria, but some are also exclusive to some or even just one. *F. pseudograminearum* shares almost all PKSs and NPRSs with the closely related *F. graminearum*, but the PKS40 and the NPRS32 are exclusively found in *F. pseudograminearum* and produce the polyketide non-ribosomal peptide fused compounds W493 A and B (Hansen et al., 2015). A further genomic analysis identified 67 putative gene clusters with a significant enrichment of predicted secondary metabolism related enzymatic functions in *F. graminearum*, of which 57 had orthologs in *F. pseudograminearum* (Sieber et al., 2014).

Recently a gene cluster has been identified in *F. pseudograminearum*, which synthesises a novel class of cytokinins, called fusatins (Sørensen et al., 2017). The gene cluster does not exist in the closely related *F. graminearum*, but orthologues could be found in *F. oxysporum*, *F. fujikuroi* and *F. verticillioides* (Sørensen et al., 2017). The gene cluster is upregulated during plant infection and the compound looks structurally similar to known plant cytokinins (Sørensen et al., 2017). Fusatin could activate cytokinin signalling in an *in vitro* assay and in *Brachypodium*, but its function during infection is still unknown (Sørensen et al., 2017).

Cytokinins had first been described as phytohormones in plants promoting cell growth and differentiation as well as delaying leaf senescence (reviewed in Ferreira and Kieber, 2005). In addition to plants, a vast array of bacteria, algae and fungi are also able to produce cytokinins. During symbiotic mycorrhizal infection of plant roots, cytokinins are produced by both the plant host as well as the mycorrhizal fungi (reviewed in Gogala, 1991) and are important for successful colonization and symbiosis, but also to prevent parasitism by the fungus (Cosme et al., 2016; Foo et al., 2013). Similarly, *Rhizobia* root nodule bacteria produce cytokinins to induce the development of symbiotic root nodules in legumes (Phillips and Torrey, 1970). Plant pathogens, such as *Agrobacterium tumefaciens*, also produce cytokinins during plant infection to manipulate their host to their own advantage (Akiyoshi et al., 1984). In addition, locally increased cytokinin levels in plants infected with the biotrophic rust and powdery mildew fungal plant pathogens delay senescence of the infected leaves which leads to the formation of green islands, though it is not known yet if the fungi produce the cytokinins themselves, or the host metabolism is altered to induce localized cytokinin production in the plant (reviewed in Ashby, 2000 and Walters and McRoberts, 2006). The

hemibiotrophic fungus *Pyrenopeziza brassicae* produces cytokinins which might suppress host cell death during brassica infection to allow the colonization of healthy tissue (Gan and Amasino, 1995; Murphy et al., 1997).

Here, the regulation of the fusatin biosynthesis cluster in *F. pseudograminearum* under different nitrogen sources, as well as the cellular development associated with the induction of the cluster, was analysed. As a similar biosynthesis regulation through specific nitrogen sources and pH had been observed before during DON production in *F. graminearum*, the production levels of fusatin and DON under these different axenic culture conditions were quantified in both *F. pseudograminearum* and *F. graminearum*.

4.2 Materials and Methods

4.2.1 Fungal strains and wheat cultivar

The *F. pseudograminearum* isolate CS3096 was used as wild type strain for the wheat seedling infections. The *F. pseudograminearum FpFCK1-GFP* fusatin reporter strain was created by Aurelie Benfield (CSIRO Agriculture & Food, Brisbane, Australia) and carries a C-terminal translational *GFP* fusion in the endogenous *FpFCK1* locus in the CS3096 *F. pseudograminearum* wild type background. The *F. graminearum* DON reporter strain *FgTRI5-GFP* also carries a translational C-terminal *GFP* fusion in the endogenous *FgTRI5* locus in the CS3005 *F. graminearum* wild type background (Blum et al., 2016). The wheat cultivar Kennedy was used for the wheat seedling infections.

4.2.2 Fusatin and DON production induction assays

For the induction assays 1000 spores were inoculated into 100 µL minimal medium per well in 96 well plates. The minimal medium used was slightly modified from Correll et al. (1987) and contained the following ingredients per litre: 30 g sucrose, 1 g KH_2PO_4, 0.5 g $MgSO_4.7H_2O$, 0.5 g KCl, 10 mg $FeSO_4.7H_2O$, 200 µL of trace element solution (per 100 mL, 5 g citric acid, 5 g $ZnSO_4.7H_2O$, 0.25 g $CuSO_4.5H_2O$, 50 mg $MnSO_4.H_2O$, 50 mg H_3BO_3, 50 mg $NaMoO_4.2H_2O$). Either 40 mM asparagine or citrulline were added as sole nitrogen sources and the pH adjusted to 4.5 with HCl and NaOH. The citrulline medium also contained 0.02 % yeast extract, because the fungus was growing very poorly in the citrulline medium without the yeast extract. After inoculation the 96 well plates were incubated at 28 °C in the dark and measured every day with a Perkin Elmer (Waltham, MA, USA)

EnVision plate reader. GFP was excited at 488 nm and detected at 509 nm and growth rates were determined by measuring the absorbance at 405 nm (OD 405). The GFP intensities were then normalised by the respective OD 405 values. Three biological replicates were averaged for each sample.

4.2.3 Fusatin and DON liquid chromatography quantification

The total amounts of fusatin and DON produced after 7 days of growth in 96 well plates were analysed from the same samples which had been analysed for the fusatin and DON production induction assays. For the high performance liquid chromatography (HPLC) quantification the metabolites from the whole fungal colony of each well, as well as the liquid medium, were extracted by adding 100 µL pure methanol and 500 µL extraction buffer (50% ethyl acetate, 33% methanol, 16% dichloromethane, 1% formic acid) to each sample. Accordingly, the samples were sonicated for ten minutes before they were centrifuged at 13000 g for five minutes. Five hundred µL of the supernatant were transferred to a new reaction tube and dried down under N_2 before being resuspended in 200 µL methanol. The samples were centrifuged again at 13000 g for five minutes and 150 µL of the supernatant were transferred into a 300 µL HPLC vial (Phenomenex, Torrance USA). The HPLC system used here was a Waters Acquity Arc UHPLC system equipped with a QDa (mass) detector. For the analysis 5 µL sample were injected and separated on a Phenomenex Kinetex phenyl–hexyl column (100 mm × 2.1 mm ID, 2.6 µm) using a flow of 0.4 mL/min with a linear water-acetonitrile gradient, where both eluents were buffered with 0.1% formic acid. The gradient started at 5% acetonitrile and reached 100% in 12 min. Afterwards the column was allowed to recover for 8 min to restore starting conditions again for the next sample. Single ion monitoring of $[M+H]^+ \pm m/z$ 0.5 was used for each compound. Five biological replicates were averaged for each sample.

4.2.4 Fluorescence microscopy

For the analysis of the subcellular localization of FCK1-GFP, wet mounts of fungal colonies from the 96 well induction assay were analysed with a ZEISS (Oberkochen, Germany) AXIO Imager.M2 with a 100× oil objective. For GFP excitation a 470/40 nm bandpass filter was used and for GFP emission detection a 525/50 nm bandpass filter.

The *FpFCK1-GFP* infected wheat seedlings were analysed with a Leica (Wetzlar, Germany) MZ16 FA fluorescence stereomicroscope with a 1,6× planapochromatic objective. For GFP detection the GFP2 filter set was used with a 425/60 nm excitation filter and a 510 nm longpass filter for emission detection.

4.2.5 Wheat seedling infection

Wheat seeds cv. Kennedy were sterilized in 10% ethanol with 0.64% sodium hypochlorite for five minutes and washed three times in sterile deionized water. Seven seeds were put onto 150 mm petri dishes containing two water soaked filter papers. The plates were wrapped in aluminium foil and placed at 4°C overnight. The next day the plates were transferred to a 20°C plant growth chamber still covered in aluminium foil. After two days the aluminium foil was removed and the seedlings were infected with 4 µL of either *F. pseudograminearum* wild type *CS3096* spores or *FpFCK1-GFP* spores (10^6 spores per mL). The spores were pipetted either onto the root or the crown of the seedlings. The crown infections were aided by slight puncturing with the pipette tip.

4.3 Results

4.3.1 Fusatin production can be induced by asparagine in *F. pseudograminearum in vitro*

Previous experiments had identified asparagine and citrulline as potential inducers of fusatin biosynthesis *in vitro* (Benfield, unpublished). These experiments were performed with a *F. pseudograminearum* fusatin reporter strain, which expresses a C-terminal translational GFP fusion of the fusatin biosynthesis enzyme FCK1 (FPSE_06372). The *FpFCK1-GFP* strain was grown in PM 3 Phenotype MicroArray plates (nitrogen utilization assays) (Biolog, Hayward, USA), which are commercially available 96 well plates, containing different nitrogen sources in each well. To confirm these preliminary results, time course experiments were performed with the *FpFCK1-GFP* reporter strain grown in asparagine, as well as in citrulline. In addition, a *F. graminearum FgTRI5-GFP* reporter strain (TRI5 is the first DON biosynthesis enzyme) was also analysed in the same manner to see if asparagine or citrulline induce DON production in *F. graminearum*.

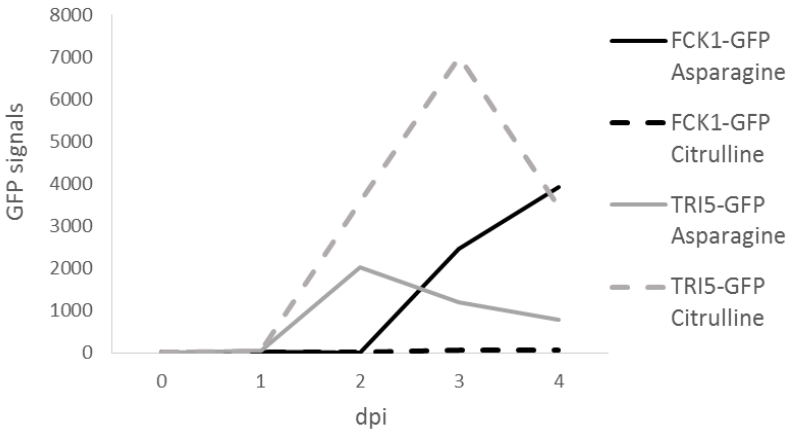

Figure 4.1. FCK1-GFP and TRI5-GFP induction in asparagine and citrulline. *FpFCK1-GFP* and *FgTRI5-GFP* spores were grown in minimal medium with either asparagine, or citrulline as sole nitrogen sources for four days. (dpi: days past inoculation)

As shown in Figure 4.1, asparagine could be confirmed as an inducer of FCK1-GFP expression in axenic culture. From three days after inoculation (dpi) strong FCK1-GFP signals could be detected in the media containing asparagine. In contrast, only background GFP signals could be detected when the *FpFCK1-GFP* reporter strain was grown in citrulline until four days after inoculation. Thus, citrulline could not be confirmed as an inducer of FCK1-GFP expression under these conditions. In *F. graminearum* both citrulline and asparagine induced TRI5-GFP expression from two dpi, which was one day earlier than FCK1-GFP induction in *F. pseudograminearum*. In contrast to FCK1-GFP induction, higher TRI5-GFP signals could be detected in citrulline than in asparagine, whereas FCK1-GFP expression was only induced by asparagine.

4.3.2 DON and fusatin quantification in *F. pseudograminearum*

To test if the FCK1-GFP signals also reflect the actual fusatin levels produced by the *FpFCK1-GFP* reporter strain, the total fusatin levels produced during the previous time course experiment (Figure 4.1) were quantified by high performance liquid chromatography (HPLC). In addition, the total DON levels were quantified in the same samples. As asparagine induced TRI5-GFP expression in *F. graminearum*, we wanted to know if *F. pseudograminearum* was also producing DON when fusatin biosynthesis was induced.

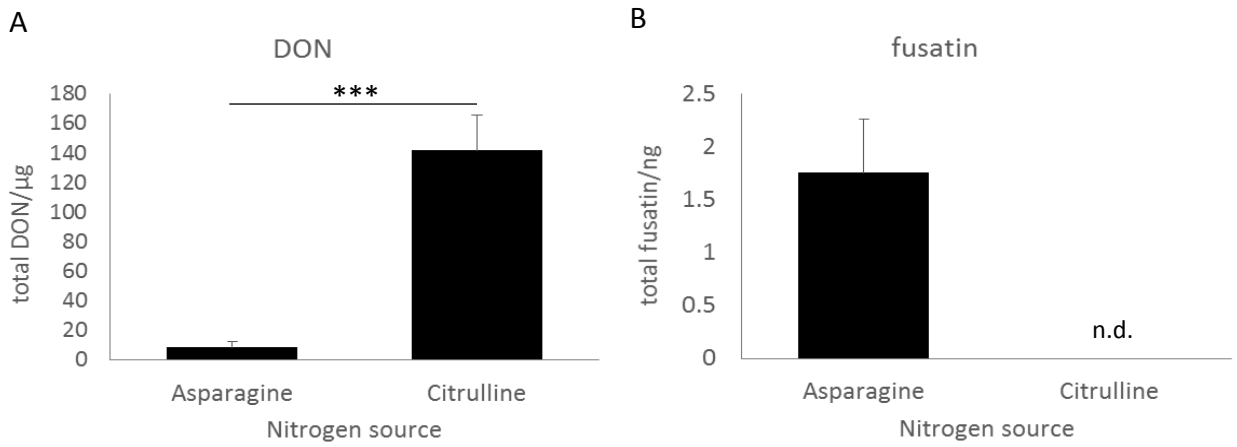

Figure 4.2. HPLC quantification of total fusatin and DON levels. The *FpFCK1-GFP* samples from the previous induction assay, grown in minimal media with asparagine or citrulline as sole nitrogen sources, were analysed 7 dpi. The asterisks indicate statistically significant differences with $p<10^{-6}$ (two tailed student's t-test type two). In the citrulline sample fusatin was not detectable (n.d.).

Similar to the TRI5-GFP induction in *F. graminearum* (Figure 4.1), the *FpFCK1-GFP F. pseudograminearum* strain produced significantly more DON when it was grown in citrulline medium than in asparagine medium (Figure 4.2 A). The fusatin levels also correlated with the FCK1-GFP induction (Figure 4.1) and in contrast to DON production, fusatin was only produced in detectable levels in asparagine medium (Figure 4.2 B).

4.3.3 The fusatin biosynthesis enzyme FCK1 is localized in the cytosol

As the *FpFCK1-GFP* reporter strain carries a translational GFP fusion, the subcellular localization of FCK1-GFP was analysed by fluorescence microscopy. Similar to the DON biosynthesis enzyme TRI5 in *F. graminearum* (Blum et al., 2016; Boenisch et al., 2017), the *F. pseudograminearum* FCK1-GFP is also localized in the cytosol (Figure 4.3). Under the fusatin biosynthesis inducing conditions *F. pseudograminearum* also developed ovoid cells (Figure 4.3, second row), which are similar to those previously observed in *F. graminearum* during DON biosynthesis inducing conditions (Blum et al., 2016; Menke et al., 2013).

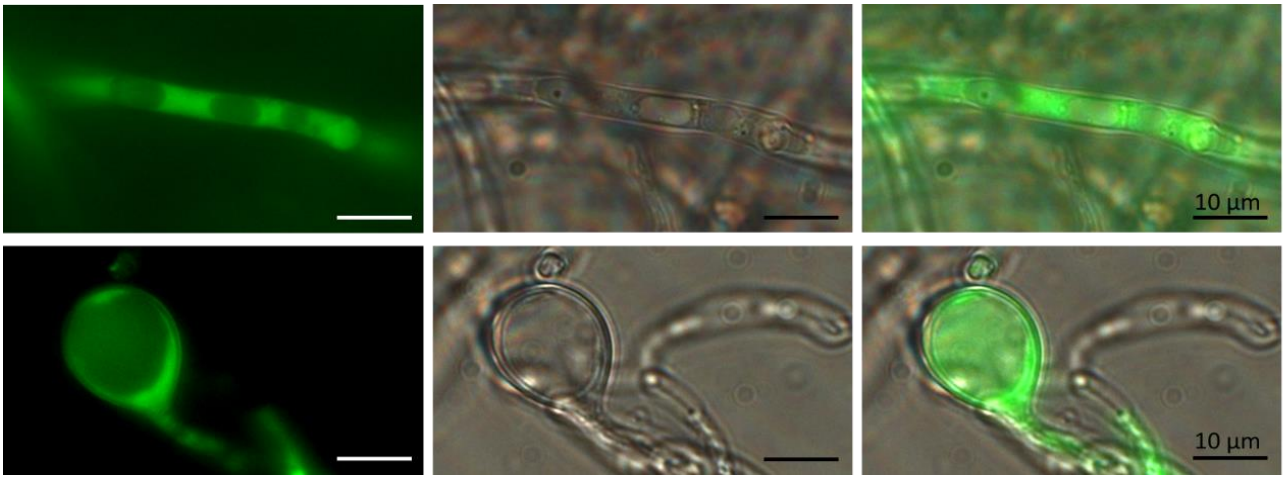

Figure 4.3. Fluorescence microscopy of *FpFCK1-GFP* hyphae. *FpFCK1-GFP* spores were grown in minimal media with asparagine as sole nitrogen source for four days. The first column shows the GFP channel, the second a DIC image and the third an overlay. In the first row a hyphae can be seen and in the second row an ovoid cell. The scale bars indicate 10 µm.

4.3.4 *F. pseudograminearum* specifically induces fusatin biosynthesis during infection in hyphae in close contact with the plant

To get a better understanding of whether fusatin is involved in plant infection in *F. pseudograminearum*, wheat seedlings were infected with the *FpFCK1-GFP* reporter strain and analysed by fluorescence microscopy. During the course of infection, there was substantial hyphal growth on the outside of the infected seedlings, yet no FCK1-GFP signals could be detected in the hyphae growing on the seedling surface (Figure 4.4 A, B). When the infection was repeated, very weak GFP signals could be seen in some hyphae above the crown and the start of the roots as well as in some hyphae growing out of the top of the coleoptile (not shown). However, when the coleoptile was pulled back 10 days after infection, clear GFP signals could be detected in densely packed hyphae on the inside of the coleoptile as well as on the pseudostem, which was previously covered in the coleoptile (Figure 4.4 C, D). In addition, after removal of the coleoptile the outer leaf was sliced open to reveal the younger leaf. Between the two leaves many fluorescing hyphae could be detected which were interconnected by hyphal clumps. The FCK1-GFP signal intensities were much higher in the hyphae growing in between the leaves and the coleoptile than the signal intensities in hyphae growing on the surface, so that no signals could be detected in the hyphae on the surface with the acquisition settings used for the hyphae in between leaves.

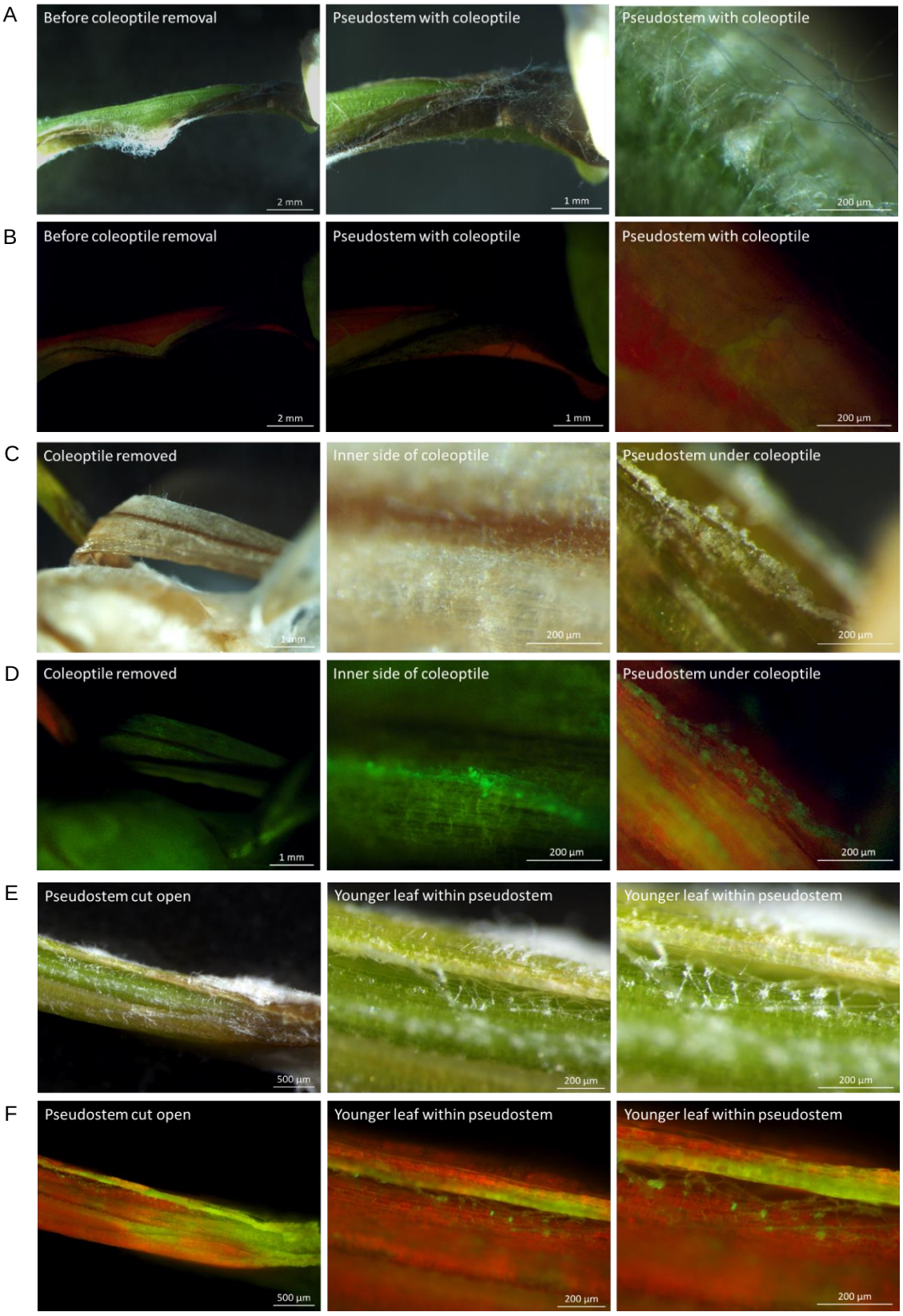

Figure 4.4. Fluorescence microscopy of *FpFCK1-GFP* infected wheat seedlings. A and **B** show hyphae growing on the surface of intact seedlings 15 dpi and 11 dpi (last column). In **C** and **D** the coleoptile was removed to show hyphae growing in between the coleoptile and the pseudostem 10 dpi. **E** and **F** show hyphae growing in between the outer and inner leaf in an open cut pseudostem of a seedling 10dpi. **A**, **C** and **E** show bright field images and **B**, **D** and **F** GFP images.

Fifteen days after infection the coleoptile was almost fully dried out and no fluorescing hyphae could be found underneath (not shown). However, when the leaves were pulled apart, strong FCK1-GFP signals could be detected in dense hyphal mats, which were in close association with the inside of the first leaf (Figure 4.5 A, B). The hyphae also seemed to have been associated with the second leaf underneath before they were pulled apart (Figure 4.5 A, B, arrow). When the second leaf was removed, the surface of the third and youngest leaf was revealed to be intensely colonised by the fungus and most hyphae showed GFP signals (Figure 4.5 C, D). The weak signals of the roots (Figure 4.5 A, B, first column) appeared to be autofluorescence of the roots. Similarly, the signals which can be seen from the dead coleoptile as well as some parts of the first and second leaves in column one of C and D of Figure 4.5, are due to autofluorescence of dead tissue.

The infections had been repeated a second time with an independent spore preparation, which also included another *FpFCK1-GFP* transformant. The above described scenarios were not specific to a certain time point after infection, but rather seemed to be dependent on the course of infection in each individual plant. Fluorescing hyphae in between the coleoptile and the pseudostem were usually found during earlier infection stages, when the crown was already brown, but the leaves did not show too many symptoms yet. The fluorescing hyphae in the pseudostem in between the leaves were found when the infection had progressed further and the leaves were showing clear symptoms. However, during final infection stages, when the plant tissue was completely necrotic, none of the hyphae within the plant were fluorescing anymore. Thus, FCK1-GFP seems to be mainly induced in hyphae growing in close association with the plant in between living plant tissue, and less in dead tissue or outside the plant.

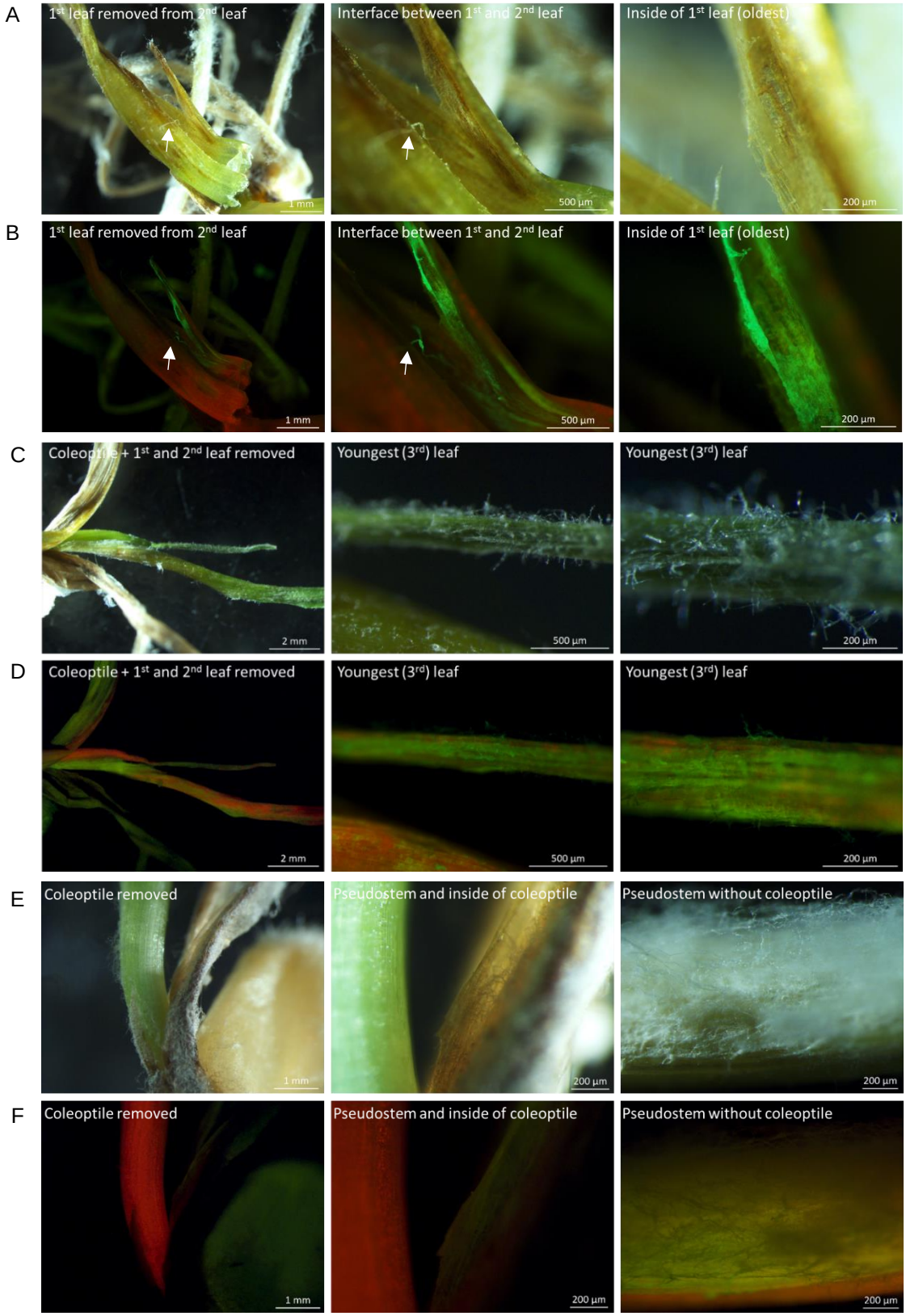

Figure 4.5. Fluorescence microscopy of *FpFCK1-GFP* (A-D) and CS3096 (E, F) infected wheat seedlings. The wheat seedlings were imaged 15 dpi. **A** and **B** show hyphae growing in between the first and second leaf, which have been pulled apart. In **C** and **D** the older first and second leaves have been removed to show hyphae growing on the youngest leaf (third) which was fully wrapped in the second leaf before. **E** and **F** show wheat seedlings infected with CS3096. **A**, **C** and **E** show bright field images and **B**, **D** and **F** GFP images.

As a negative control, wheat seedlings were also infected with the CS3096 *F. pseudograminearum* wild type strain (Figure 4.5 E, F). A similar auto fluorescence could be observed from dead plant tissue, which can be seen in the background in Figure 4.5 F, but as expected no fluorescence could be detected in the hyphae.

4.4 Discussion

Here we show that the expression of the *F. pseudograminearum* fusatin biosynthesis enzyme FCK1 can be induced *in vitro* by specific nitrogen sources, similar to the DON biosynthesis enzyme TRI5 in *F. graminearum*. During the four day time course experiment asparagine induced FCK1-GFP, as well as TRI5-GFP, whereas citrulline only induced TRI5-GFP but not FCK1-GFP. The time course also showed that TRI5-GFP was induced one day earlier in *F. graminearum* than FCK1-GFP in *F. pseudograminearum*.

The HPLC DON quantifications in the *FpFCK1* strain showed that the DON production in this *F. pseudograminearum* strain reflected the TRI5-GFP expression under the different conditions in the *FgTRI5-GFP F. graminearum* strain. Hence, DON production seems to be regulated similarly in *F. graminearum* and *F. pseudograminearum* under the axenic culture conditions used here. On the other hand, fusatin production was induced in an opposite manner to DON production in *F. pseudograminearum*, indicating differing regulatory mechanisms which allow the fine tuning of the different expression patterns of FCK and TRI5.

Similar to DON production in *F. graminearum*, *F. pseudograminearum* develops ovoid cells in asparagine containing medium, however as the fungus also produces DON under these conditions, the cellular development could also be linked to DON production. Nevertheless, in *F. pseudograminearum* FCK1-GFP is expressed in these ovoid cells and is localised in the cytosol, similar to TRI5-GFP in *F. graminearum* (Blum et al., 2016; Boenisch et al., 2017).

Although, previous experiments indicated that fusatin is most likely a cytokinin and that it can induce cytokinin signalling in *Brachypodium* (Sørensen et al., 2017), the actual function of fusatin in *F. pseudograminearum* is still unknown. The microscopic analysis of *FpFCK1-GFP* infected wheat seedlings indicates that fusatin might play a role during wheat infection, as FCK1-GFP is mainly induced in hyphae growing in close association with living plant tissue within the plant. However, not all hyphae growing in between leaves were fluorescing. This seemed to be most often the case, when the plant tissue showed

substantial cell death, but also when there was no cell death at all. Often, FCK1-GFP positive hyphae could be found in a zone in between mainly dead tissue and the still healthy tissue, where cell death was starting to occur in some isolated cell groups. Thus, fusatin might play a role during a very specific time point of infection, which seems to be in between the biotrophic and the necrotrophic phase of infection. Although *in vitro* fusatin production inducing conditions also induce DON production, this does not necessarily mean that they would be coproduced during the same infection stages or in the same hyphae at the same time. It would be interesting to introduce a DON reporter construct, like TRI5-RFP, into the *FpFCK1-GFP* strain to analyse the production of these two secondary metabolites during plant infection at the same time.

In other plant pathogenic fungi cytokinins are produced during plant infection to delay senescence and to allow the colonization of healthy plant tissue by the fungus (reviewed in Ashby, 2000 and in Walters and McRoberts, 2006; Gan and Amasino, 1995; Murphy et al., 1997). Accordingly, fusatin could play a similar role in *F. pseudograminearum* during wheat infection and suppress host cell death to allow the spread of the fungus in the still healthy plant tissue before the fungus switches to the necrotrophic infection phase during which DON production is potentially induced to kill the plant cells. In addition to delaying senescence, plant cytokinins also increase the sink strength, especially in younger plant tissue (Leopold and Kawase, 1964; Richmond and Lang, 1957; Roitsch and Ehneß, 2000). Hence, *F. pseudograminearum* could produce fusatin to manipulate the tissue it is infecting to become a sink tissue, so there will be more nutrients available for the fungus. On the other hand, cytokinins have also been shown to regulate the accumulation of defense metabolites in different plant species (Brütting et al., 2017; Dervinis et al., 2010; Schäfer et al., 2015; Smigocki et al., 1993) which would be counterproductive for the fungus during infection. Thus, it would be very interesting to see if the fungal fusatins are able to only activate certain cytokinin signalling pathways in the plant which are beneficial for the fungus, but are able to avoid those that would induce plant defense responses. However, the cost of the plant defense metabolite accumulation might also be less than the benefit of the nutrient accumulation for the fungus. In addition, *F. pseudograminearum* is able to detoxify wheat benzoxazolinone defense metabolites (Kettle et al., 2015) and thus may have evolved to tolerate the accumulation of certain plant defense metabolites. In summary, the data so far support a potential role of the *F. pseudograminearum* produced cytokinins during wheat infection, however the exact mechanisms of action still remain to be revealed.

5 Discussion

In this thesis, the regulation and cell biology of secondary metabolites was investigated using deoxynivalenol (DON) and fusatin biosynthesis in *Fusarium graminearum* and *F. pseudograminearum* as examples.

First a novel high throughput mutant screen was developed to identify regulators of secondary metabolite production. Here, a gain-of-function allele of the *F. graminearum* adenylyl cyclase was identified, which resulted in DON production under repressive conditions. This is the first gain-of-function adenylyl cyclase allele described in filamentous fungi. In addition, this is also the first mutant to be described, which develops cellular structures associate with toxin production under repressive conditions.

The results of the second chapter present the first super resolution SIM analyses in *Fusarium* and, to my knowledge, the first quantitative analyses of accumulation patterns of cytosolic proteins in filamentous fungi. The significant clustering of TRI5-GFP around toxisomes shows that the cytosol is not just a homogenous soup after all and that cytosolic proteins can exhibit more complex localization patterns.

The results presented in the third chapter showed for the first time that the production of the novel *F. pseudograminearum* cytokinins is partially co-regulated with DON production and that cytokinins are produced during wheat infection in hyphae in close association with the plant. Microscopically the production of this compound also appears to occur in structures similar to those observed during DON biosynthesis. The identification of likely shared regulatory and developmental processes during DON and fusatin production presents the question: how are the production of the vast array of different secondary metabolites regulated temporally and spatially during the fungal development not only in the different life and infection stages, but also within a fungal colony as well as within individual cells?

5.1 Adenylyl cyclase signalling network regulating DON production in *F. graminearum*

At the beginning of this PhD project a mutant screen was developed to identify regulators of DON production in *F. graminearum*. In this mutant screen a gain of function mutant of the *F. graminearum* adenylyl cyclase FAC1 was identified, which causes overproduction of DON under repressive conditions. This confirmed previous results, which had shown that FAC1 is essential for DON production, as a Δ*fac1* knockout was unable to produce DON (Bormann

et al., 2014). Adenylyl cyclases are universal regulatory proteins which can be found ubiquitous throughout nature from uni- to multicellular organisms where they regulate a vast array of different biological processes (Båhzu and Danchin, 1994; Linder, 2006). However, because adenylyl cyclase mediated cAMP signalling is involved in so many different biological processes, the activity of these master regulators needs to be tightly regulated as well. Heterotrimeric G-proteins are known regulators of adenylyl cyclases. Yu et al. (2008) reported that the knockout mutants of the *F. graminearum* heterotrimeric G-protein subunits α 1, Δ*gpa1*, and β 1, Δ*gpb1* produce more DON. Thus the G-protein subunit α 1 (GPA1) and β 1 (GPB1) might be negative regulators of DON production. However, separate knockout mutants of *GPA2* and *GPA3* did not alter DON production, but Δ*gpa2* was less virulent on wheat heads, thus GPA2 and perhaps also GPA3 might be redundant positive regulators of DON production. A potential role of GPA2 as a positive regulator for DON production is supported by studies of a constitutive active signalling GPA2^{Q207L} mutant which overproduces DON (Park et al., 2012). Perhaps the binding site for one of the afore-mentioned G protein subunits is mutated in the *g8* FAC1. This could block the binding of potentially negative regulators like GPA1 or GPB1 or conversely mimic binding of potentially positive regulators like GPA2 or GPA3.

Hypothetical cAMP signalling cascade:

Taken together the results to date draw a complex picture of how cAMP signalling could regulate DON production in *F. graminearum* (Figure 5.1). Extracellular signals are perceived by membrane associated G-protein coupled receptors, of which 116 have been annotated in *F. graminearum* (Ma et al., 2010). This activates the coupled heterotrimeric G-proteins, which allows the dissociation of the different subunits and the exchange of GDP to GTP. In the GTP bound state the G-proteins are active and can thus regulate downstream proteins like the adenylyl cyclase. Based on the elevated DON levels in the Δ*gpa1* and Δ*gpb1* knockout mutants, GPA1 and GPB1 subunits might repress adenylyl cyclase activity, whereas GPA2 might activate it, as its constitutive active mutant over induces DON (Park et al., 2012; Yu et al., 2008). However, G-protein regulating proteins interact with GPA subunits and promote hydrolysis of GTP to GDP, which puts the GPA back into its inactive state (Chidiac and Roy, 2011). A knockout of the G-protein regulating protein FlbA resulted in increased DON production (Park et al., 2012), indicating that FlbA might be a negative regulator of GPA2 and thus inhibiting its activation of the adenylyl cyclase, which is required

for DON production. A common target activated by adenylyl cyclase produced cAMP are protein kinases A (PKA), which in filamentous fungi consist of two catalytic subunits, whereas one of the subunits usually mediates most of the PKA activities. In *F. graminearum* CPK1 is the major PKA catalytic subunit and its knockout results in decreased expression of DON synthesis genes (Hu et al., 2014). PKA regulates other proteins through phosphorylation. The global nitrogen regulator AreA is important for DON production and carries a putative PKA phosphorylation site (Hou et al., 2015; Min et al., 2012). Min et al. (2012) also showed that AreA interacts with TRI10 which together with TRI6 regulates DON production through transcriptional regulation of the *TRI* gene cluster (Seong et al., 2009). Similar to other organisms, the cAMP levels in *F. graminearum* are further regulated through phosphodiesterases (PDEs) PDE1 and PDE2 which hydrolyse cAMP to 5'AMP, whereas only PDE2 is negatively regulating DON production, although PDE1 and PDE2 have redundant functions in regulating growth, development and pathogenesis (Jiang et al., 2016).

However G-proteins do not only regulate adenylyl cyclases, but for example also mitogen-activated-protein kinases (MAPK). These are involved in MAPK signalling cascades, in which sequential phosphorylation of MAPK kinase kinase (MAPKKK), to MAPKK to MAPK mediates downstream regulation of transcription factors by the activated terminal MAPK (Bardwell, 2005). In *F. graminearum*, the MAPKs MGV1, MAP1 as well as the MAPKKK Os4, the MAPKK Os5 and the MAPK Os2 have been shown to be involved in the regulation of DON production (Hou et al., 2002; Ochiai et al., 2007; Urban et al., 2003; Van Thuat et al., 2012). Hence, it still needs to be shown if the respective G-protein knockout phenotypes are due to altered MAPK or cAMP signalling, e. g. by phosphorylation studies of the respective MAPKs and cAMP quantifications in the G-protein knockout mutants.

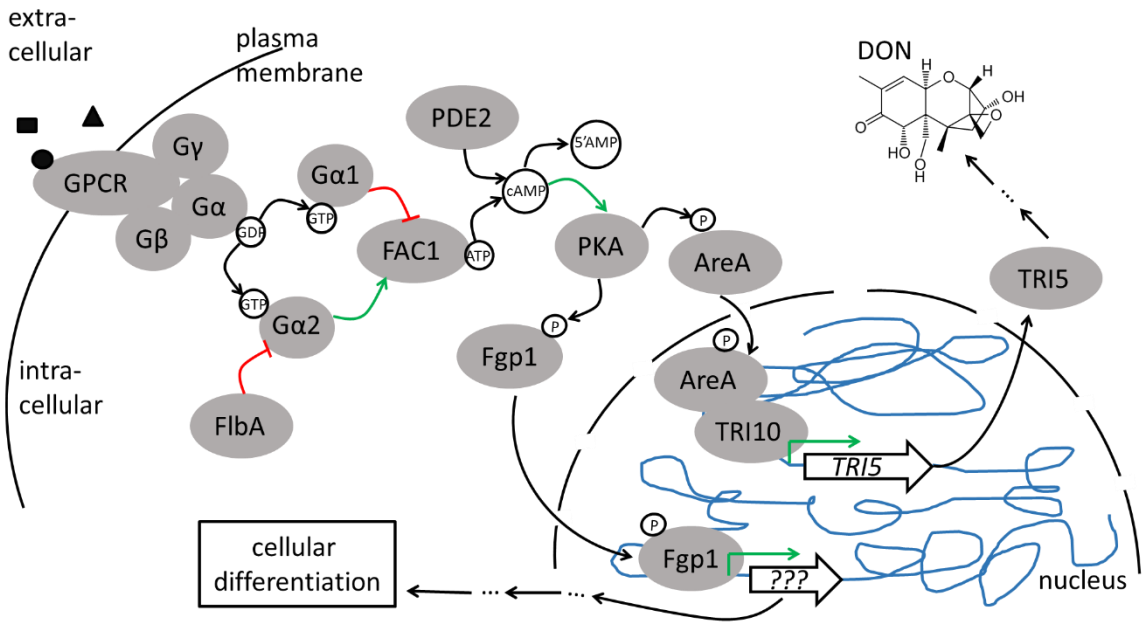

Figure 5.1. Hypothetical signalling network regulating DON production in *F. graminearum*. GPCRs (G-protein coupled receptor) can perceive extracellular signals, causing the dissociation of Gα, Gβ, Gγ G-protein subunits, which in turn regulate the activity of FAC1 (*F. graminearum* adenylyl cyclase). G-proteins are regulated by regulators of G-protein signalling, like e.g. FlbA. FAC1 converts ATP (adenosine triphosphate) to cAMP (cyclic adenosine monophosphate), which activates PKA (protein kinase A). The cAMP levels are controlled by PDEs (phosphodiesterases), which convert cAMP to 5'AMP. The *F. graminearum* global nitrogen regulator AreA has a conserved PKA phosphorylation site. AreA has been shown to interact with TRI10, a major transcription factor regulating *TRI* gene expression, like e.g. TRI5, which is the trichothecene synthase required for DON (deoxynivalenol) biosynthesis. Fgp1 (Wor1-like protein) also has a conserved PKA phosphorylation site and might act as a transcription factor to mediate the cAMP dependent cellular differentiations during toxin production.

In addition, the *F. graminearum* adenylyl cyclase is probably not only regulated by G-proteins. Mammalian adenylyl cyclases for example are complexly regulated by e. g. Ca^{2+}, Ca^{2+}-calmodulin, the plant diterpene forskolin, phosphorylation by protein kinases A and C (PKA,PKC), adenosine analogues, bicarbonate and by catechol estrogens (Desaubry et al., 1996; Iyengar, 1993; Sunahara et al., 1996; Tesmer et al., 1997; Xia and Storm, 1997). Accordingly, the *F. graminearum* adenylyl cyclase could potentially also be regulated by plant derived secondary metabolites, which could mediate an infection specific increase in cAMP which could then in turn activate DON production. Furthermore, mammalian adenylyl cyclases are also known to specifically regulate their targets through tissue specific expression as well as subcellular compartmentalization (Cooper, 2003). It would be very interesting to fluorescently label the *F. graminearum* adenylyl cyclase in the TRI5-GFP DON

production reporter strain to see if the expression of the adenylyl cyclase is upregulated in toxin-producing hyphae, or if its subcellular localization is altered in comparison to non-toxin-producing hyphae.

As mentioned above, GPCRs are upstream regulators of adenylyl cyclases, which perceive extracellular signals. Hence, GPCRs are interesting candidates which could detect plant derived signals during infection, which could allow the infection specific regulation of DON production in *F. graminearum*.

Further, adenylyl cyclase mutants are not only altered in DON production, but also in cellular development, as the Δ*fac1* knockout mutant is unable to produce infection structures (Bormann et al., 2014) and the gain of function mutant develops ovoid and bulbous cells during toxin production repressing conditions (Blum et al., 2016). It will be discussed below, how cAMP signalling could regulate cellular development.

5.2 Cellular developmental changes and subcellular reorganization of the smooth ER during toxin production

In addition to the complex signalling network, DON production in *F. graminearum* also involves developmental changes of cellular structures, as well as subcellular reorganization of the smooth ER.

The cAMP signalling network not only regulates DON production, but also cellular differentiation associated with toxin production. Thus, the question arises how cAMP signalling might be linked to cellular development. The Wor1-like transcription factor Fgp1 is a positive regulator of DON production (Jonkers et al., 2012) and like AreA also has a putative PKA phosphorylation site. A Δ*fgp1* knockout mutant develops less ovoid cells in DON-production-inducing medium (Jonkers et al., 2012) and thus Jiang et al. (2016) hypothesize that cAMP dependent cellular differentiation during toxin production might be mediated through transcriptional regulation of Fgp1, which in turn might be regulated through PKA phosphorylation (Figure 5.1). The development of the ovoid cells also seems to be independent of DON production, as a Δ*tri6* knockout mutant, which does not produce any detectable DON, is still able to develop ovoid cells *in vitro* (Jonkers et al., 2012) and a Δ*gpmk1* (pathogenicity mitogen-activated protein kinase) knockout mutant can still produce DON, but does not develop bulbous cells *in planta* (Rittenour and Harris, 2010). Hence, DON production and the associated cellular differentiations share regulatory signalling

pathways, but are still differentially regulated, suggesting a divergence of the regulatory pathway, e.g. through the regulation of different transcription factors by PKA (Figure 5.1). As already stated by Menke et al. (2012) as well as in the first chapter here, the morphological changes of hyphae observed during toxin production *in vitro* are similar to those observed during plant infection (Boddu et al., 2006; Brown et al., 2010; Ilgen et al., 2009; Jansen et al., 2005; Pritsch et al., 2000; Rittenour and Harris, 2010). The bulbous hyphae resemble infection hyphae which can be found growing within the infected plant tissue, however the actual function of the ovoid cells observed *in vitro* is still unknown. The ovoid cells usually contain large vacuoles (Menke et al., 2012), thus they could potentially store secondary metabolites.

Another developmental change which can be observed during toxin production *in vitro* but also *in planta* during infection is the proliferation of the smooth ER into toxisomes (Boenisch et al., 2017). It is still unknown if the development of toxisomes is specific to DON production or a general stress response of *F. graminearum* to e.g. the growth conditions. To this end a Δ*tri6* knockout mutant which is unable to produce DON could be grown under DON-production-inducing conditions. If this mutant still develops toxisomes, the toxisome development in the Δ*fac1* adenylyl cyclase knockout mutant could be analysed, as this is further upstream in the signalling cascade. To exclude a general stress response to the DON-production-inducing medium, the *FAC1*^{P1441S} adenylyl gain-of-function mutant could be analysed in DON-production-repressing medium, as this mutant still produces DON under repressing conditions. In mammalian cells, yeast cells and plant cells, smooth ER proliferations can be induced by overexpressing ER resident transmembrane proteins, like e.g. HMR1 (Gong et al., 1996; Ohkuma et al., 1995; Sandig et al., 1999; Snapp et al., 2003; Takei et al., 1994; Vergeres et al., 1993; Wright et al., 1990; Yamamoto et al., 1996). Thus, as the expression of *HMR1* is also upregulated during toxin production *in vitro* in *F. graminearum* (Boenisch et al., 2017), it could be the driving force behind the development of toxisomes.

It was shown here that the cytosolic TRI5-GFP accumulates around toxisomes and sometimes even co-localizes with them. This led to the hypothesis that the accumulation around toxisomes allows a more efficient biosynthesis of DON, as it brings the cytosolic TRI5 into close proximity of the ER resident TRI1 and TRI4. However, it is not known how the accumulation of the cytosolic TRI5-GFP is mediated, nor how important it actually is for DON production. A potential candidate which could be involved in the clustering of

TRI5-GFP is TRI14. TRI14 is important for DON production *in planta* but not *in vitro* (Dyer et al., 2005) and it is localized at toxisomes (Boenisch et al., 2017), but its function is still unknown. TRI14 could be a scaffolding protein, which could mediate the accumulation of TRI5-GFP around the toxisomes. Thus, the localization of TRI5-GFP could be analysed in a Δ*tri14* knockout mutant to see if TRI5-GFP still accumulates around toxisomes. Another potential function of TRI14 could be as a scaffolding protein during the formation of the potential DON-biosynthesis multi-enzyme complex. To address this question the Δ*tri14* knockout mutant could be analysed, to see if there are still FRET events detectable between TRI1 and TRI4 and HMR1 in the absence of TRI14.

As HMS1-RFP and HMS1-GFP both accumulated around toxisomes in some cells, it was hypothesized, that HMS1 might accumulate more around toxisomes at different time points. Accordingly, the accumulation patterns of HMS1 could be analysed at earlier and later time points. As HMS1 is involved in the biosynthesis of farnesyl pyrophosphate, the precursor for DON biosynthesis, it could potentially be accumulating more frequently around toxisomes at earlier time points. However, the analysis would be difficult, as less toxisomes will have developed at earlier time points. Further, it would be of interest to analyse if HMS1 accumulates around the ER under DON-production-repressing conditions, though this analysis would probably be impossible, as there are no toxisomes under repressing conditions and the fine reticulate ER network exhibits too weak signals to allow SIM analysis.

Although our understanding of the cell biology behind DON biosynthesis has advanced significantly in the past five years, it still remains unclear where the final DON biosynthesis steps are happening and where it is stored, or if it is directly secreted. The subcellular localization of TRI8, the last enzyme in the DON biosynthesis pathway, could give further hints, but has not been published yet. Immunofluorescence staining could potentially reveal where DON is stored in the cell, if it is at all, but it would also be very challenging as DON is a very small and highly soluble compound, which makes antibody staining within cells very hard.

In summary, the results presented here highlight that the production of the secondary metabolite DON in *F. graminearum* requires more than just the expression of the biosynthesis gene cluster, which provides indications as to why only so few secondary metabolite clusters have been functionally characterised, even though the genomic data of thousands of different microbes is available (Schmidt-Dannert, 2015). In addition, it seems that different filamentous fungi seem to have developed slightly different cell biological

mechanisms for their toxin production. However, as described above every fungal species probably produces many more secondary metabolites, some of which might be produced at the same time. Thus, it still remains to be revealed how the production of the different metabolites is coordinated. Are different metabolites produced by different cells within a fungal colony? Are the metabolites, which are produced in the same cells spatially separated within different cellular compartments? If different metabolites are synthesised in the same compartment, are there microdomains within the same cellular organelle? How are precursor pools distributed and shared between different metabolic pathways?

5.3 How is the production of the two secondary metabolites DON and fusatin coordinated in *F. pseudograminearum*?

A novel biosynthesis cluster has been characterised recently in *F. pseudograminearum* which produces the cytokinin-like compound fusatin (Sørensen et al., 2017). Here, the analysis of the *in vitro* conditions inducing fusatin production revealed that the fusatin production inducing conditions also induce DON production in *F. pseudograminearum*. Similar to DON production, fusatin production can also be induced by specific nitrogen sources *in vitro*. This raises the question why both DON and fusatin can be induced *in vitro* by specific nitrogen sources and if this is related to the fact that both DON and fusatin are involved in plant infection.

Are different nitrogen sources accumulating in different tissues or at different time points in plants during infection? Polyamines, the main inducers of DON production, have been reported to accumulate in wheat infected with *F. graminearum* (Gardiner et al., 2010). Similar, asparagine (fusatin production inducer) levels were increased in DON treated wheat plants (Nussbaumer et al., 2015), but increased asparagine levels could also be detected in resistant wheat cultivars in comparison to susceptible cultivars constitutively but also induced by *F. graminearum* infection (Paranidharan et al., 2008). Hence, the concentrations of different nitrogen sources changes in infected plants, probably both due to defence responses of the plants as well as due to host manipulation by the fungus. Accordingly, the specific induction of DON and fusatin production in *F. pseudograminearum* may have been adapted to the specific host conditions that the fungus encounters during infection and might allow the induction of different secondary metabolites during different time points of infection. It could for example be possible, that fusatin production is induced at earlier time points during infection to allow the spread of the fungus through the still healthy tissue and to induce

nutrient accumulation in the plant tissue prior to the switch to necrotrophic infection stages, during which the fungus kills plant cells with mycotoxins like DON to feed on the dead tissue.

However, the induction of both DON and fusatin production by the different nitrogen sources *in vitro* could also just be due to secondary effects mediated for example through the acidification of the medium, which happens when for example putrescine is taken up by *F. graminearum* (Gardiner et al., 2009c). Thus, DON production and fusatin production in *F. pseudograminearum* seem to share regulatory networks, as both are induced by asparagine, however their regulatory networks also seem to diverge at some point, as more DON is produced in citrulline than in asparagine, but no fusatin could be detected in citrulline. As DON and fusatin production seem to share some regulatory pathways, it would be interesting to see if fusatin production in *F. pseudograminearum* is also regulated through cAMP signalling. Accordingly, repressing *in vitro* cultures could be treated with exogenous cAMP to see if the cAMP treatment would be able to overcome the repressive conditions and fusatin would be produced. To identify regulators of fusatin production the FACS based mutant screen presented here could be performed with mutagenised *FpFCK1* fusatin reporter strain spores. The identification of fusatin production regulators could provide novel hints to the potential function of fusatins during plant infection, as well as how their induction is regulated during plant infection. The identification of plant derived inducing signals would then in turn provide new starting points for the development of control strategies against *F. pseudograminearum* infections.

5.4 FACS mutant screen to characterize other secondary metabolites

As mentioned before, only very few microbial secondary metabolites have been characterized to date, even though they could have great potential e.g. as pharmaceuticals. Most secondary metabolite clusters are not expressed under standard *in vitro* culture conditions, which hinders their characterization. The FACS based mutant screen developed during this PhD project could be adapted to other secondary metabolite clusters to create mutants which express the cluster under the preferred culture conditions. The mutant screen can also be of industrial interest, as it could facilitate the creation of mutants which produce higher amounts of a desired compound or allow the production of the compound in cheaper growth conditions.

5.5 Final remarks

The investigations here add to our overall understanding of the complex regulation and cell biology of toxin production. We are only starting to understand these biological mechanisms involved in the biosynthesis of metabolites which have been known for a long time and yet there is still a vast array of secondary metabolites which have not been characterized at all. Whilst only two species and compounds were studied here, it is likely that the findings will have relevance to a vast number of different fungi and metabolites.

6 References

Akiyoshi, D.E., Klee, H., Amasino, R.M., Nester, E.W., Gordon, M.P., 1984. T-DNA of Agrobacterium tumefaciens encodes an enzyme of cytokinin biosynthesis. Proc. Natl. Acad. Sci. 81, 5994–5998.

Alexander, N.J., McCormick, S.P., Hohn, T.M., 1999. TRI12, a trichothecene efflux pump from Fusarium sporotrichioides : gene isolation and expression in yeast. Mol. Gen. Genet. MGG 261, 977–984.

Alexander, N.J., McCormick, S.P., Larson, T.M., Jurgenson, J.E., 2004. Expression of Tri15 in Fusarium sporotrichioides. Curr. Genet. 45, 157–62.

Alexander, N.J., Proctor, R.H., McCormick, S.P., 2009. Genes, gene clusters, and biosynthesis of trichothecenes and fumonisins in Fusarium. Toxin Rev. 28, 198–215.

Ashby, A.M., 2000. Biotrophy and the cytokinin conundrum. Physiol. Mol. Plant Pathol. 57, 147–158.

Audenaert, K., Callewaert, E., Höfte, M., De Saeger, S., Haesaert, G., 2010. Hydrogen peroxide induced by the fungicide prothioconazole triggers deoxynivalenol (DON) production by *Fusarium graminearum*. BMC Microbiol. 10, 112–133.

Bae, H., Gray, J.S., Li, M., Vines, L., Kim, J., Pestka, J.J., 2010. Hematopoetic Cell Kinase Associates with the 40S Ribosomal Subunit and Mediates the Ribotoxic Stress Response to Deoxynivalenol in Mononuclear Phagocytes. Toxicol. Sci.

Bae, H.K., Pestka, J.J., 2008. Deoxynivalenol induces p38 interaction with the ribosome in monocytes and macrophages. Toxicol. Sci. 105, 59–66.

Bagga, S., Straney, D., 2000. Modulation of cAMP and phosphodiesterase activity by flavonoids which induce spore germination of *Nectria haematococca* MP VI (*Fusarium solani*). Physiol. Mol. Plant Pathol. 56, 51–61.

Båhzu, O., Danchin, A., 1994. Adenylyl Cyclases: A Heterogeneous Class of ATP-Utilizing Enzymes. Prog. Nucleic Acid Res. Mol. Biol. 49, 241–283.

Bai, G.-H., Desjardins, A.E., Plattner, R.D., 2002. Deoxynivalenol-nonproducing Fusarium graminearum Causes Initial Infection, but does not Cause DiseaseSpread in Wheat Spikes. Mycopathologia 153, 91–98.

Baldwin, T.K., Urban, M., Brown, N., Hammond-Kosack, K.E., 2010. A role for topoisomerase I in Fusarium graminearum and F. culmorum pathogenesis and sporulation. Mol. Plant. Microbe. Interact. 23, 566–77.

Bardwell, L., 2005. A walk-through of the yeast mating pheromone response pathway. Peptides 26, 339–350. doi:10.1016/j.peptides.2004.10.002

Bentley, A.R., Tunali, B., Nicol, J.M., Burgess, L.W., Summerell, B.A., 2006. A survey of Fusarium species associated with wheat and grass stem bases in northern Turkey.

Beyer, M., Klix, M.B., Klink, H., Verreet, J.-A., 2006. Quantifying the effects of previous crop, tillage, cultivar and triazole fungicides on the deoxynivalenol content of wheat grain – a review. J. Plant Deseases Prot.113, 241–246.

Bin-Umer, M.A., McLaughlin, J.E., Basu, D., McCormick, S., Tumer, N.E., 2011. Trichothecene mycotoxins inhibit mitochondrial translation--implication for the mechanism of toxicity. Toxins (Basel). 3, 1484–501.

Bin-Umer, M.A., McLaughlin, J.E., Butterly, M.S., McCormick, S., Tumer, N.E., 2014. Elimination of damaged mitochondria through mitophagy reduces mitochondrial oxidative stress and increases tolerance to trichothecenes. Proc. Natl. Acad. Sci. U. S. A. 111, 11798–803.

Blum, A., Benfield, A.H., Stiller, J., Kazan, K., Batley, J., Gardiner, D.M., 2016. High-throughput FACS-based mutant screen identifies a gain-of-function allele of the Fusarium graminearum adenylyl cyclase causing deoxynivalenol over-production. Fungal Genet. Biol. 90, 1–11.

Boddu, J., Cho, S., Kruger, W.M., Muehlbauer, G.J., 2006. Transcriptome analysis of the barley-*Fusarium graminearum* interaction. Mol. Plant. Microbe. Interact. 19, 407–417.

Boenisch, M.J., Broz, K.L., Purvine, S.O., Chrisler, W.B., Nicora, C.D., Connolly, L.R., Freitag, M., Baker, S.E., Kistler, H.C., 2017. Structural reorganization of the fungal endoplasmic reticulum upon induction of mycotoxin biosynthesis. Sci. Rep. 7, 44296.

Boenisch, M.J., Schäfer, W., 2011. *Fusarium graminearum* forms mycotoxin producing infection structures on wheat. BMC Plant Biol. 11, 110–128.

Booth, C., 1971. The genus Fusarium. Kew, UK, Commonwealth Mycological Institute.

Bormann, J., Boenisch, M.J., Brückner, E., Firat, D., Schäfer, W., 2014. The adenylyl cyclase plays a regulatory role in the morphogenetic switch from vegetative to pathogenic lifestyle of *Fusarium graminearum* on wheat. PLoS One 9, e91135.

Boutigny, A.-L., Barreau, C., Atanasova-Penichon, V., Verdal-Bonnin, M.-N., Pinson-Gadais, L., Richard-Forget, F., 2009. Ferulic acid, an efficient inhibitor of type B trichothecene biosynthesis and Tri gene expression in Fusarium liquid cultures. Mycol. Res. 113, 746–53.

Bowden, R.L., Leslie, J.F., 1999. Sexual Recombination in *Gibberella zeae*. Phytopathology 89, 182–188.

Brown, D.W., McCormick, S.P., Alexander, N.J., Proctor, R.H., Desjardins, A.E., 2002. Inactivation of a cytochrome P-450 is a determinant of trichothecene diversity in Fusarium species. Fungal Genet. Biol. 36, 224–233.

Brown, D.W., McCormick, S.P., Alexander, N.J., Proctor, R.H., Desjardins, A.E., 2001. A genetic and biochemical approach to study trichothecene diversity in Fusarium sporotrichioides and Fusarium graminearum. Fungal Genet. Biol. 32, 121–33.

Brown, J.S., Aufauvre-Brown, A., Holden, D.W., 1998. Insertional mutagenesis of *Aspergillus fumigatus*. Mol. Gen. Genet. 259, 327–335.

Brown, N.A., Urban, M., van de Meene, A.M.L., Hammond-Kosack, K.E., 2010. The infection biology of *Fusarium graminearum*: defining the pathways of spikelet to spikelet colonisation in wheat ears. Fungal Biol. 114, 555–571.

Brütting, C., Schäfer, M., Vanková, R., Gase, K., Baldwin, I.T., Meldau, S., 2017. Changes in cytokinins are sufficient to alter developmental patterns of defense metabolites in Nicotiana attenuata. Plant J. 89, 15–30.

Burgess, L., Backhouse, D., Summerell, B., Swan, L., 2001. Crown rot of wheat, in: Summerell B, Leslie J, Backhouse D, Bryden W, Burgess L (Eds.), Fusarium: Paul E. Nelson Memorial Symposium. APS Press, St Paul, MN, USA, pp. 271–294.

Bushnell, W.R., Hazen, B.E., Pritsch, C., Leonard, K.J., 2003. Histology and physiology of Fusarium head blight. Bushnell, W. R., Hazen, B. E., Pritsch, C., & Leonard, K. (2003).

Histology and physiology of Fusarium head blight. Fusarium Head Blight of Wheat and Barley (Leonard, KJ and Bushnell, WR, eds). St. Paul, MN: APS Press. 44–83.

Cappellini, R.A., Peterson, J.L., 1965. Macroconidium formation in submerged cultures by a non-sporulating strain of *Gibberella zeae*. Mycologia 57, 962–966.

Chidiac, P., Roy, A.A., 2003. Activity, Regulation, and Intracellular Localization of RGS Proteins. Recept. Channels 9, 135–147.

Chung, K.-R., Ehrenshaft, M., Wetzel, D.K., Daub, M.E., 2003. Cercosporin-deficient mutants by plasmid tagging in the asexual fungus *Cercospora nicotianae*. Mol. Genet. Genomics 270, 103–113.

Comeau, A., Langevin, F., Caetano, V.R., Haber, S., Savard, M.E., Voldeng, H., Fedak, G., Dion, Y., Rioux, S., Gilbert, J., Martin, R.A., Eudes, F., Scheeren, P.L., 2011. A Different Path to the Summit of Fusarium Head Blight Resistance in Wheat: Developing Germplasm with a Systemic Approach. Plant Breed. Seed Sci. 63, 39–48.

Conservation Technology Information Centre, n.d. Crop Residue Management Survey [WWW Document]. URL http://www.ctic.purdue.edu/CRM (accessed 9.26.14).

Cooper, D.M.F., 2003. Regulation and organization of adenylyl cyclases and cAMP. Biochem. J. 375, 517–529.

Correll, J.C., Klittich, C.J.R., Leslie, J.., 1987. Nitrate nonutilizing mutants of *Fusarium oxysporum* and their use in vegetative compatibility tests. Phytopathology 77, 1640–1646.

Cosme, M., Ramireddy, E., Franken, P., Schmülling, T., Wurst, S., 2016. Shoot- and root-borne cytokinin influences arbuscular mycorrhizal symbiosis. Mycorrhiza 26, 709–720.

Cuomo, C.A., Güldener, U., Xu, J.-R., Trail, F., Turgeon, B.G., Di Pietro, A., Walton, J.D., Ma, L.-J., Baker, S.E., Rep, M., Adam, G., Antoniw, J., Baldwin, T., Calvo, S., Chang, Y.-L., Decaprio, D., Gale, L.R., Gnerre, S., Goswami, R.S., Hammond-Kosack, K., Harris, L.J., Hilburn, K., Kennell, J.C., Kroken, S., Magnuson, J.K., Mannhaupt, G., Mauceli, E., Mewes, H.-W., Mitterbauer, R., Muehlbauer, G., Münsterkötter, M., Nelson, D., O'donnell, K., Ouellet, T., Qi, W., Quesneville, H., Roncero, M.I.G., Seong, K.-Y., Tetko, I. V, Urban, M., Waalwijk, C., Ward, T.J., Yao, J., Birren, B.W., Kistler, H.C., 2007. The *Fusarium graminearum* genome reveals a link between localized polymorphism and pathogen specialization. Science 317, 1400–1402.

De Nijs, M., Rombouts, F., Notermans, S., 1996. FUSARIUM MOLDS AND THEIR MYCOTOXINS. J. Food Saf. 16, 15–58.

Dervinis, C., Frost, C.J., Lawrence, S.D., Novak, N.G., Davis, J.M., 2010. Cytokinin Primes Plant Responses to Wounding and Reduces Insect Performance. J. Plant Growth Regul. 29, 289–296.

Desaubry, L., Shoshani, I., Johnson, R.A., 1996. 2',5'-Dideoxyadenosine 3'-Polyphosphates Are Potent Inhibitors of Adenylyl Cyclases. J. Biol. Chem. 271, 2380–2382.

Desjardins, A., Maragos, C., Norred, W., Pestka, J., Phillips, T., Vardon, P., Whitaker, T., Wood, G., Egmond, H. van, 2003. Mycotoxins: Risks in plant, animal, and human systems - CAST task force report 139.

Desjardins, A.E., 2006. *Fusarium* mycotoxins: chemistry, genetics, and biology. American Phytopathological Society (APS Press), Minnesota.

Desmond, O.J., Manners, J.M., Stephens, A.E., Maclean, D.J., Schenk, P.M., Gardiner,

D.M., Munn, A.L., Kazan, K., 2008. The *Fusarium* mycotoxin deoxynivalenol elicits hydrogen peroxide production, programmed cell death and defence responses in wheat. Mol. Plant Pathol. 9, 435–445.

Dyer, R.B., Plattner, R.D., Kendra, D.F., Brown, D.W., 2005. Fusarium graminearum TRI14 is required for high virulence and DON production on wheat but not for DON synthesis in vitro. J. Agric. Food Chem. 53, 9281–7.

Elliott, C.E., Howlett, B.J., 2006. Overexpression of a 3-ketoacyl-CoA thiolase in *Leptosphaeria maculans* causes reduced pathogenicity on *Brassica napus*. Mol. Plant. Microbe. Interact. 19, 588–596.

Fawcett, D.W., 1955. Observations on the cytology and electron microscopy of hepatic cells. J. Natl. Cancer Inst. 15, 1475–503.

Ferreira, F.J., Kieber, J.J., 2005. Cytokinin signaling. Curr. Opin. Plant Biol. 8, 518–525.

Firon, A., Villalba, F., Beffa, R., D'Enfert, C., 2003. Identification of essential genes in the human fungal pathogen *Aspergillus fumigatus* by transposon mutagenesis. Eukaryot. Cell 2, 247–255.

Foo, E., Ross, J.J., Jones, W.T., Reid, J.B., 2013. Plant hormones in arbuscular mycorrhizal symbioses: an emerging role for gibberellins. Ann. Bot. 111, 769–779.

Galbraith, C.G., Galbraith, J.A., 2011. Super-resolution microscopy at a glance. J. Cell Sci. 124.

Gan, S., Amasino, R.M., 1995. Inhibition of leaf senescence by autoregulated production of cytokinin. Science (80-.). 270.

Gardiner, D.M., Kazan, K., Manners, J.M., 2009a. Nutrient profiling reveals potent inducers of trichothecene biosynthesis in *Fusarium graminearum*. Fungal Genet. Biol. 46, 604–613.

Gardiner, D.M., Kazan, K., Manners, J.M., 2009b. Novel genes of *Fusarium graminearum* that negatively regulate deoxynivalenol production and virulence. Mol. Plant. Microbe. Interact. 22, 1588–1600.

Gardiner, D.M., Kazan, K., Praud, S., Torney, F.J., Rusu, A., Manners, J.M., 2010. Early activation of wheat polyamine biosynthesis during Fusarium head blight implicates putrescine as an inducer of trichothecene mycotoxin production. BMC Plant Biol. 10, 289–313.

Gardiner, D.M., Osborne, S., Kazan, K., Manners, J.M., 2009c. Low pH regulates the production of deoxynivalenol by *Fusarium graminearum*. Microbiology 155, 3149–56.

Geng, Z., Zhu, W., Su, H., Zhao, Y., Zhang, K.-Q., Yang, J., 2014. Recent advances in genes involved in secondary metabolite synthesis, hyphal development, energy metabolism and pathogenicity in Fusarium graminearum (teleomorph Gibberella zeae). Biotechnol. Adv. 32, 390–402.

Giese, H., Sondergaard, T.E., Sørensen, J.L., 2013. The AreA transcription factor in *Fusarium graminearum* regulates the use of some nonpreferred nitrogen sources and secondary metabolite production. Fungal Biol. 117, 814–821.

Gilbert, J., Haber, S., 2013. Overview of some recent research developments in Fusarium head blight of wheat. Can. J. Plant Pathol. 35, 37–41.

Gogala, N., 1991. Regulation of mycorrhizal infection by hormonal factors produced by hosts and fungi. Experientia 47, 331–340.

Gong, F.C., Giddings, T.H., Meehl, J.B., Staehelin, L.A., Galbraith, D.W., 1996. Z-membranes: artificial organelles for overexpressing recombinant integral membrane proteins. Proc. Natl. Acad. Sci. 93, 2219–2223.

Guenther, J.C., Trail, F., 2005. The development and differentiation of Gibberella zeae (anamorph: Fusarium graminearum) during colonization of wheat. Mycologia 97, 229–37.

Güldener, U., Mannhaupt, G., Münsterkötter, M., Haase, D., Oesterheld, M., Stümpflen, V., Mewes, H.-W., Adam, G., 2006. FGDB: a comprehensive fungal genome resource on the plant pathogen *Fusarium graminearum*. Nucleic Acids Res. 34, D456–D458.

Guo, X.W., Fernando, W.G.D., Bullock, P., Sapirstein, H., 2010. Quantifying cropping practices in relation to inoculum levels of Fusarium graminearum on crop stubble. Plant Pathol. 59, 1107–1113.

Gustafsson, M.G.L., 2000. Surpassing the lateral resolution limit by a factor of two using structured illumination microscopy. J. Microsc. 198, 82–87.

Haggag, W.M., Abd-El-Kareem, F., 2009. Methyl jasmonate stimulates polyamines biosynthesisand resistance against leaf rust in wheat plants. Arch. Phytopathol. Plant Prot. 42, 16–31.

Hanoune, J., Defer, N., 2001. Regulation and role of adenylyl cyclase isoforms. Annu. Rev. Pharmacol. Toxicol. 41, 145–74.

Hansen, F.T., Gardiner, D.M., Lysøe, E., Fuertes, P.R., Tudzynski, B., Wiemann, P., Sondergaard, T.E., Giese, H., Brodersen, D.E., Sørensen, J.L., 2015. An update to polyketide synthase and non-ribosomal synthetase genes and nomenclature in Fusarium. Fungal Genet. Biol. 75, 20–29.

Hatley, M.E., Benton, B.K., Xu, J., Manfredi, J.P., Gilman, A.G., Sunahara, R.K., 2000. Isolation and characterization of constitutively active mutants of mammalian adenylyl cyclase. J. Biol. Chem. 275, 38626–38632.

Heier, T., Jain, S.K., Kogel, K.-H., Pons-Kuhnemann, J., 2005. Influence of N-fertilization and Fungicide Strategies on Fusarium Head Blight Severity and Mycotoxin Content in Winter Wheat. J. Phytopathol. 557, 551–557.

Hoffman, C.S., 2005. Glucose sensing via the protein kinase A pathway in Schizosaccharomyces pombe. Chemical Soc. Trans. Volume 33, 257–260.

Hohn, T.M., Beremand, P.D., 1989. Isolation and nucleotide sequence of a sesquiterpene cyclase gene from the trichothecene-producing fungus Fusarium sporotrichioides. Gene 79, 131–138.

Hohn, T.M., Krishna, R., Proctor, R.H., 1999. Characterization of a transcriptional activator controlling trichothecene toxin biosynthesis. Fungal Genet. Biol. 26, 224–35.

Hohn, T.M., Vanmiddlesworth, F., 1986. Purification and characterization of the sesquiterpene cyclase trichodiene synthetase from *Fusarium sporotrichioides*. Arch. Biochem. Biophys. 251, 756–761.

Hollingsworth, C.R., Motteberg, C.D., Thompson, W.G., 2006. Assessing Fungicide Efficacies for the Management of Fusarium Head Blight on Spring Wheat and Barley Plant Health Progress Plant Health Progress.

Hoppert, M., Gentzsch, C., Schörgendorfer, K., 2001. Structure and localization of cyclosporin synthetase, the key enzyme of cyclosporin biosynthesis in Tolypocladium

inflatum. Arch. Microbiol. 176, 285–293.

Horevaj, P., Bluhm, B.H., 2012. BDM1, a phosducin-like gene of Fusarium graminearum, is involved in virulence during infection of wheat and maize. Mol. Plant Pathol. 13, 431–44.

Hou, R., Jiang, C., Zheng, Q., Wang, C., Xu, J.-R., 2015. The AreA transcription factor mediates the regulation of deoxynivalenol (DON) synthesis by ammonium and cyclic adenosine monophosphate (cAMP) signalling in *Fusarium graminearum*. Mol. Plant Pathol.

Hou, Z., Xue, C., Peng, Y., Katan, T., Kistler, H.C., Xu, J.-R., 2002. A mitogen-activated protein kinase gene (MGV1) in Fusarium graminearum is required for female fertility, heterokaryon formation, and plant infection. Mol. Plant. Microbe. Interact. 15, 1119–27.

Howard, D.H., 2002. FUSARIUM MOLDS AND THEIR MYCOTOXINS. CRC Press.

Hu, S., Zhou, X., Gu, X., Cao, S., Wang, C., Xu, J.-R., 2014. The cAMP-PKA pathway regulates growth, sexual and asexual differentiation, and pathogenesis in *Fusarium graminearum*. Mol. Plant-Microbe Interact. 27, 557–566.

Huang, M., Bai, Y., Sjostrom, S.L., Hallström, B.M., Liu, Z., Petranovic, D., Uhlén, M., Joensson, H.N., Andersson-Svahn, H., Nielsen, J., 2015. Microfluidic screening and whole-genome sequencing identifies mutations associated with improved protein secretion by yeast. Proc. Natl. Acad. Sci. 112, E4689–E4696.

Ilgen, P., Hadeler, B., Maier, F.J., Schäfer, W., 2009. Developing kernel and rachis node induce the trichothecene pathway of *Fusarium graminearum* during wheat head infection. Mol. Plant. Microbe. Interact. 22, 899–908.

Iyengar, R., 1993. Molecular and functional diversity of mammalian Gs-stimulated adenylyl cyclases. FASEB J 7, 768–775.

Jansen, C., von Wettstein, D., Schäfer, W., Kogel, K.-H., Felk, A., Maier, F.J., 2005. Infection patterns in barley and wheat spikes inoculated with wild-type and trichodiene synthase gene disrupted *Fusarium graminearum*. Proc. Natl. Acad. Sci. U. S. A. 102, 16892–16897.

Jelinek, C.F., Pohland, A.E., Wood, G.E., 1989. Worldwide occurrence of mycotoxins in foods and feeds--an update. Assoc. Off. Anal. Chem. 72, 223–230.

Jiang, C., Zhang, C., Wu, C., Sun, P., Hou, R., Liu, H., Wang, C., Xu, J.-R., 2016. TRI6 and TRI10 play different roles in the regulation of DON production by cAMP signaling in Fusarium graminearum. Environ. Microbiol. 18, 3689–3701.

Jiang, J., Liu, X., Yin, Y., Ma, Z., 2011a. Involvement of a velvet protein FgVeA in the regulation of asexual development, lipid and secondary metabolisms and virulence in Fusarium graminearum. PLoS One 6, e28291.

Jiang, J., Yun, Y., Fu, J., Shim, W.-B., Ma, Z., 2011b. Involvement of a putative response regulator FgRrg-1 in osmotic stress response, fungicide resistance and virulence in Fusarium graminearum. Mol. Plant Pathol. 12, 425–36.

Jiang, J., Yun, Y., Liu, Y., Ma, Z., 2012. FgVELB is associated with vegetative differentiation, secondary metabolism and virulence in Fusarium graminearum. Fungal Genet. Biol. 49, 653–62.

Jiang, J., Yun, Y., Yang, Q., Shim, W.-B., Wang, Z., Ma, Z., 2011c. A type 2C protein phosphatase FgPtc3 is involved in cell wall integrity, lipid metabolism, and virulence in

Fusarium graminearum. PLoS One 6, e25311.

Jiao, F., Kawakami, A., Nakajima, T., 2008. Effects of different carbon sources on trichothecene production and Tri gene expression by *Fusarium graminearum* in liquid culture. FEMS Microbiol. Lett. 285, 212–219.

Jonkers, W., Dong, Y., Broz, K., Kistler, H.C., 2012. The Wor1-like protein Fgp1 regulates pathogenicity, toxin synthesis and reproduction in the phytopathogenic fungus Fusarium graminearum. PLoS Pathog. 8, e1002724.

Kachroo, A., He, Z., Patkar, R., Zhu, Q., Zhong, J., Li, D., Ronald, P., Lamb, C., Chattoo, B.B., 2003. Induction of H2O2 in Transgenic Rice Leads to Cell Death and Enhanced Resistance to Both Bacterial and Fungal Pathogens. Transgenic Res. 12, 577–586.

Kakimoto, T., 2001. Identification of Plant Cytokinin Biosynthetic Enzymes as Dimethylallyl Diphosphate:ATP/ADP Isopentenyltransferases. Plant Cell Physiol. 42, 677–685.

Kazan, K., Gardiner, D.M., Manners, J.M., 2012. On the trail of a cereal killer : recent advances in *Fusarium graminearum* pathogenomics and host resistance. Mol. Plant Pathol. 13, 399–413.

Kettle, A.J., Batley, J., Benfield, A.H., Manners, J.M., Kazan, K., Gardiner, D.M., 2015. Degradation of the benzoxazolinone class of phytoalexins is important for virulence of Fusarium pseudograminearum towards wheat. Mol. Plant Pathol. 16, 946-962.

Kim, H.-K., Lee, S., Jo, S.-M., McCormick, S.P., Butchko, R. a E., Proctor, R.H., Yun, S.-H., 2013. Functional roles of FgLaeA in controlling secondary metabolism, sexual development, and virulence in Fusarium graminearum. PLoS One 8, e68441.

Kistler, H.C., Broz, K., 2015. Cellular compartmentalization of secondary metabolism. Front. Microbiol. 6, 68.

Klittich, C., Leslie, J.F., 1987. Nitrate reduction mutants of *Fusarium moniliforme* (*Gibberella fujikuroi*). Genetics 118, 417–423.

Knight, N.L., Sutherland, M.W., 2013. Histopathological assessment of wheat seedling tissues infected by *Fusarium pseudograminearum*. Plant Pathol. 62, 679–687.

Kokkonen, M., Ojala, L., Parikka, P., Jestoi, M., 2010. Mycotoxin production of selected *Fusarium* species at different culture conditions. Int. J. Food Microbiol. 143, 17–25.

Kronstad, J., De Maria, A., Funnell, D., Laidlaw, R.D., Lee, N., de Sá, M.M., Ramesh, M., 1998. Signaling via cAMP in fungi: interconnections with mitogen-activated protein kinase pathways. Arch. Microbiol. 170, 395–404.

Kurakawa, T., Ueda, N., Maekawa, M., Kobayashi, K., Kojima, M., Nagato, Y., Sakakibara, H., Kyozuka, J., 2007. Direct control of shoot meristem activity by a cytokinin-activating enzyme. Nature 445, 652–655.

Lee, J., Myong, K., Kim, J.-E., Kim, H.-K., Yun, S.-H., Lee, Y.-W., 2012. FgVelB globally regulates sexual reproduction, mycotoxin production and pathogenicity in the cereal pathogen Fusarium graminearum. Microbiology 158, 1723–33.

Leopold, A.C., Kawase, M., 1964. Benzyladenine Effects on Bean Leaf Growth and Senescence. Am. J. Bot. 51, 294.

Li, L., Wright, S.J., Krystofova, S., Park, G., Borkovich, K.A., 2007. Heterotrimeric G protein signaling in filamentous fungi. Annu. Rev. Microbiol. 61, 423–452.

Li, M., Gong, X., Zheng, J., Jiang, D., Fu, Y., Hou, M., 2005. Transformation of *Coniothyrium*

minitans, a parasite of *Sclerotinia sclerotiorum*, with *Agrobacterium tumefaciens*. FEMS Microbiol. Lett. 243, 323–329.

Li, Y., Wang, C., Liu, W., Wang, G., Kang, Z., Kistler, H.C., Xu, J.-R., 2011. The HDF1 histone deacetylase gene is important for conidiation, sexual reproduction, and pathogenesis in Fusarium graminearum. Mol. Plant. Microbe. Interact. 24, 487–96.

Linder, J.U., 2006. Class III adenylyl cyclases: molecular mechanisms of catalysis and regulation. Cell. Mol. Life Sci. 63, 1736–1751.

Liu, X., Jiang, J., Yin, Y., Ma, Z., 2013. Involvement of FgERG4 in ergosterol biosynthesis, vegetative differentiation and virulence in Fusarium graminearum. Mol. Plant Pathol. 14, 71–83.

Lysøe, E., Pasquali, M., Breakspear, A., Kistler, H.C., 2011. The transcription factor FgStuAp influences spore development, pathogenicity, and secondary metabolism in Fusarium graminearum. Mol. Plant. Microbe. Interact. 24, 54–67.

Ma, L.-J., van der Does, H.C., Borkovich, K.A., Coleman, J.J., Daboussi, M.-J., Di Pietro, A., Dufresne, M., Freitag, M., Grabherr, M., Henrissat, B., Houterman, P.M., Kang, S., Shim, W.-B., Woloshuk, C., Xie, X., Xu, J.-R., Antoniw, J., Baker, S.E., Bluhm, B.H., Breakspear, A., Brown, D.W., Butchko, R.A.E., Chapman, S., Coulson, R., Coutinho, P.M., Danchin, E.G.J., Diener, A., Gale, L.R., Gardiner, D.M., Goff, S., Hammond-Kosack, K.E., Hilburn, K., Hua-Van, A., Jonkers, W., Kazan, K., Kodira, C.D., Koehrsen, M., Kumar, L., Lee, Y.-H., Li, L., Manners, J.M., Miranda-Saavedra, D., Mukherjee, M., Park, G., Park, J., Park, S.-Y., Proctor, R.H., Regev, A., Ruiz-Roldan, M.C., Sain, D., Sakthikumar, S., Sykes, S., Schwartz, D.C., Turgeon, B.G., Wapinski, I., Yoder, O., Young, S., Zeng, Q., Zhou, S., Galagan, J., Cuomo, C.A., Kistler, H.C., Rep, M., 2010. Comparative genomics reveals mobile pathogenicity chromosomes in Fusarium. Nature 464, 367–73.

Ma, P., Wera, S., Van Dijck, P., Thevelein, J.M., 1999. The *PDE1*-encoded low-affinity phosphodiesterase in the yeast *Saccharomyces cerevisiae* has a specific function in controlling agonist-induced cAMP signaling. Mol. Biol. Cell 10, 91–104.

Maier, F.J., Miedaner, T., Hadeler, B., Felk, A., Salomon, S., Lemmens, M., Kassner, H., Schäfer, W., 2006. Involvement of trichothecenes in fusarioses of wheat, barley and maize evaluated by gene disruption of the trichodiene synthase (Tri5) gene in three field isolates of different chemotype and virulence. Mol. Plant Pathol. 7, 449–61.

McLaughlin, J.E., Bin-Umer, M.A., Tortora, A., Mendez, N., McCormick, S., Tumer, N.E., 2009. A genome-wide screen in Saccharomyces cerevisiae reveals a critical role for the mitochondria in the toxicity of a trichothecene mycotoxin. Proc. Natl. Acad. Sci. U. S. A. 106, 21883–8.

McMullen, M., Halley, S., Schatz, B., Meyer, S., Jordahl, J., Ransom, J., 2008. Integrated strategies for Fusarium head blight management in the United States. Cereal Res. Commun. 36, 563–568.

McMullen, M., Jones, R., Gallenberg, D., 1997. Scab of Wheat and Barley: A Re-emerging Disease of Devastating Impact - PDIS.1997.81.12.1340. Plant Dis. 81.

Menke, J., Dong, Y., Kistler, H.C., 2012. *Fusarium graminearum* Tri12p influences virulence to wheat and trichothecene accumulation. Mol. Plant. Microbe. Interact. 25, 1408–1418.

Menke, J., Weber, J., Broz, K., Kistler, H.C., 2013. Cellular development associated with induced mycotoxin synthesis in the filamentous fungus *Fusarium graminearum*. PLoS One 8, e63077.

Merhej, J., Richard-Forget, F., Barreau, C., 2011. The pH regulatory factor Pac1 regulates *Tri* gene expression and trichothecene production in *Fusarium graminearum*. Fungal Genet. Biol. 48, 275–84.

Merhej, J., Urban, M., Dufresne, M., Hammond-Kosack, K.E., Richard-Forget, F., Barreau, C., 2012. The velvet gene , FgVe1 , affects fungal development and positively regulates trichothecene biosynthesis and pathogenicity in Fusarium graminearum 13, 363–374.

Miller, J.D., Blackwell, B.A., 1996. Biosynthesis of 3-acetyldeoxynivalenol and other metabolites by Fusarium culmorum HLX 1503 in a stirred jar fermentor. Can. J. Bot. 64, 1–5.

Miller, J.D., Greenhalgh, R., 1985. Nutrient effects on the biosynthesis of trichothecenes and other metabolites by *Fusarium graminearum*. Mycologia 77, 130–136.

Miller, J.D., Taylor, A., Greenhalgh, R., 1983. Production of deoxynivalenol and related compounds in liquid culture by *Fusarium graminearum*. Can. J. Microbiol. 29, 1171–1178.

Min, K., Shin, Y., Son, H., Lee, J., Kim, J.-C., Choi, G.J., Lee, Y.-W., 2012. Functional analyses of the nitrogen regulatory gene *areA* in *Gibberella zeae*. FEMS Microbiol. Lett. 334, 66–73.

Mudge, A.M., Dill-Macky, R., Dong, Y., Gardiner, D.M., White, R.G., Manners, J.M., 2006. A role for the mycotoxin deoxynivalenol in stem colonisation during crown rot disease of wheat caused by Fusarium graminearum and Fusarium pseudograminearum. Physiol. Mol. Plant Pathol. 69, 73–85.

Müller, W.H., Bovenberg, R.A.L., Groothuis, M.H., Kattevilder, F., Smaal, E.B., Van der Voort, L.H.M., Verkleij, A.J., 1992. Involvement of microbodies in penicillin biosynthesis, Biochimica et Biophysica Acta (BBA) - General Subjects. 210-213.

Murphy, A., Pryce-Jones, E., Johnstone, K., Ashby, A., 1997. Comparison of cytokinin production *in vitro* by *Pyrenopeziza brassicae* with other plant pathogens. Physiol. Mol. Plant Pathol. 50, 53–65.

Murray, G.M., Brennan, J.P., 2010. Estimating disease losses to the Australian barley industry. Australas. Plant Pathol. 39, 85–96.

Murray, G.M., Brennan, J.P., 2009. Estimating disease losses to the Australian wheat industry. Australas. Plant Pathol. 38, 558–570.

Nganje, W.E., Bangsund, D.A., Leistritz, F.L., Wilson, W.W., Tiapo, N.M., 2002. Estimating the economic impact of a crop disease: the case of Fusarium head blight in US wheat and barley, in: National Fusarium Head Blight Forum Proceedings.

Nguyen, L.N., Bormann, J., Le, G.T.T., Stärkel, C., Olsson, S., Nosanchuk, J.D., Giese, H., Schäfer, W., 2011. Autophagy-related lipase FgATG15 of Fusarium graminearum is important for lipid turnover and plant infection. Fungal Genet. Biol. 48, 217–24.

Nishiuchi, T., Masuda, D., Nakashita, H., Ichimura, K., Shinozaki, K., Yoshida, S., Kimura, M., Yamaguchi, I., Yamaguchi, K., 2006. Fusarium phytotoxin trichothecenes have an elicitor-like activity in Arabidopsis thaliana, but the activity differed significantly among their molecular species. Mol. Plant. Microbe. Interact. 19, 512–20.

Nussbaumer, T., Warth, B., Sharma, S., Ametz, C., Bueschl, C., Parich, A., Pfeifer, M., Siegwart, G., Steiner, B., Lemmens, M., Schuhmacher, R., Buerstmayr, H., Mayer, K.F.X., Kugler, K.G., Schweiger, W., 2015. Joint Transcriptomic and Metabolomic Analyses Reveal Changes in the Primary Metabolism and Imbalances in the

Subgenome Orchestration in the Bread Wheat Molecular Response to Fusarium graminearum. G3 Genes, Genomes, Genet. 5.

O'Donnell, K., Rooney, A.P., Proctor, R.H., Brown, D.W., McCormick, S.P., Ward, T.J., Frandsen, R.J.N., Lysøe, E., Rehner, S.A., Aoki, T., Robert, V.A.R.G., Crous, P.W., Groenewald, J.Z., Kang, S., Geiser, D.M., 2013. Phylogenetic analyses of RPB1 and RPB2 support a middle Cretaceous origin for a clade comprising all agriculturally and medically important fusaria. Fungal Genet. Biol. 52, 20–31.

O'Donnell, K., Ward, T.J., Geiser, D.M., Corby Kistler, H., Aoki, T., 2004. Genealogical concordance between the mating type locus and seven other nuclear genes supports formal recognition of nine phylogenetically distinct species within the *Fusarium graminearum* clade. Fungal Genet. Biol. 41, 600–623.

Ochiai, N., Tokai, T., Nishiuchi, T., Takahashi-Ando, N., Fujimura, M., Kimura, M., 2007. Involvement of the osmosensor histidine kinase and osmotic stress-activated protein kinases in the regulation of secondary metabolism in Fusarium graminearum. Biochem. Biophys. Res. Commun. 363, 639–44.

Ohkuma, M., Park, S.M., Zimmer, T., Menzel, R., Vogel, F., Schunck, W.-H., Ohta, A., Takagi, M., 1995. Proliferation of intracellular membrane structures upon homologous overproduction of cytochrome P-450 in Candida maltosa. Biochim. Biophys. Acta - Biomembr. 1236, 163–169.

Palazzini, J.M., Ramirez, M.L., Torres, A.M., Chulze, S.N., 2007. Potential biocontrol agents for Fusarium head blight and deoxynivalenol production in wheat. Crop Prot. 26, 1702–1710.

Palecek, S.P., Parikh, A.S., Kron, S.J., 2002. Sensing, signalling and integrating physical processes during Saccharomyces cerevisiae invasive and filamentous growth. Microbiology 148, 893–907.

Paranidharan, V., Abu-Nada, Y., Hamzehzarghani, H., Kushalappa, A.C., Mamer, O., Dion, Y., Rioux, S., Comeau, A., Choiniere, L., 2008. Resistance-related metabolites in wheat against *Fusarium graminearum* and the virulence factor deoxynivalenol (DON). Botany 86, 1168–1179.

Parent, C.A., Devreotes, P.N., 1996. Constitutively active adenylyl cyclase mutant requires neither G proteins nor cytosolic regulators. J. Biol. Chem. 271, 18333–18336.

Park, A.R., Cho, A.-R., Seo, J.-A., Min, K., Son, H., Lee, J., Choi, G.J., Kim, J.-C., Lee, Y.-W., 2012. Functional analyses of regulators of G protein signaling in *Gibberella zeae*. Fungal Genet. Biol. 49, 511–520.

Peñalva, M.A., Tilburn, J., Bignell, E., Arst, H.N., 2008. Ambient pH gene regulation in fungi: making connections. Trends Microbiol. 16, 291–300.

Peplow, A.W., Tag, A.G., Garifullina, G.F., Beremand, M.N., 2003. Identification of new genes positively regulated by Tri10 and a regulatory network for trichothecene mycotoxin production. Appl. Environ. Microbiol. 69, 2731–2736.

Pestka, J.J., 2010. Deoxynivalenol-induced proinflammatory gene expression: mechanisms and pathological sequelae. Toxins (Basel). 2, 1300–17. doi:10.3390/toxins2061300

Phillips, D.A., Torrey, J.G., 1970. Cytokinin Production by Rhizobium japonicum. Physiol. Plant. 23, 1057–1063.

Pinson-Gadais, L., Richard-Forget, F., Frasse, P., Barreau, C., Cahagnier, B., Richard-Molard, D., Bakan, B., 2008. Magnesium represses trichothecene biosynthesis and

modulates Tri5, Tri6, and Tri12 genes expression in Fusarium graminearum. Mycopathologia 165, 51–9.

Ponts, N., Pinson-Gadais, L., Barreau, C., Richard-Forget, F., Ouellet, T., 2007. Exogenous H_2O_2 and catalase treatments interfere with Tri genes expression in liquid cultures of *Fusarium graminearum*. FEBS Lett. 581, 443–447.

Ponts, N., Pinson-Gadais, L., Boutigny, A.-L., Barreau, C., Richard-Forget, F., 2011. Cinnamic-derived acids significantly affect *Fusarium graminearum* growth and in vitro synthesis of type B trichothecenes. Phytopathology 101, 929–934.

Ponts, N., Pinson-Gadais, L., Verdal-Bonnin, M.-N., Barreau, C., Richard-Forget, F., 2006. Accumulation of deoxynivalenol and its 15-acetylated form is significantly modulated by oxidative stress in liquid cultures of *Fusarium graminearum*. FEMS Microbiol. Lett. 258, 102–107.

Powell, J.J., Carere, J., Fitzgerald, T.L., Stiller, J., Covarelli, L., Xu, Q., Gubler, F., Colgrave, M.L., Gardiner, D.M., Manners, J.M., Henry, R.J., 2017. The Fusarium crown rot pathogen *Fusarium pseudograminearum* triggers a suite of transcriptional and metabolic changes in bread wheat (*Triticum aestivum* L .). Ann. Bot. 119, 853–867.

Pritsch, C., Muehlbauer, G.J., Bushnell, W.R., Somers, D.A., Vance, C.P., 2000. Fungal development and induction of defense response genes during early infection of wheat spikes by *Fusarium graminearum*. Mol. Plant. Microbe. Interact. 13, 159–169.

Proctor, R.H., Hohn, T.M., McCormick, S.P., 1995a. Reduced Virulence of Gibberella zeae Caused by Disruption of a Trichothecene Toxin Biosynthetic Gene. Mol. Plant. Microbe. Interact. 8, 593–601.

Proctor, R.H., Hohn, T.M., McCormick, S.P., Desjardins, A.E., 1995b. Tri6 encodes an unusual zinc finger protein involved in regulation of trichothecene biosynthesis in Fusarium sporotrichioides. Appl. Envir. Microbiol. 61, 1923–1930.

Profant, D.A., Roberts, C.J., Koning, A.J., Wright, R.L., 1999. The role of the 3-hydroxy 3-methylglutaryl coenzyme A reductase cytosolic domain in karmellae biogenesis. Mol. Biol. Cell 10, 3409–23.

Repka, V., 1999. Improved Histochemical Test for In Situ Detection of Hydrogen Peroxide in Cells Undergoing Oxidative Burst or Lignification. Biol. Plant. 42, 599–607.

Reyes-Dominguez, Y., Boedi, S., Sulyok, M., Wiesenberger, G., Stoppacher, N., Krska, R., Strauss, J., 2012. Heterochromatin influences the secondary metabolite profile in the plant pathogen Fusarium graminearum. Fungal Genet. Biol. 49, 39–47.

Richmond, A.E., Lang, A., 1957. Effect of Kinetin on Protein Content and Survival of Detached Xanthium Leaves. Science. 125, 650-651.

Riley, B.B., Barclay, S.L., 1990. Conditions that alter intracellular cAMP levels affect expression of the cAMP phosphodiesterase gene in *Dictyostelium*. Proc. Natl. Acad. Sci. U. S. A. 87, 4746–4750.

Rittenour, W.R., Harris, S.D., 2010. An in vitro method for the analysis of infection-related morphogenesis in *Fusarium graminearum*. Mol. Plant Pathol. 11, 361–369.

Roitsch, T., Ehneß, R., 2000. Regulation of source/sink relations by cytokinins. Plant Growth Regul. 32, 359–367.

Roze, L. V., Chanda, A., Linz, J.E., 2011. Compartmentalization and molecular traffic in secondary metabolism: A new understanding of established cellular processes. Fungal

Genet. Biol. 48, 35–48.

Sandig, G., Kaergel, E., Menzel, R., Vogel, F., Zimmer, T., Schunck, W.-H., 1999. Regulation of Endoplasmic Reticulum Biogenesis in Response to Cytochrome P450 Overproduction. Drug Metab. Rev. 31, 393–410.

Schäfer, M., Meza-Canales, I.D., Brütting, C., Baldwin, I.T., Meldau, S., 2015. Cytokinin concentrations and CHASE-DOMAIN CONTAINING HIS KINASE 2 (NaCHK2)- and NaCHK3-mediated perception modulate herbivory-induced defense signaling and defenses in *Nicotiana attenuata*. New Phytol. 207, 645–658.

Schmidt-Dannert, C., 2015. NextGen microbial natural products discovery. Microb. Biotechnol. 8, 26–28.

Seong, K.-Y., Pasquali, M., Zhou, X., Song, J., Hilburn, K., McCormick, S., Dong, Y., Xu, J.-R., Kistler, H.C., 2009. Global gene regulation by *Fusarium* transcription factors Tri6 and Tri10 reveals adaptations for toxin biosynthesis. Mol. Microbiol. 72, 354–367.

Seong, K., Hou, Z., Tracy, M., Kistler, H.C., Xu, J.-R., 2005. Random insertional mutagenesis identifies genes associated with virulence in the wheat scab fungus *Fusarium graminearum*. Phytopathology 95, 744–750.

Seong, K., Li, L., Hou, Z., Tracy, M., Kistler, H.C., Xu, J.-R., 2006. Cryptic promoter activity in the coding region of the HMG-CoA reductase gene in Fusarium graminearum. Fungal Genet. Biol. 43, 34–41.

Sieber, C.M.K., Lee, W., Wong, P., Münsterkötter, M., Mewes, H.-W., Schmeitzl, C., Varga, E., Berthiller, F., Adam, G., Güldener, U., 2014. The Fusarium graminearum Genome Reveals More Secondary Metabolite Gene Clusters and Hints of Horizontal Gene Transfer. PLoS One 9, e110311.

Smigocki, A., Neal, J.W., McCanna, I., Douglass, L., 1993. Cytokinin-mediated insect resistance in Nicotiana plants transformed with the ipt gene. Plant Mol. Biol. 23, 325–335.

Smiley, R.W., Backhouse, D., Lucas, P., Paulitz, T.C., 2009. Diseases Which Challenge Global Wheat Production - Root, Crown, and Culm rots, in: Carver, B.F. (Ed.), Wheat: Science and Trade. Wiley-Blackwell, Ames, IA, USA, 125–153.

Smiley, R.W., Patterson, L.-M., 1996. Pathogenic fungi associated with Fusarium foot rot of winter wheat in the semiarid Pacific Northwest. Plant Dis. 80, 944–949.

Snapp, E.L., Hegde, R.S., Francolini, M., Lombardo, F., Colombo, S., Pedrazzini, E., Borgese, N., Lippincott-Schwartz, J., 2003. Formation of stacked ER cisternae by low affinity protein interactions. J. Cell Biol. 163, 257-269.

Son, H., Lee, J., Park, A.R., Lee, Y.-W., 2011a. ATP citrate lyase is required for normal sexual and asexual development in Gibberella zeae. Fungal Genet. Biol. 48, 408–17.

Son, H., Seo, Y.-S., Min, K., Park, A.R., Lee, J., Jin, J.-M., Lin, Y., Cao, P., Hong, S.-Y., Kim, E.-K., Lee, S.-H., Cho, A., Lee, S., Kim, M.-G., Kim, Y., Kim, J.-E., Kim, J.-C., Choi, G.J., Yun, S.-H., Lim, J.Y., Kim, M., Lee, Y.-H., Choi, Y.-D., Lee, Y.-W., 2011b. A phenome-based functional analysis of transcription factors in the cereal head blight fungus, Fusarium graminearum. PLoS Pathog. 7, e1002310.

Sørensen, J.L., Benfield, A.H., Wollenberg, R.D., Westphal, K., Wimmer, R., Nielsen, K.F., Carere, J., Covarelli, L., Beccari, G., Powell, J., Yamashino, T., Kogler, H., Sondergaard, T.E., Gardiner, D.M., 2017. Reprogramming of the host by a cereal pathogen using a cytokinin mimic. Environ. Microbiol. submitted.

Summerell, B., Burgess, L., 1988. Stubble Management Practices and the Survival of Fusarium Graminearum Group 1 in Wheat Stubble Residues. Australas. Plant Pathol. 17, 88.

Sunahara, R.K., Dessauer, C.W., Gilman, A.G., 1996. Complexity and Diversity of Mammalian Adenylyl Cyclases - annurev.pa.36.040196.002333. Annu. Rev. Pharmacol. Toxicol. 36, 461–480.

Takei, K., Mignery, G.A., Mugnaini, E., Südhof, T.C., De Camilli, P., 1994. Inositol 1,4,5-Trisphosphate receptor causes formation of ER cisternal stacks in transfected fibroblasts and in cerebellar purkinje cells. Neuron 12, 327–342.

Takei, K., Sakakibara, H., Sugiyama, T., 2001. Identification of genes encoding adenylate isopentenyltransferase, a cytokinin biosynthesis enzyme, in Arabidopsis thaliana. J. Biol. Chem. 276, 26405–10.

Tang, W., Gilman, A., 1995. Construction of a soluble adenylyl cyclase activated by Gs alpha and forskolin. Science. 268, 1769–1772.

Tesmer, J.J.G., Sunahara, R.K., Gilman, A.G., Sprang, S.R., 1997. Crystal Structure of the Catalytic Domains of Adenylyl Cyclase in a Complex with Gs·GTPS. Science. 278, 1907–1916.

The world health organisation IARC working group on the evaluation of carcinogenic risks to humans, 1992. Toxins derived from *Fusarium graminearum*, *F. culmorum* and *F. crookwellense*: Zearalenone, deoxynivalenol, nivalenol and fusarenone X. Lyon, France.

Trail, F., 2009. For blighted waves of grain: Fusarium graminearum in the postgenomics era. Plant Physiol. 149, 103–10.

Tsuyuki, R., Yoshinari, T., Sakamoto, N., Nagasawa, H., Sakuda, S., 2011. Enhancement of trichothecene production in *Fusarium graminearum* by cobalt chloride. J. Agric. Food Chem. 59, 1760–1766.

Tunali, B., Nicol, J.M., Hodson, D., Uçkun, Z., Büyük, O., Erdurmuş, D., Hekimhan, H., Aktaş, H., Akbudak, M.A., Bağci, S.A., 2008. Root and Crown Rot Fungi Associated with Spring, Facultative, and Winter Wheat in Turkey. Plant Dis. 92, 1299–1306.

Upadhyay, S., Xu, X., Lowry, D., Jackson, J.C., Roberson, R.W., Lin, X., 2016. Subcellular Compartmentalization and Trafficking of the Biosynthetic Machinery for Fungal Melanin. Cell Reports. 14, 2511-2518.

Urban, M., Mott, E., Farley, T., Hammond-Kosack, K., 2003. The Fusarium graminearum MAP1 gene is essential for pathogenicity and development of perithecia. Mol. Plant Pathol. 4, 347–359.

van de Kamp, M., Driessen, A.J.M., Konings, W.N., 1999. Compartmentalization and transport in β-lactam antibiotic biosynthesis by filamentous fungi. Antonie Van Leeuwenhoek 75, 41–78.

van der Lende, T.R., van de Kamp, M., Berg, M. van den, Sjollema, K., Bovenberg, R.A.L., Veenhuis, M., Konings, W.N., Driessen, A.J.M., 2002. δ-(l-α-Aminoadipyl)-l-cysteinyl-d-valine synthetase, that mediates the first committed step in penicillin biosynthesis, is a cytosolic enzyme. Fungal Genet. Biol. 37, 49–55.

Van Thuat, N., Schäfer, W., Bormann, J., 2012. The stress-activated protein kinase FgOS-2 is a key regulator in the life cycle of the cereal pathogen Fusarium graminearum. Mol. Plant. Microbe. Interact. 25, 1142–56.

van Wyk, P.S., Los, O., Pauer, G.D.C., Marasas, W.F.O., 1987. Geographic distribution and pathogenecity of Fusarium species associated with crown rot of wheat in the Orange Free State, South Africa. Phytophylactica 19, 271–274.

Vergeres, G., Yen, T.S., Aggeler, J., Lausier, J., Waskell, L., 1993. A model system for studying membrane biogenesis. Overexpression of cytochrome b5 in yeast results in marked proliferation of the intracellular membrane. J. Cell Sci. 106.

Vlaardingerbroek, I., Beerens, B., Shahi, S., Rep, M., 2015. Fluorescence Assisted Selection of Transformants (FAST): Using flow cytometry to select fungal transformants. Fungal Genet. Biol. 76, 104–109.

Voigt, C. a., von Scheidt, B., Gácser, A., Kassner, H., Lieberei, R., Schäfer, W., Salomon, S., 2006. Enhanced mycotoxin production of a lipase-deficient Fusarium graminearum mutant correlates to toxin-related gene expression. Eur. J. Plant Pathol. 117, 1–12.

Voigt, C. a, Schäfer, W., Salomon, S., 2005. A secreted lipase of Fusarium graminearum is a virulence factor required for infection of cereals. Plant J. 42, 364–75.

Walters, D., 2002. Methyl jasmonate alters polyamine metabolism and induces systemic protection against powdery mildew infection in barley seedlings. J. Exp. Bot. 53, 747–756.

Walters, D.R., McRoberts, N., 2006. Plants and biotrophs: a pivotal role for cytokinins? Trends Plant Sci. 11, 581–586.

Wang, G., Wang, C., Hou, R., Zhou, X., Li, G., Zhang, S., Xu, J.-R., 2012. The AMT1 arginine methyltransferase gene is important for plant infection and normal hyphal growth in Fusarium graminearum. PLoS One 7, e38324.

Wang, Y., Liu, W., Hou, Z., Wang, C., Zhou, X., Jonkers, W., Ding, S., Kistler, H.C., Xu, J.-R., 2011. A novel transcriptional factor important for pathogenesis and ascosporogenesis in Fusarium graminearum. Mol. Plant. Microbe. Interact. 24, 118–28.

Watanabe, C.M.., Townsend, C.A., 2002. Initial Characterization of a Type I Fatty Acid Synthase and Polyketide Synthase Multienzyme Complex NorS in the Biosynthesis of Aflatoxin B1. Chem. Biol. 9, 981–988.

Weld, R.J., Plummer, K.M., Carpenter, M.A., Ridgway, H.J., 2006. Approaches to functional genomics in filamentous fungi. Cell Res. 16, 31–44.

Wong, P., Walter, M., Lee, W., Mannhaupt, G., Münsterkötter, M., Mewes, H.-W., Adam, G., Güldener, U., 2011. FGDB: revisiting the genome annotation of the plant pathogen *Fusarium graminearum*. Nucleic Acids Res. 39, D637–D639.

Wright, R., Keller, G., Gould, S.J., Subramani, S., Rine, J., 1990. Cell-type control of membrane biogenesis induced by HMG-CoA reductase. New Biol. 2, 915–21.

Wuchiyama, J., Kimura, M., Yamaguchi, I., 2000. A Trichothecene Efflux Pump Encoded by TriIO2 in the Biosynthetic Gene Cluster of Fusarium graminearum. Appl. Microbiol. Biotechnol. 53, 196–200.

Xia, Z., Storm, D.R., 1997. Calmodulin-regulated adenylyl cyclases and neuromodulation. Curr. Opin. Neurobiol. 7, 391–396.

Xue, A.G., Voldeng, H.D., Savard, M.E., Fedak, G., 2009. Biological management of Fusarium head blight and mycotoxin contamination in wheat. World Mycotoxin J. Volume 2.

Yaguchi, A., Yoshinari, T., Tsuyuki, R., Takahashi, H., Nakajima, T., Sugita-Konishi, Y.,

Nagasawa, H., Sakuda, S., 2009. Isolation and identification of precocenes and piperitone from essential oils as specific inhibitors of trichothecene production by Fusarium graminearum. J. Agric. Food Chem. 57, 846–51.

Yamamoto, A., Masaki, R., Tashiro, Y., 1996. Formation of crystalloid endoplasmic reticulum in COS cells upon overexpression of microsomal aldehyde dehydrogenase by cDNA transfection. J. Cell Sci. 109, 1727-1738.

Yin, W., Keller, N.P., 2011. Transcriptional regulatory elements in fungal secondary metabolism. J. Microbiol. 49, 329–339.

Yu, H.-Y., Seo, J.-A., Kim, J.-E., Han, K.-H., Shim, W.-B., Yun, S.-H., Lee, Y.-W., 2008. Functional analyses of heterotrimeric G protein G alpha and G beta subunits in *Gibberella zeae*. Microbiology 154, 392–401.

Zhang, S., Schisler, D.A., Boehm, M.J., Slininger, P.J., 2007. Utilization of chemical inducers of resistance and Cryptococcus flavescens OH 182.9 to reduce Fusarium head blight under greenhouse conditions. Biol. Control 42, 308–315.

Zhou, H.-R., 2003. Rapid, Sequential Activation of Mitogen-Activated Protein Kinases and Transcription Factors Precedes Proinflammatory Cytokine mRNA Expression in Spleens of Mice Exposed to the Trichothecene Vomitoxin. Toxicol. Sci. 72, 130–142.

Zhou, W., Kolb, F.L., Riechers, D.E., 2005. Identification of proteins induced or upregulated by Fusarium head blight infection in the spikes of hexaploid wheat (Triticum aestivum). Genome 48, 770–80.

Zhou, X., Heyer, C., Choi, Y.-E., Mehrabi, R., Xu, J.-R., 2010. The CID1 cyclin C-like gene is important for plant infection in Fusarium graminearum. Fungal Genet. Biol. 47, 143–51.